BIOS

Research Doctorate School in

BIOmolecular Sciences

Ph.D. in BIOMATERIALS – *XXIII Cycle (2009-2011)*

"POLYMERIC AND CERAMIC BIOMATERIALS IN BONE REGENERATION"

Dr. Francesca Veronesi

Supervisor: Prof. Roberto Giardino

Tutor: Dr. Milena Fini

Laboratory of Preclinical and Surgical Studies

Rizzoli Orthopaedic Institute

-CONTENTS-

1. SKELETAL SYSTEM

1.1 BONE STRUCTURE

Bone is a dynamic, vascular, living tissue that changes throughout life, is one of the so-called "connective tissues" of the body and thus comprises cells that become embedded in their own extracellular matrix. Bone is highly specialized with a complex, hierarchical structure over multiple levels (Standring S, 2008). Given bone tissue's ability to adapt its mass and morphology to functional demands, its ability to repair itself without leaving a scar, and its capacity to rapidly mobilize mineral stores on metabolic demand, bone is considered the ultimate "smart" material and a dynamic example of "form follows function" in biological systems. The principal role of the bone is to provide structural support for the body and while the bone also serves as the body's mineral reservoir and producer of blood cells, the mineralized structure is the very basis of posture, opposes muscular contraction resulting in motion, withstands functional load bearing, and protects internal organs (Kneser U, et al., 2006).

It is composed of an extracellular matrix (ECM) which has been represented as a two-phases composite, characterized by an organic phase (35%) composed by 90% of collagenous proteins (97% collagen I and 3% collagen III, IV and V) and 10% of non collagenous proteins (mainly osteocalcin, osteonectin, sialoproteins, proteoglycans, osteopontin, fibronectin, Growth Factors and bone morphogenetic proteins), reinforced with inorganic (65%) component, characterized by calcium phosphate hydroxyapatite [$(Ca_{10}(PO_4)_6(OH)_2)$] crystals (HA, TCP) with a Ca:P ratio of 5:3, sodium (Na), magnesium (Mg) and potassium (K) (Figure 1). Apatite crystals are nanoscale, elongate, plate-like and orientated in relation to the direction of primary stress (Amizuka N, 2004).

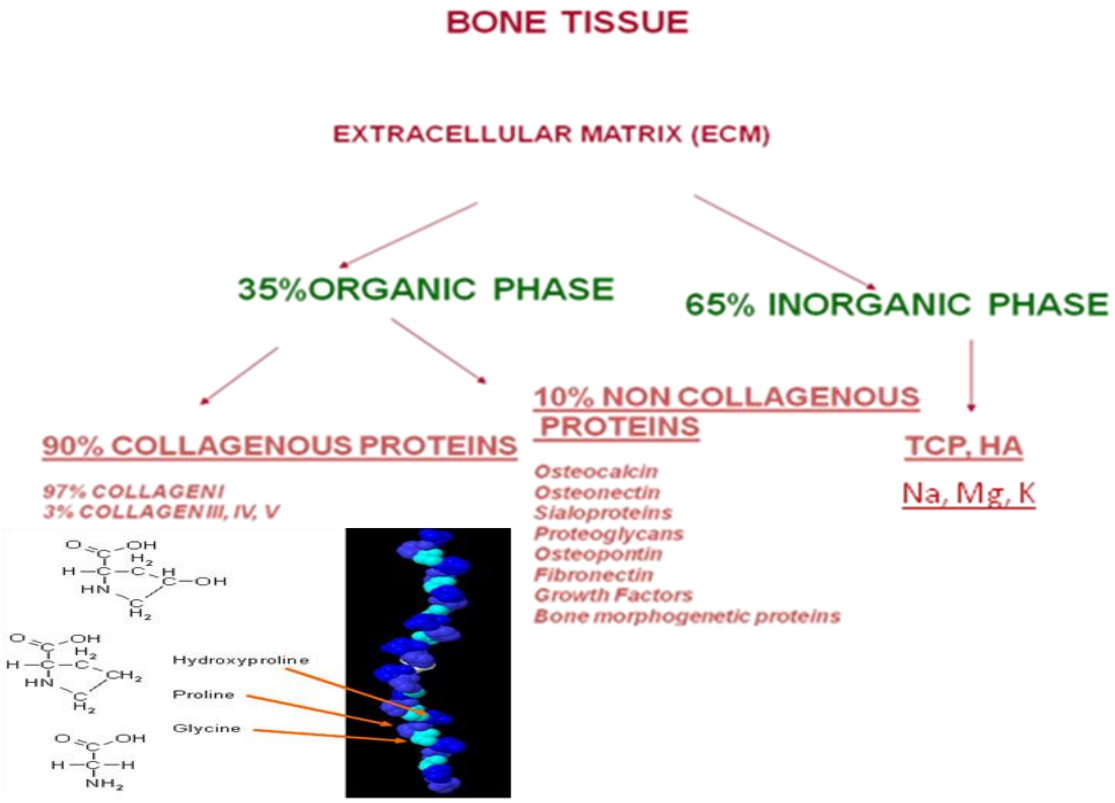

Fig. 1. Bone extracellular matrix (ECM) composition.

Bone growth factors (GFs) and cytokines influence the synthesis and resorption of bone by acting on the local cell population present in bone marrow and on bone. They are local regulators of cell growth, function and angiogenesis. Bone matrix contains a great number of GFs and cytokines such as, Interleukin I , VI and IX (IL-I, VI, IX), Tumor necrosis factor α (TNF-α), Transforming growth factor beta supergene family (TGF-β1-5 and Bone Morphogenetic Proteins-BMPs), Platelet-derived growth factors (PDGFs), insulin-like growth factor I and II (IGF-I and-II), fibroblast growth factors (FGFs), as indicated in Table 1 (Soheim E, 1998).

Tab. 1. Cytokine and GF functions and sources in bone.

CYTOKINES AND GFs	BONE FORMATION	BONE RESORPTION	POTENTIAL SOURCES IN BONE
IL-I	+	+++	Osteoblasts
IL-VI	?	+/-	Osteoblasts
IL-IX	++	++	Osteoblasts
TNF-α	+	+++	Osteoblasts
TGF-β and BMPs	++	++	Osteoblasts, bone matrix
PDGFs	++	++	Platelets, osteoblasts, bone matrix
IGF-I	+++		Osteoblasts, bone matrix
IGF-II	+++		Osteoblasts, bone matrix
FGFs	+++		Osteoblasts, bone matrix

Histologically (Figure 2), bone is identified as lamellar bone, consisting of lamellae (3-7 μm in thickness) composed of bone matrix and osteocytes each occupating a cavity (lacuna). Canaliculi penetrate the lamellae of adjacent lacunae. The osteon or Haversian system is formed by arranged lamellae around a longitudinal vascular channel. The osteons are parallel to one another in skeletrical districts where tension forces prevail. Vascular anastomosis are present between vascular channels of adjacent osteons, as branches that run perpendicular to Haversian channels (Volkmann channels) (Laz PJ, et al., 2007).

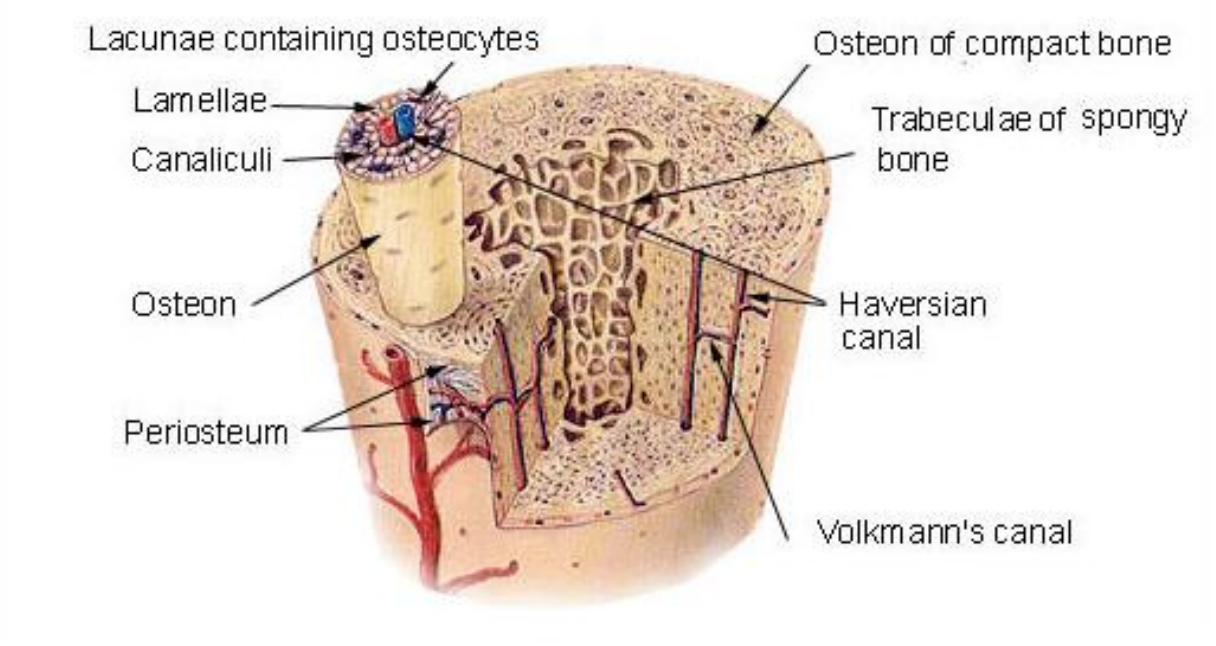

Fig.2. Bone structure. (Image from http://training.seer.cancer.gov/anatomy/skeletal/tissue.html).

Bone tissue is arranged in two macroarchitectural forms-cortical (or compact) and cancellous (or trabecular, or spongy)- which are employed in various proportions and geometries to form the individual bones of the body (Figure 3). The latter can be broadly subdivided into four groups: long bones (femur, tibia, fibula, humerus, radius, and ulna); short bones such as those of the carpus (wrist) and tarsus (ankle); flat bones such as those of the calvaria (skull vault); and irregular bones (the remaining bones of the skull, the scapula, and pelvic bones).

In cortical bone, densely packed collagen fibrils form concentric lamellae, and the fibrils in adjacent lamellae run in perpendicular planes as in plywood, whereas, cancellous bone has a loosely organized, porous matrix. Cortical bone is almost solid with less than 10% of porosity, in contrast, cancellous bone is organized in a porous sponge-like pattern. Cortical bone has loading fibers orientated along the loading axis with highly organized structures such as the Haversian system. Cancellous bone has a cortex of cortical tissue consisting of longitudinally oriented osteons that are typically of the order of 200 μm in diameter and 10-20 mm in length. The cortical

has greater apparent modulus of elasticity, tensile strength, and fracture toughness than cancellous bone. However, owing to the highly porous structure (cancellous bone 75-90%; cortical bone 5-10%), relative properties of the ECM are similar (Davies JE, 2003). In general, strength of bone depends on the hardness of the compact cortical bone and on the underlying scaffolding effect of the trabeculae of cancellous bone.

The cortical bone has evolved to withstand torsional loading, while the function of cancellous bone is to withstand predominantly compressive loading.

About 3-5 % of one's skeleton is being eaten away by osteoclasts and replaced by osteoblasts, throughout life from six weeks *in utero*, when bone first forms, until we die. This constant remodeling of bone tissue provides a mechanism for scar-free healing and regeneration of damaged bone tissue, and results in the exquisite lamellar microarchitecture of both cortical and trabecular mature bone.

From this perspective, therefore, trabecular bone represents a biologically superior tissue, ideally evolved for rapid bone healing, when compared to the slowly remodeling healing pattern typical of cortical bone. On the other hand, cancellous bone is finer and more delicate in appearance. Its physical arrangement of broad plates, connected by thin struts, provides for maximum support but with a minimum of raw material. The metabolic activity of cancellous bone is thought to be considerably higher than that of cortical bone, with the result that diseases, which are caused by aberrations of metabolism, are invariably seen in the cancellous compartment first.

Cancellous bone has a very high surface area, which is contiguous with the marrow compartment. Since marrow contains not only mesenchymal progenitor cells, that can give rise to osteoblasts, but also a rich vasculature that can supply both the circulating mononuclear precursors to osteoclasts (needed for remodeling) and the endothelial population needed for angiogenesis, it is

not surprising that trabecular bone can remodel more quickly than cortical bone (Henriksen K, et al., 2009).

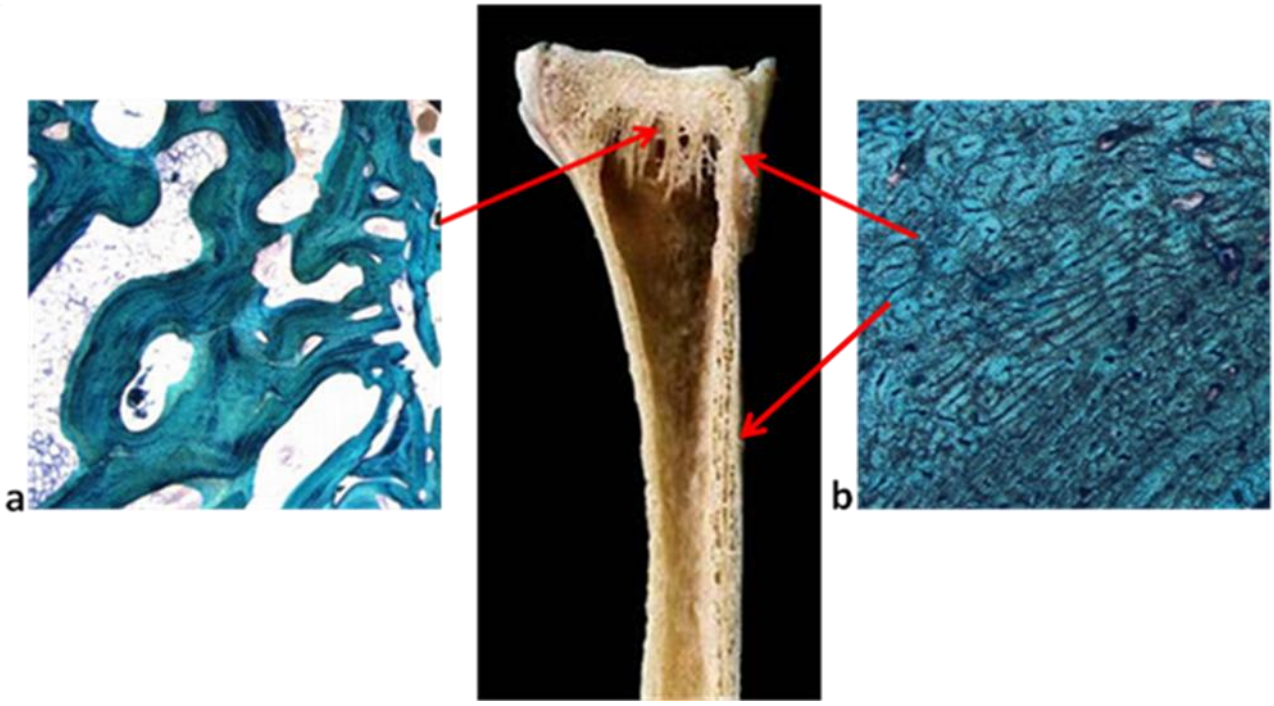

Fig.3. Bone structure. a) Cancellous and b) cortical bone. Toluidine blue, fast green staining. Magnification 10x. (Image from Laboratory of Preclinical and Surgical Studies-IOR).

The entire surface of bone, except where articular cartilage is present, is covered by specialized dense connective tissue known as periosteum. This layer is attached to the cortical bone below by a series of collagenous bundles known as Sharpey fibers and the strength of these attachments varies between different bones. The internal surface of bone, which includes the medullary cavity, cavities of the haversian system of compact bones and the trabeculae of cancellous bone, is lined with another connective layer, endosteum (Hing KA, 2004).

1.2 BONE CELLS

Bone is composed of four different cell types: **osteoblasts, osteocytes, osteoclasts** and **osteoprogenitor cells.**

1.2.1 Osteoblasts

Osteoblasts (Figure 4) are epithelial-like cells that are fully differentiated and polarized cells (20-30µm of diameter) within bone and derived by the differentiation of osteoprogenitor cells.

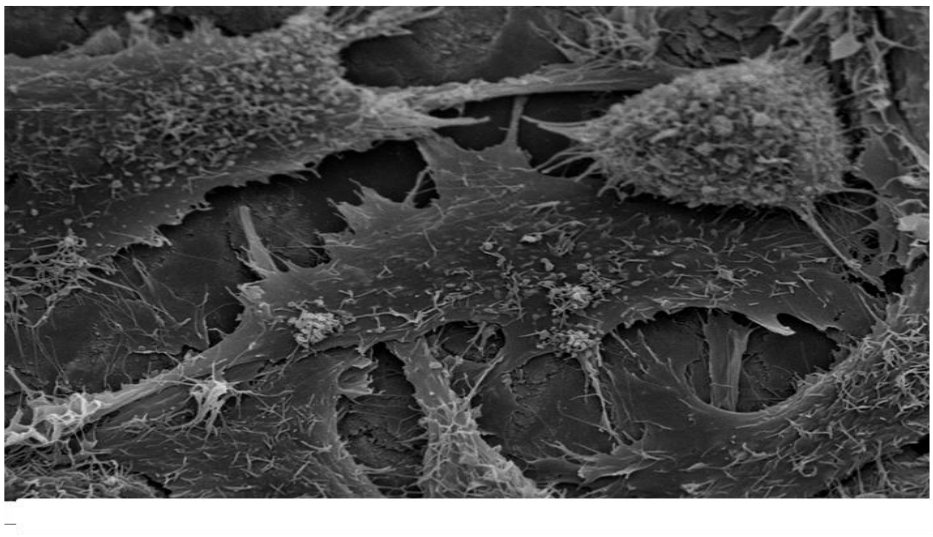

Fig.4. Osteoblasts. Scanning electron Microscopy (SEM). Magnification 1950x. (Image from laboratory of Preclinical and Surgical Studies-IOR).

They have a spherical or ovoid nucleus, lay down the extracellular matrix and regulate mineralization, depositing osteoid, nonmineralized organic matrix and initiating the subsequent mineralization of the osteoid. They secrete the type I Collagen and the non collagenous proteins of the bone matrix such as osteocalcin, osteopontin, bone sialoproteins and GFs such as BMPs. Morphologically, they are cuboidal or columnar in shape and located at the bone surface together with their precursors, where they form a tight layer of cells. The lifespan of an osteoblast ranges between 3 days in young rabbits up to 8 weeks in humans, during which time it lays down 0.5-1.5

µm osteoid per day. Eventually, some osteoblasts may become trapped in their own calcified matrix, changing their phenotype and developing into osteocytes. In fact, when bone formation is completed, osteoblasts flatten out and transform into osteocytes (Henriksen K, et al., 2009).

1.2.2 Osteocytes

Osteocytes (Figure 5) are the most abundant resident cells (>90%) in bone tissue. They are regularly spaced in lacunae throughout the calcified bone matrix and communicate with each other as well as with the cells on bone surface, osteoblasts and osteoprogenitor cells, through a large number of cytoplasmic processes running in bone canaliculi. Osteocytes are no longer involved in bone formation. Due to their inaccessibility and difficulty in cell culture, osteocytes have not received enough attention and little is known about their function for a long time.

However, in recent years, these mysterious cells shed new light on their pivotal function in regulation of new bone formation and remodeling (Huang CP, et al., 2008; Takai E, et al., 2004). The large population, ideal location and unique morphologies make osteocytes ideal candidates for detection of external stimulations and generation of signals that affect osteoblasts, osteoclasts and their progenitors in the bone marrow. An analogy might be made between the bone cells network and neuronal system.

Osteocytes may play the role as the ‘‘brain center’’, and their principal function is thought to be in intercellular signaling by the extensive cellular network (Huang CP, et al., 2008).

Osteocytes form extensive interconnected 3D cellular networks that position them to be suitable sensors of changes in the local mechanical and hormonal environment in bone tissue.

Mechanical stimuli such as hydrostatic pressure, fluid shear, and load-induced strain have been shown to elicit a response from osteocytes both *in vitro* and *in vivo*. Unlike other *in vitro* applications of mechanical stimuli such as membrane stretch, which can induce concomitant fluid

flow-induced effects (e.g., shear stress, streaming potentials, nutrient convection), and fluid shear stress, which is driven by a pressure gradient, hydrostatic pressure can be applied uniformly to all cells without other modes of mechanical stimulation (Warden SJ, 2006).

Osteocytes are not capable of division and are lost when the bone in which they reside is degraded, so the osteocyte's lifespan is dictated by the lifespan of the bone and they can remain alive for years provided vascularization is continuous.

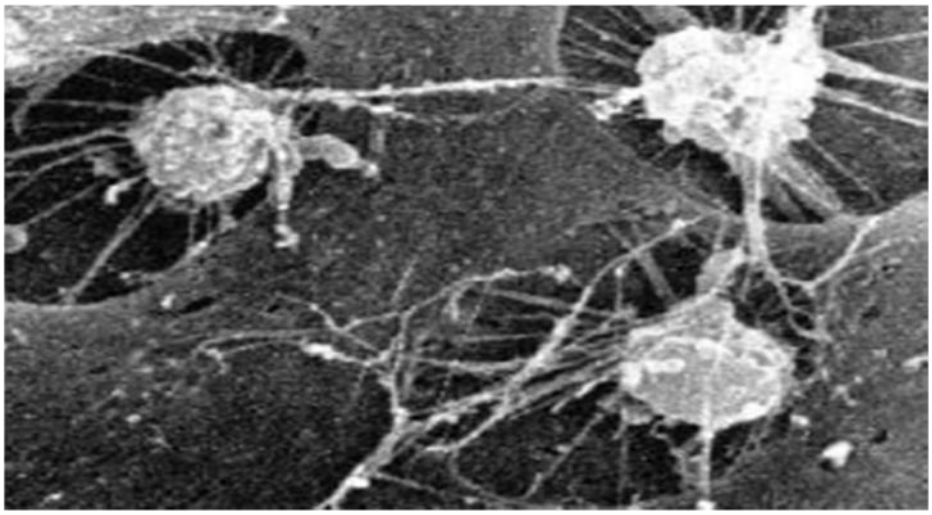

Fig.5. Osteocytes in lacunae. Scanning electron Microscopy (SEM). Magnification 1950x. (Image from laboratory of Preclinical and Surgical Studies-IOR).

1.2.3 Osteoclasts

Osteoclasts (Figure 6) are large (from 20 to 100µm in diameter), highly migratory and multinucleated cells that resorb bone and when active, they rest directly on the bone surface and have two plasma membrane specializations. They are highly polarized cells that occupy the Howship's lacuna.

The main feature of osteoclasts is their ability to resorb fully mineralized bone at Howship's lacunae. Both macrophages and osteoclasts are derived from hematopoietic stem cells (monocyte-macrophage progenitor cell lineage) and, similar to macrophages, they carry an arsenal of

lysosomal enzymes. A resorption bay is formed underneath the cell into which the lytic enzymes are secreted. In addition, proton pumps lower the pH in this subosteoclastic space to values between 2 and 4, activating the secreted enzymes such as tartrate-resistant acid phosphatase. Osteoclasts are transiently active in response to a metabolic demand for the mobilization of calcium from bone into blood. An activated osteoclast, with an average lifespan of 15-20 days, is able to resorb 200,00 μm^3/day, an amount of bone formed by seven to ten generations of osteoblasts (Standring S, 2008).

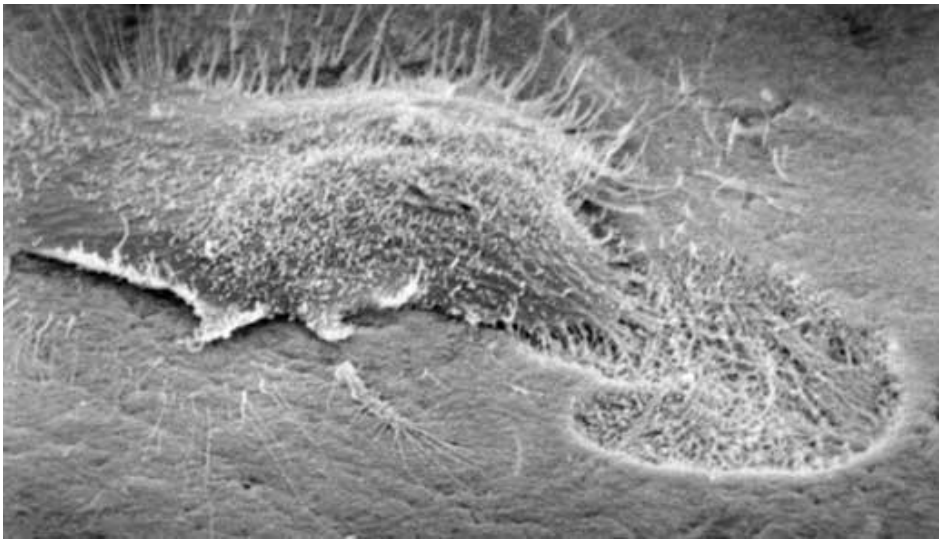

Fig.6. Osteoclast. Scanning electron Microscopy (SEM). Magnification 1950x. (Image from laboratory of Preclinical and Surgical Studies-IOR).

1.2.4 Osteoprogenitor cells

The regenerative potential of our body depends on specialized stem cells, characterized by their functions to differentiate into different cell lineages and to self-renew for the maintenance of the stem cell pool. Since the late 19^{th} century, bone marrow (BM) has been known to host mesenchymal stem cells (MSCs), also called osteoprogenitor cells or bone-lining cells, which are able to differentiate into multiple mesodermal tissues such as bone, cartilage, adipose, muscle, tendon, stroma, and neuronal cells (Figure 7).

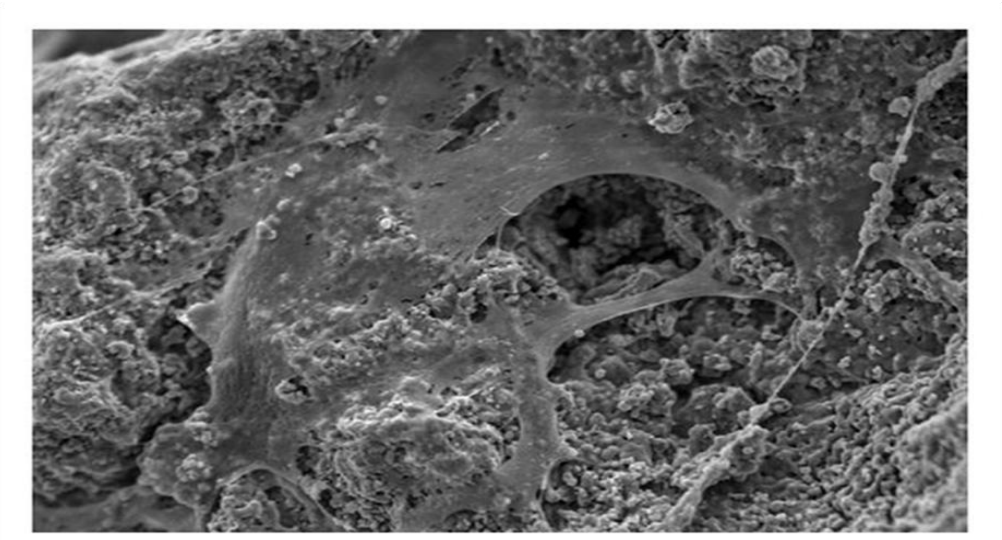

Fig. 7. Osteoprogenitor cells. Scanning electron Microscopy (SEM). Magnification 1950x. (Image from laboratory of Preclinical and Surgical Studies-IOR).

These cells have a direct role in the maintenance of bone balance. They act as a source of progenitors for osteoblasts and moreover, constitutively secrete a distinct set of cytokines, suggesting that they serve specific supportive functions in the microenvironment of BM. MSCs are the cells competent for bone tissue maintenance and regeneration: their self-renewal and differentiating properties in an osteogenic lineage make them very useful tools in tissue engineering and regenerative medicine. Osteoprogenitor cells differentiation toward a specific lineage is dependent on hormonal and local factors, commonly called the microenvironment (e.g., leptin, cell-cell-signaling, extracellular matrix, and cytokines), which can activate specific transcription factors. Although it has been reported their use as a part of bone grafting procedures, that have a clinical potential, many clinical variables (e.g., the anatomic site of BM harvest, recent trauma, local or systemic bone diseases, menopausal status, use of tobacco or pharmaceutical agents, age and gender) might contribute to differences in MSC samples.

Osteoprogenitor cells persist throughout postnatal life as bone-lining cells and they are reactivated in the adult, during the repair of bone fractures and other injuries (Veronesi F, et al., 2011).

1.3 BONE MODELING AND REMODELING

Already in 1892, Wolff found that the orientation of trabeculae coincides with the direction of the stress trajectories. He proposed that bone loading is somehow sensed and that the bone adapts its structure accordingly. This principle of functional adaptation is generally known as "Wolff's Law" (Wolff J, 1892). The ability of bone to adapt to mechanical loads is brought about by continuous bone resorption and bone formation. If these processes occur at different locations, the bone morphology is altered. Frost defined this as modeling (Frost HM, 2001).

In a homeostatic equilibrium, resorption and formation are balanced and, in that case, old bone is continuously replaced by new tissue. This ensures that the mechanical integrity of the bone is maintained but it causes no global changes in morphology. Frost defined this as remodeling (Frost HM, 2001). The modeling and remodeling processes are not very different at the cellular level. They are based on the separate actions of bone resorbing cells (osteoclasts) and bone forming cells (osteoblasts). Approximately 10% of the skeleton is renewed each year by remodeling. This process is necessary to repair skeletal microfractures, to prevent accumulation of older and weaker bone, and to maintain mineral homeostasis (Fini M, et al., 2010).

This process is complex and characterized by the coordinated actions of osteoclasts and osteoblasts, organized in basic multicellular units (BMU) that follow a cycle of resorption, reversal, formation, and resting phases (Figure 8). Remodeling begins with the migration of partially differentiated mononuclear pre-osteoclasts to the bone surface where they form multinucleated

osteoclasts. The signal that initiates the resorption phase is thought to be the mechanical stress that alters local bone architecture and is sensed and transduced by osteocytes. After osteoclastic resorption, which takes about 3 weeks, there is a reversal phase when mononuclear cells on the bone surface provide signals for osteoblast differentiation and migration and this phase lasts up to 4-5 weeks. In the formation phase, osteoblasts lay down bone until the resorbed bone is completely replaced by new bone; this phase may last for about 3 months. Eventually, bone surface is covered with flattened lining cells and a resting period follows. This dynamic process occurs in BMUs at multiple sites simultaneously throughout the skeleton (Gallagher CJ, 2008).

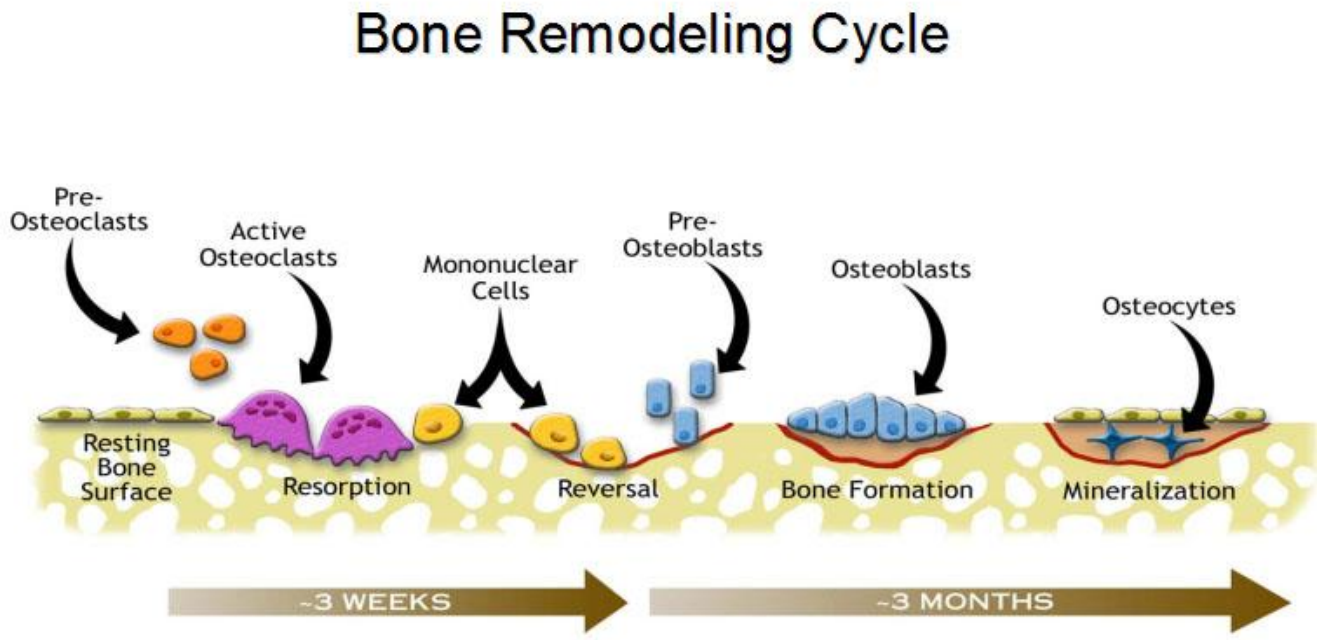

Fig.8. Bone remodeling cycle in healthy conditions. (Image fromhttp://www.ns.umich.edu).

1.4 BONE HEALING

A fracture or a bone defect means that the continuity of a bone is disrupted. During the course of healing, different types of tissues can be seen in a lesion area, whereby one substitutes the other (Figure 9).

The striking feature of bone healing, compared to healing in other tissues, is that repair doesn't create a scar tissue. This is linked to the capacity for remodeling which intact bone possesses.

The healing of bone fracture and defect has traditionally been described in four phases.

1) Haematoma formation (inflammation or granulation) phase

Initially, a hematoma is found between the fragment ends. The hematoma might well act as a guiding structure which, as a spacer, determines the size and shape of the callus.

Activated platelets release a variety of products, including fibronectin, PDGF and TGF-β, which trigger the influx of inflammatory cells. The subsequent cytokine cascade brings the cells of repair (fibroblasts, endothelial cells and osteoblasts) into the fracture gap.

2) Soft callus formation (proliferative) phase.

This is characterised by the formation of connective tissues, including cartilage, and formation of new capillaries from pre-existing vessels (angiogenesis). In detail, during the first few days the hematoma changes to become granulation tissue. Capillary sprouts, mononuclear cells, fibroblasts, and fibrocytes are present. During the process of healing, a maturation of this granulation tissue is observed and it is transformed into connective tissue with its collagen fibers. This maturation results in an increase in stiffness.

3) Hard callus formation (maturing or modeling) phase.

This phase leads to woven bone, either directly from mesenchymal tissue (intramembranous) or via an intermediate stage of cartilage (endochondral or chondroid routes). Osteoblasts can form

woven bone rapidly, but it is randomly arranged and mechanically weak. During this step, in both fibrous tissue and fibrocartilage, mineralization occurs.

4) Remodeling phase.

Woven bone is remodeled into stronger lamellar bone by the orchestrated action of osteoclast bone resorption and osteoblast bone formation. In this phase the mineralization is followed by local resorption of the mineralized cartilage, whereby new vessels enter the fracture area. The walls of the resorption spaces are then covered with lamellar bone, thus forming new bone trabeculae. A further bone deposition, combined with local resorption, leads to a reshaping of those trabeculae (Marsh DR and Li G, 1999).

Thus, a gradual increase in strength and stiffness occurs, along with a reduction of the ability to elongate (Dimitriou R, et al., 2005; Gerstenfeld LC, et al., 2003).

In terms of extracellular matrix formation, type III collagen predominates at the inflammatory stage, followed by type II collagen in the cartilaginous phase and type I collagen production at the ossification and remodeling stages.

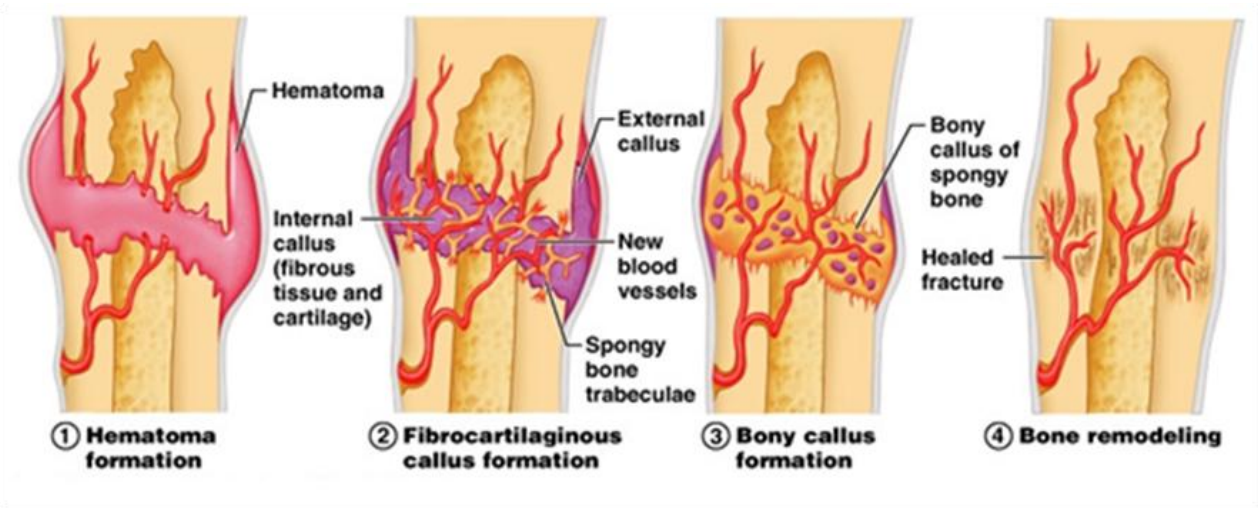

Fig.9. Steps of the bone healing process. (Image from http://apbrwww5.apsu.edu).

Bone regeneration is a highly efficient and tightly regulated process that involves all the above-mentioned components of bone tissue. Bone regeneration is the result of a continuous interplay between GFs and cytokines for both initiation and regulation of the remodeling process. The majority of fractures heals well under standard conservative or surgical therapy. However, extended bone defects, following trauma or cancer resection or non-unions of fractures, may require more sophisticated treatments. In these cases bone grafting procedures, segmental bone transport, distraction osteogenesis or biomaterials are applied for reconstruction (Kneser U, et al., 2006).

1.4.1 Bone healing complications

Bone tissue, usually, has the ability to repair itself, but when complicated fractures and large bone defects have to be bridged, the healing process fails in many cases. Despite the advent of modern techniques, individual fractures occasionally refuse to heal and a non-union or pseudoarthrosis can occur. Insufficient blood supply and infections of the callus or the surrounding tissue or even systemic diseases can have further negative effects on bone regeneration, resulting in the formation of a non-union (Janicki P and Schmidmaier G, 2011).

The healing process may be classified into 4 separate entities: union, malunion, non-union, and pseudoarthrosis. Union is used to described a fracture that has united; in malunion the fracture has united but the union is incorrectly aligned; non-union occurs when the apposed ends of the fracture have failed to unite and to ossify. The amount of healing, that has occurred, may vary from a cartilaginous bridge, which has failed to ossify, to fibrous-connective tissue, or to an absolute lack of bridging. Non-unions can also occur after the bone resection caused by cysts, benignant and malignant tumors and by congenital malformations and osteomyelitis (Sumner-

Smith G, 2002). Pseudoarthrosis indicates a true false-joint formation when bone needs are joined by a fibrous joint-capsule-like structure, which contains synovial-like fluid originating from local serum production.

Nearly 5-10% of all fractures is associated with impaired healing, resulting in delayed union or non-union.

Bone defects are very challenging in orthopaedic practice; they can result from a high-energy traumatic event, from large bone resection for different pathologies such as tumor or infection, or from the treatment of complex non-unions (en-bloc resection). They can be considered critical in relation to the skeletal segment involved and the length of bone loss: 3 cm for the forearm, 5 cm in the femur and tibia, 6 cm in the humerus (Janicki P and Schmidmaier G, 2011).

The main clinical pathologies that could require a graft or a biomaterial implantation are, as well as the above mentioned non-unions and pseudoarthrosis, the bone fractures with loss of substance. For these defects, there is a constant demand for substitutes which can effectively bridge long segmental defect or fill loss of substances with minimal morbidity and accelerating healing times. Tissue regeneration has become a great challenge for many illness, traumatic lesions or reconstructive needs (Fini M, et al., 2005).

The amount of repair, however, depends on the size of the bone defect, the lesion site and the patient's health status, the age and lifestyle. For critical size defects (would not fully heal spontaneously) and for the above mentioned defects, or even to accelerate or geode the repair process, the use of bioactive scaffolding materials could be of great advantage. The use of bone-filling materials with the properties of adsorption, osteopromotion, safety and ease of sterilizing, manufacture and surgical use may improve the healing rate, making the difference between success and failure (Yamada Y, et al., 2003).

Nevertheless, it is still a great challenge in reconstructive surgery to treat large bone defects or non-unions. The therapy concept, based on bone substitutes, includes the possibility to rebuild bone lacking structure and to allow migration, proliferation and differentiation of bone cells and to promote vascularisation (Nandi SK, et al., 2010).

Approximately 2.2 million bone graft procedures are performed each year worldwide to repair bone defects in orthopaedics, neurosurgery and oral and maxillofacial surgery with a yearly estimated costs of $ 2.5 billion.

2. BONE GRAFTS

A tissue graft is a medical procedure in which tissue from a donor is used to replace missing or damaged tissue on a patient. Numerous types of human tissue can be used including veins, skin, tendons, bone, and ocular materials. In general, tissue grafting can be divided into 3 major categories according to the genetic relationship between the donor and the recipient. They are a) **autogenous** tissue graft (**autograft**): a tissue graft from one site to another within the same individual; b) **allogenous** tissue graft (**allograft**): a tissue graft between individuals of the same species; d) **xenogenous** tissue graft (**xenograft**): donor and recipient are individuals from different species (Delloye C, et al., 2003).

In orthopaedic field, regarding bone healing, bone grafts can be osteogenic, osteoinductive and osteoconductive.

A graft that supplies and supports bone forming cells is termed osteogenic.

Osteoinductive agents (proteins) induce proliferation or differentiation of undifferentiated stem cells to osteogenic cells. A graft that has the capacity to induce bone formation when placed into a site where no bone formation will occur is termed osteoinductive. Osteoconduction is the process whereby scaffolding is provided for inward migration of cellular elements involved in bone formation (mesenchymal cells, osteoblasts, osteoclasts and vasculature) (Kneser U, et al., 2006).

Autogenous bone graft is the transplantation of bone taken from one anatomic site to another site in the same individual. It is defined as the 'gold standard' for regeneration, is a safe solution for compatibility and the absence of immune response, and it is considered to be the most suitable material, because the graft has osteogenic (marrow-derived osteoblastic cells as well as preosteoblastic precursor cells), osteoinductive (noncollagenous bone matrix proteins, including GFs) and osteoconductive properties (bone mineral and collagen) (Kneser U, et al., 2006).

Moreover, the differences in histocompatibility and the risk of transferring a disease are not existent. On the other hand, the autograft drawbacks include: an insufficient amount of graft material necessary to replace the missing portion, particularly in children or in bone loss due to tumors; a significant postsurgical morbidity at the donor site; increased surgical time and blood loss and an additional cost due to a possible prolongation of the hospitalization. The different types of autogenous bone grafts are represented by autologous cancellous bone, autologous cortical bone and vascularized autografts. Autologous cancellous bone plays a dominant role in bone-transplant surgery because osteogenic stem cells can survive in an autogenic spongiosa and it has a clinical success in the treatment of a wide range of diseases, such as delayed fracture healing, pseudoarthrosis, bone defects and infections. It has a robust biological activity in inducing and producing new bone (Sen MK and Miclau T, 2007). It has been considered more osteogenic as compared to cortical bone graft because the presence of spaces within its structure, allowing the diffusion of nutrients and limited revascularization, but it does not provide substantial structural support. The principle advantage of autologous cancellous grafts is the potential to transfer osteoprogenitor cells combined with matrix and signals, provided by the cancellous particles, yielding a mixture that contains other factors of bone regenerative strategy.

Another example of an osteogenic material is bone marrow. Bone marrow aspirates contain MSC, cells already committed to osteogenic or chondrogenic lineage, and some biologically active proteins that stimulate bone regeneration in similar manner to naturally occurring fracture clot, many from platelet degranulation. However, use of bone marrow does not yield the magnitude of osteogenesis observed with cancellous bone for several reasons. Aspiration results in varying quality of bone marrow depending on technique and patient. Osteoprogenitor cell content can be

low and most importantly, bone marrow lacks the necessary scaffold or osteoconductive material to be efficacious on its own (Kolk A, et al., 2012).

Autologous cortical bone graft has little or no osteoinductive properties, is mostly osteoconductive, and the surviving osteoblasts provide some osteogenic properties as well. It is much less important, for bone regeneration, than cancellous bone due to its poor vascularity and its low content of osteogenic stem cells. Thus, the only role for free cortical autografts in bone regeneration is the temporary increase in mechanical stability (Beaman FD, et al., 2006). Autologous cortical bone grafts are good choices for segmental defects of bone of 5 to 6 cm, which require immediate structural support.

Vascularized cortical autograft heals rapidly at the host-graft-interface, and its remodeling is similar to that of normal bone. It improves osteocyte survival and enhances bony incorporation. It appears to demonstrate less bony necrosis with no subsequent trabecular collapse and no architectural disorganization, when compared with the non-vascularized grafts (Kawamura K, et al., 2008).

The limitation associated with the procurement of autograft for bone grafting and the development of modern tissue banks have resulted in a supply of high-quality allogenic tissue for reconstructive orthopaedic surgery. **Allograft** overcomes the limitations associated with the procurement of autografts for bone grafting. It may be derived from cadaveric bone sources or from living donors harvested during hip arthroplasty, and has both osteoinductive (they release bone morphogenic proteins that act on bone cells) and osteoconductive properties, but it lacks osteogenic properties because of the absence of viable cells. Beside limitations in the essential bone graft characteristics, there is an ongoing controversial discussion about the association of allogenic material with a risk of transmission of infectious agents such as the human

immunodeficiency virus (HIV), hepatitis B and C viral infection (HBV/HCV), malignancies, systemic disorders (autoimmune disease), or toxins. Removal of osteoarthritic femoral heads throughout hip arthroplasty shows an 8% evidence of diseases not previously known. Elimination of this major concern of allogenic material requires tissue-processing, sterilization and a deactivation process of proteins in the extracellular matrix which contains bone growth factors, proteins, and other bioactive substances necessary for osteoinduction and, ultimately, successful bone healing. Although the risk of transmission of disease is much lower than with blood products, it is still possible. The more aggressive the allograft processing, the less intense immunologic responses will occur, but this results in a decrease of the osteoinductive properties. For this reason fresh allografts are clinically no longer used. Frozen allografts induce stronger immune responses than freeze-dried allografts (Habibovic P and de Groot K, 2007).

Compared with autologous cancellous bone, allograft cancellous bone is a poor promoter of bone healing. Allogenic cortical bone incorporation occurs by sporadic formation of new appositional bone and the lack of vascularization leads to weakness of the graft. It is used in replacing segments of bone after tumor excision, in lengthening bones and in treating selected non-unions.

Massive osteochondral allografts (diaphyseal cortical bone, metaphyseal cancellous bone and articular cartilage) are used in joint reconstruction after limb salvage procedures for tumor resection and in traumatic bone loss. Some complications are represented by allograft fracture, articular cartilage degeneration, osteoarthritis, deep infections and non-unions.

Xenograft is a tissue graft between two different species and despite its wide availability, the untreated xenogenic bone is an unsuitable transplant material because it provokes a strong immunodefensive reactions. Porous natural hydroxyapatite (HA) can be obtained from animal bones or seaweeds. Xenogenic HA is the preferred biological material because of its stability

concerning absorption (i.e. dependent on the porosity value, crystallinity, crystal structure, etc.) (Kolk A, et al., 2012).

In the last few years, Demineralized Bone Matrix (DBM) has attracted attention as bone graft.

DBM consists of sponge-like collagen from human, bovine or equine origin that has undergone decalcification and sterilization, so it can be classified as allogenic or xenogenic material dependent on the origin. The trabecular structure of the original tissue remains, therefore maintaining its biological structure. DBM has been shown to have osteoconductive and osteoinductive properties, but it provides no structural stability and therefore should only be applied in a structurally stable environment (Naujoks C, et al., 2011).

It is mainly used as a ‘‘bone graft extender’’, revascularizes quickly and acts as suitable carrier for autologous bone marrow, it does not evoke any appreciable local foreign body reaction as the antigenic surface structure of the bone is destroyed during demineralization. More growth factors are available after the removal of bone minerals, so the bone inductance of DBM is higher than that associated with mineralized allogenic transplants. DBM is a derivative of allograft bone and it could be prepared by pulverization of allogenic bone to a consistent size, followed by mild acid extraction of the mineralized phase of bone. This process, principally developed by Urist et al in 1965, results in a composite of non-collagenous proteins, growth factors, and collagen (Urist MR and Dawson E, 1981).

Nowadays, bone graft materials with completely different origins are commercially available for many applications throughout the human body. They are variable in their composition, their mechanism of action and, therefore, their indications. In conclusion, problems related to the availability of graft material, donor-site morbidity, immunogenicity and biomechanical integrity represent some limitations of bone grafts and clinical success.

Bone substitute materials are generally considered to be a highly important alternative to bone grafting.

Due to the numerous disadvantages present in all kinds of grafts, there is a rationale for the designing and developing of artificial supports (scaffolds) for tissue engineering applications and their demand is growing steadily. The alternative to tissue grafting is the use of artificial designed scaffolds or implants, fabricated using various materials (biomaterials). Nowadays, materials, including metals, polymers, ceramics and composites, are used clinically for implants and medical devices in many medical areas (Yan Y et al., 2009).

3. BIOMATERIALS

The term “Biomaterial” can be defined as “a material intended to interface with biological systems to evaluate, treat, augment or replace any tissue, organ or function of the body”. This is still a good conceptual definition, but should be modified to take into account the extended applications of biomaterials. Moreover, the variety and complexity of these applications is such that a classification of biomaterials might be considered. A slightly modified definition of biomaterial is proposed as follows: “ a material intended to interface with biological systems as an integral part of a process designed to evaluate, monitor or treat tissues of the body, to replace or augment tissues or to facilitate the regeneration of tissues” (ESB satellite Consensus Conference, Sorrento, September 2005).

Current requirements for an ideal biomaterial as bone substitute are rigorous as listed below:

- Resorbability/degradability and sterility
- Biocompatibility
- Osteoinduction, osteoconduction, osseointegration

Resorption of the material and replacement by normal bone are either biologically based on the influence of cells or by chemical-physical dissolving processes, and should occur simultaneously in the ideal case. The biomaterial should be easy to use, should withstand sterilization and should come in sufficient quantities. In a time of global economic downturns, costs are an important issue in clinical applications (Kao ST and Scott DD, 2007).

3.1 BIOCOMPATIBILITY

Biocompatibility ensures the absence of toxicity, teratogenicity or carcinogenicity. The lack of antigenicity guarantees the avoidance of pro-inflammatory and immunogenic reactions. All such requirements serve as a basis for effective long-term tolerance and such criteria are mainly fulfilled by available synthetic materials (Williams DF, 2008).

Biocompatibility is a fundamental requirement of biomaterials and is defined as “the ability of a material to perform with an appropriate host response in a specific application” (Williams DF, 1987). It is the essential requisite for the employment of a material in the biomedical field, is strictly related to the specific application and location of the biomedical device and can be defined as its substantial property of not alter the physiologic environment and not cause pathological outcomes. Since at the present time no absolutely inert materials exist, so it is probably more correct to describe biocompatibility as biotolerability. In 1995 Wintermantel and Mayer modified the definition of biocompatibility into surface and structural compatibility of implants, involving appropriate chemical, biological and physical characteristics, including surface morphology (for cell anchorage and guidance) (Wintermantel E and Mayer J, 1995).

The assessment of biocompatibility is a mandatory prerequisite for all materials and devices before their clinical application. The evaluation of the biocompatibility of a material, assigned to clinical use, is a long trial that requires a well planned sequence of steps. The assessment of biocompatibility of a particular biomaterial entails the consecutive execution of well accepted scientific evaluations. Considered together, the results of these evaluations help to provide an objective picture of the associated composite biocompatibility and in general, the sequence of evaluations increases in complexity and scope over time, from basic *in vitro* cell culture

cytotoxicity evaluation to *in vivo* large animal anatomically relevant evaluations of biocompatibility and biofunctionality.

These procedures are now standardized at an international level, in particular in the European Community, the rules of EN ISO 10993 provide the guide-lines for each investigation in this field. The International Organization for Standardization (ISO) is a worldwide federation of national standards bodies for the biological evaluation of medical devices. ISO 10993 refers to the fundamental principles governing the biological evaluation of medical devices, the definition of categories of devices based on the nature and duration of the contact with the body, and the selection of appropriate tests to be performed. Biocompatibility tests must be performed on the final product or material, taking into account the type, duration and conditions of the exposure in the human body, the physical and chemical features of the product, the toxicological activity of the chemical elements or compounds and the presence of leachable materials. It is not required that a material or device will be submitted to all the tests, but only to those related to the specific contact with the body environment (Gatti AM and Knowles JC, 2002).

The capability of a biomaterial to perform a specific function cannot be evaluated by single *in vitro* or single *in vivo* methodology. *In vitro* methods provide necessary and useful results that precede and complete the *in vivo* testing. *In vitro* tests decrease the number of animals required for *in vivo* biocompatibility evaluation, while *in vivo* evaluations allow long-term investigations, by reproducing the complex biological environment and are suitable for the evaluation of biofunctionality.

A research project that adopts only an *in vitro* or an *in vivo* method is considered limited and a study conducted only *in vitro* is acceptable as a first step and becomes ethically unacceptable if

performed only *in vivo* with no preliminary *in vitro* information on the biomaterial biocompatibility (Fini M and Giardino R, 2003).

In vitro cell cultures. The *in vitro* evaluation provides the initial biocompatibility screening and it is represented by target cell assays, making use of the most sensitive cells pertinent to the application for which the biomaterial is developed. Table.2 shows the benefits and limits of *in vitro* studies and some relevant negative aspects of the *in vitro* screening are represented by the minimization of the variables of metabolism, distribution, and adsorption, and the maximization of the cell line exposure to any potential toxicity. Moreover, there is difficulty to extrapolate the results to the clinical population. Consequently, an *in vivo* evaluation must be conducted.

The impossibility of predicting, *in vitro*, the effect of biological fluids on biomaterials, which is responsible for the side-effects, as well as long-term prosthetic device behaviour, represents a real drawback of cell culture systems. On the other hand *in vitro* tests provide detailed information on particulate debris toxicity when identified.

Osteosarcoma and immortalized cell lines are used, as well as primary cells from several species and anatomical locations. If human-derived primary cells are employed, they usually come from the surgical residues obtained during surgery (i.e. bone fragments unusable for tissue banking). Human osteosarcoma cell lines show the absence of individual variability observed when primary lines are used, as well as better repeatability and reproducibility.

In vitro test sensitivity, in discriminating between safe and toxic biomaterials, is of great importance in rejecting inappropriate materials prior to the *in vivo* implantation. It is recognized that *in vitro* tests can be limited due to their relative simplicity when compared to the complex interactions occurring in an organism *in toto*, because of the lack of systemic and local factors due to the complexity of cell and tissue response (Negrou G, et al., 2008).

In vivo animal models. Animal models provide important biomaterial knowledge that leads to the development of more effective clinical treatments of diseases in both humans and animals, acting as a bridge between *in vitro* studies and clinical trials. Depending on the purpose of the study, biomaterials are usually implanted in the diaphyseal (cortical bone and medullar cavity), metaphyseal or epiphyseal part of long bones (cancellous bone). Common bone implant tests are histologic, histomorphometric and biomechanical investigations that can provide a complete characterization of the osteogenic and osteointegration properties of the material. Performing *in vivo* studies requires, first of all, compliance to ethical and legal rules on animal experimentation. Every Country has its own regulations, but a regional local ethical committee exists to approve every research protocol. Biomedical research, using animals, is regulated worldwide by precise rules. In the United States, the Animal Welfare Act dated from 1966 and this was followed in 1986 by the Public Health Service Policy on Care and Use of Laboratory Animals. All of these documents contain guidelines about the animal environmental, housing and management as well as veterinary care. In the European Union, the Directive 86/609_Protection of Experimental Animals gives, to the state members of the European Community, indications to be applied in the regulation of animal research. According to this directive, the Italian Government, with the Law by decree number 116 of January 27,1992 on the protection of animals used for scientific purpose, settles the guidelines for this matter. Considering the biological evaluation of medical devices, part 2 of ISO 10993 "Animal Welfare Requirements" contains the directives to be followed when animal tests are to be performed (Andersson M, et al., 2007; Andersson M, et al., 2008).

The tests are justified only when the resulting data are not otherwise available and essential for the material characterization, when no other scientifically validated method not involving animals is available, and when strategies to minimize pain, suffering, distress and lasting harm have been

identified and implemented. Animal tests must be carried out in authorized laboratories, with appropriate facilities for animal stabling and welfare and must not be conducted before appropriate preliminary *in vitro* tests have been carried out with favorable results. Surgical procedures must be performed in general anaesthesia and in well equipped operatory rooms, under the control and responsibility of well trained scientists. *In vivo* tests for biocompatibility may use the biomaterials themselves or may utilize extracts of them to determine the toxicity and bioactivity of potential leachable, dissolution products, or other materials utilized in the synthesis and production of the biomaterial. Important limits of an *in vivo* study (Table 2) include the presence of differences that are so great between humans and animals, data on animal bone remodeling and formation that cannot be representative of bone healing in humans, the need for appropriate facilities and complex professional expertise, prolonged time and high costs (Buma P, et al., 2004).

Tab.2. Benefits and limits of *in vitro* and *in vivo* studies.

	BENEFITS	**LIMITS**
***IN VITRO* STUDIES**	High sensitivity; Standard experimental conditions; Human cells and tissues; No ethical drawbacks; Easy to perform, manage, interpret; Fast and inexpensive screening; Reduction of animal use and suffering.	Specific sensitivity; Deposition of metabolic and toxic products (in static cultures); Partial information on biofunctionality and mechanical osteointegration; Lack of systemic factors; Difficulty in long-term studies.
***IN VIVO* STUDIES**	Long-term investigations; Biofunctionality and effectiveness of the final prosthetic device; Presence of systemic factors; Biological environment.	Ethical drawbacks; Legal authorization requirements; Appropriate facilities; Complex professional expertise; Prolonged time, high costs; Differences between humans and animals.

3.2 OSTEOINDUCTION, OSTEOCONDUCTION AND OSSEOINTEGRATION

Osteoinduction is the ability to actively stimulate or promote bone formation. Osteoinductive biomaterials provide a biological stimulus for induction, recruitment, stimulation and differentiation of primitive, undifferentiated and pluripotent stromal cells into osteoblasts or preosteoblasts, the initial cellular phase of a bone-forming lineage (Calori GM, et al., 2011).

Osteoconduction is defined as the process of bony ingrowth from local osseous tissue onto surfaces. Osteoconductivity is a property of the biomaterial that allows the colonization and ingrowth of new bone cells and sprouting capillaries due to its three-dimensional structure. The original definition is not strictly restricted to biomaterials, however, the contemporary concept of an osteoconductive material is one where bone formation is promoted to appose and conform to its surface, when the material is placed into bone, by virtue of its composition, shape or surface texture. Osteoconduction is mainly determined by the porosity properties of the biomaterials and also, in a lesser extent, by the chemical and physical properties of the substrate that promote cell adhesion and growth. Osteoconductivity is, by definition, a passive process (LeGeros RZ, 2002).

For some biomaterials and dependent on implantation site, **osseointegration** is the process of achieving stable direct anchorage and contact between bone and biomaterials and it was firstly described by Branemark in 1977 and defined by Albrektsson in 1981 (Branemark PI, et al., 1977; Albrektsson T, et al., 1981). At an histological level it is defined as the direct anchorage of a biomaterial by formation of bony tissue around the implant without the growth of fibrous tissue at the bone-implant interface. A biomechanical definition has also evolved stating that osseointegration is “a process whereby clinically asymptomatic rigid fixation of alloplastic materials is achieved and maintained, in bone, during functional loading” (Zarb G and Albrektsson T, 1991).

Osteoinduction, osteoconduction and osseointegration are powerful inter-related phenomena in bone regeneration and intrinsically related to bone morphogenetic proteins, bone growth factors and direct bone anchorage factors, respectively.

To date, no bone substitute biomaterial is available that is equal to autogenous bone, and current biomaterials serve primarily as filling and frame building materials, mostly providing osteoconductivity for the bone healing process.

Ideally, the healing process of the bone defects should result in regenerated and vital bone, without foreign bodies (Horch HH, et al., 2006).

To reach this aim, **tissue engineering** applications are developed.

4. TISSUE ENGINEERING

During the 1st Tissue Engineering Symposium (California 1988), tissue engineering was defined, for the first time, as "application of the principles and methods of engineering and life sciences towards the fundamental and pathological mammalian tissues and the development of biological substitutes that restore, maintain or improve tissue function"(Fox CF and Skalak R, 1988). It was considered the point that best marked the transition to a new era of research. This large area confronts and engages different sciences such as engineering, chemistry, physics, biology, biotechnology and medicine in a multi-disciplinary approach for the development of functional tissues and organs *in vitro*, for their implantation *in vivo* or for direct remodeling and regeneration of tissue *in vivo* to repair, replace, preserve or enhance tissue or organ functions lost due to disease, injury or aging (Ingber DE, et.al,2006).

The new therapeutic strategy consists in the use of tissue-engineered living cells (and / or their products) and innovative supports, to develop bioactive tissue substitutes as an alternative to inert systems and it is clear that the complexity of biological tissues in terms of macromolecular composition, organization and ultrastructural interactions between cells and the environment, makes it difficult the passage of engineered constructs from the experimental field to the clinic. Tissue engineering offers the potential to eliminate re-operation and to solve implant rejection, transmission of diseases and shortage in organ donations by using biological substitutes, providing long term solutions in tissue repair or treatment of diseases, and offering treatments for medical conditions that are untreatable (McIntire LV, 2003). So, aided by advances in biological and medical sciences, materials science and engineering, tissue engineering has triumphed in recent decades by providing various implant biomaterials for human tissue repair for millions of patients all over the world. The design and fabrication of **scaffolds**, with required properties, are key

components for tissue engineering. Tissue engineering typically uses artificial extracellular matrix, named scaffolds, to engineer new tissues. Scaffolds are tissue engineered product biomaterials defined as degradable materials used, through implantation or injection, in a host for the purpose of stimulating tissue engineering or cell therapy process. A porous structure, usually polymeric, serves as substrate and guide for tissue regeneration. Usually the terms scaffold and matrix are used interchangeably in this aspect (ESB satellite Consensus Conference, Sorrento, September 2005).

Tissue engineering proposes different alternative routes for all tissue repair and the bone scaffold based most important methodologies are the ***in vitro*** **tissue engineering** and the **in situ tissue regeneration**.

The first involves the preparation of an *in vitro* engineered tissue, where autologous osteoprogenitor cells and signaling molecules are *ex vivo* seeded and differentiated onto a scaffold; engineered constructs as well, once re-implanted into the patient, should be gradually resorbed and replaced by viable tissue with vascular and nervous contribution (Figure 10). In this way the tissue is regenerated outside the human body (Thompson MS , et al., 2010).

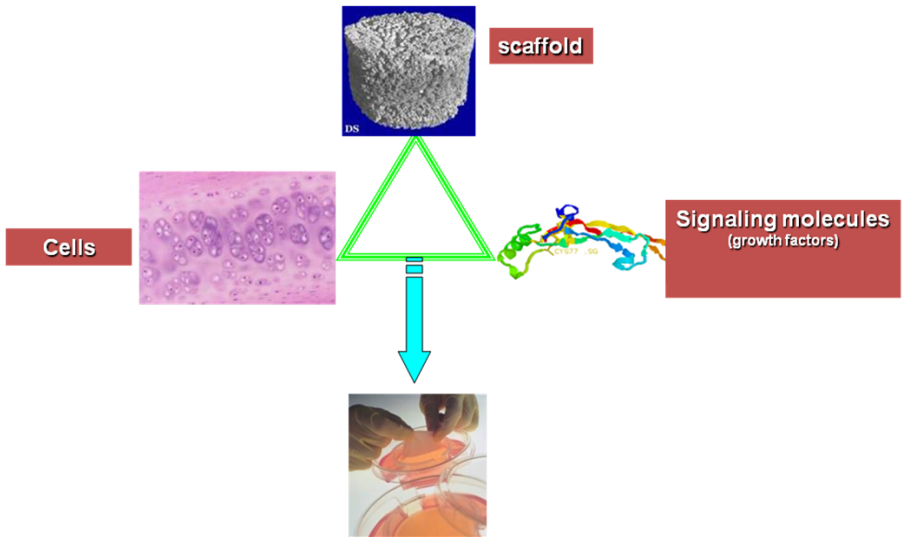

Fig.10. *In vitro* tissue engineering with the use of scaffolds, autologous cells and signaling molecules.

The advantage of this methodology is the transplantation of a prefabricated functional tissue that releases cells and osteogenic factors, is incorporated and revascularized in the host body and starts the remodeling process. The disadvantages are represented by the law requirements, high costs and times of the different techniques for the fabrication of these constructs.

The second approach (Figure 11), also called *in vivo* regeneration, is characterized by the *in vivo* implant of biological factors or scaffolds (with or without signaling molecules) in order to stimulate tissue regeneration. It is characterized by an acellular scaffold implantation, that stimulates the extracellular matrix and recruits or maintains, in the lesion site, cells and biological factors also from other body seats (Wan AC and Ying JY, 2010).

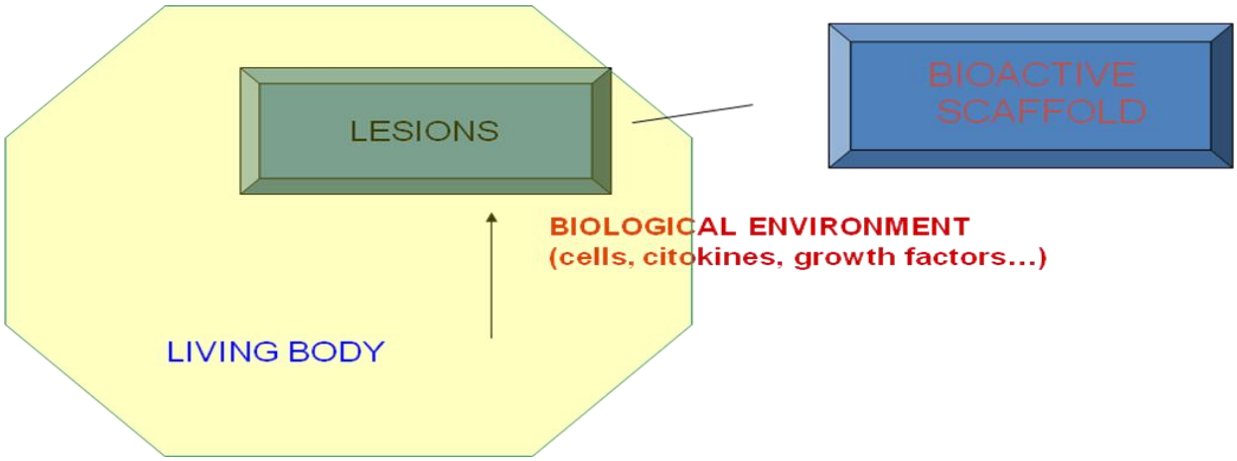

Fig.11. In situ tissue regeneration is modeled as if it takes place inside a bioreactor which is surrounded by a reservoir. Exudate, that contains cells, cytokines and several other substances but not matrix components, flows continuously from the reservoir to the bioreactor. In in situ tissue regeneration the bioreactor is the living body and the reservoir the biological environment typical of a wound healing.

In situ tissue engineering requires the use of bioactive scaffolds.

Bioactivity is a very widely used term. The definition, agreed at the second ESB Consensus Conference, Sorrento 2005, is as follows: “Phenomenon by which a biomaterial elicits or modulates biological activity”. However, there could be some forms of classification of bioactivity that reflect the nature of the modulation of biological activity. *In vitro* bone bioactivity is the up-regulation of calcium phosphate deposition on a scaffold surface. *In vivo* bone bioactivity is the up-regulation of the process of bone formation on the surface of a scaffold (ESB Consensus Conference, Sorrento 2005).

Bioactivity is a phenomenon through which, a scaffold stimulates or modulates a biological response and creates an interaction between scaffold and living body through the activation of a specific physiological process (Ohtsuki C, et al., 2009).

4.1 SCAFFOLDS

Currently, scaffolds can be divided into two categories: **natural and synthetic**.

Natural materials. Natural polymer-based materials consist of structural and functional proteins (such as collagens), proteoglycans, glycoproteins, and glycosaminoglycans found in a natural tissue, and they have been implanted for constructive remodeling of many tissues in preclinical and human clinical trials (Table 3). They are formed in nature during the growth cycles of all organisms, hence they are also referred to as biopolymers. Advantages of biopolymers over synthetics are their excellent physiological activities such as a selective adhesion and a similar mechanical properties to natural tissues, moreover, they have excellent biological properties, including cell adhesion, biodegradability and biocompatibility. The natural polymers mimic the decellularized native extracellular matrix down to the molecular level because many of them

possess the property of self-assembly, and are better materials for the biological system to recognize. They are degraded into noninflammatory products (a significant advantage over their synthetic counterparts), but their exact composition is often difficult to ascertain and reproduce and may be immunogenic because they carry a risk of microbiological contamination. Their relatively poor mechanical properties, undefined rate of degradation and propensity to induce an inflammatory response limit their range of applications (Fini M, 2005).

Tab.3. Natural materials. Biocompatibility, disadvantages and applications.

POLYMERS	BIOCOMPATIBILITY	DISADVANTAGES	APPLICATIONS
Collagen	Minimal cytotoxicity, Mild foreign body reaction, Minimal inflammation	Proteolytic removal of small nonhelical telopepties	Skin; cartilage; **bone**; ligament; tendons; vessels; nerves; bladder; liver
Hyaluronic acid	Mild foreign body reaction, No inflammation	Highly viscous solution, Many purification steps after chemical modification	Skin; cartilage; **bone**; ligament; vessels; nerves; liver
Alginic acid	Minimal foreign body reaction, No inflammation	Uncontrollable dissolution of hydrogel	Skin; cartilage; **bone**; nerves; muscle; pancreas
Chitosan	Minimal foreign body reaction, No inflammation	Uncontrollable deacetylation and molecular weight	Skin; cartilage; **bone**; nerves; vessels; liver; pancreas
Gelatin	Minimal cytotoxicity, Mild foreign body reaction, Minimal inflammation	Weak mechanical property	Skin; cartilage; **bone**; ligaments; breast
Fibrin	Minimal cytotoxicity, Mild foreign body reaction, Minimal inflammation	Weak mechanical property	Skin; **bone**; cartilage; liver; tendons; ligament; vessels
Poly(hydroxyalkanoate)	Minimal cytotoxicity, Mild foreign body reaction, Minimal inflammation	Pyrogen removed	Skin; **bone**; tendons; cartilage; nerves; ligaments; heart; vessels; muscle
Silk	Minimal cytotoxicity, Mild foreign body reaction, Minimal inflammation	Inflammation of sericin	Skin; ligaments; **bone**; cartilage; tympanic membrane; vessels; tendons

Collagen based scaffolds have been used for bone tissue engineering, in fact, type I collagen is a major component of bone and leads to new bone from stem/progenitor cells via the developmental cascade. Therefore, type I collagen might be a good candidate material for a biomimetic approach to design artificial scaffolds for bone tissue engineering (Kim BS, et al., 2011). Another example of natural-based scaffolds is represented by the silk fibroin hydrogel that, in a Fini M et al. study, was comparatively investigated in terms of osteoblast function and healing of confined critical size cancellous bone defects. *In vitro* results on osteoblasts, showed the absence of inflammatory effects and a stimulation of TGF-β1 production. *In vivo*, it permitted the healing of critical size defects in the trabecular bone and silk fibroin hydrogel improved bone remodeling and maturation greatly. Therefore, it is considered potentially useful as bone replacement material in reconstructive orthopaedic surgery, being a readily available injectable biomaterial able to improve bone healing and maturation (Fini M, et al., 2005).

Synthetic materials. These materials are attractive because they can be fabricated into various shapes and phases with desired pore morphologic features for tissue in-growth, and have the ability to tailor mechanical properties and degradation kinetics to suit various applications in repair and reconstruction of diseased and damaged parts of the human body. In orthopaedic, they provide mechanical support during tissue growth, can incorporate cells and growth factors and provide osteoconductive environments.

The synthetic materials are usually classified in non-polymeric (metals and ceramics), polymeric and composites materials and are spreadly used in many human districts (Gunatillake PA and Adhikari R, 2003).

Non-polymeric materials, including metallic and ceramic materials, have been used for bone tissue engineering. Metals are used in implant fabrication mainly because of their excellent mechanical

properties and the extensive knowledge-base of mankind with regard to their processing, properties and structures. They generally possess higher strength, ductility and water resistance, and they are used as passive substitutes and as supports for hard tissue repair or replacement in load-bearing applications such as total hip and knee joint replacements, for fracture healing aids such as bone plates, screws and wires, spinal fixation devices and for dental implants. Stainless steel and titanium or titanium alloys are the materials that usually comprise the basis of metal implants for bone regeneration (Wang W, et al., 2011). Generally, the mechanical properties of metallic materials are superior to those of polymeric ones. However, there are several disadvantages, such as the lack of tissue adherence, low rate of degradation, toxicity due to accumulation of metal ions due to corrosion, and mismatch of Young's modulus between metallic materials and bone.

The thermal and chemical stability of ceramics, high strength, wear resistance and durability, all contribute to make ceramics good candidate scaffolds for surgical implants. Bioceramics, especially calcium phosphates and HA, are preferred materials as bone grafts because of their excellent chemical stability, low density and compositional similarities with bone mineral phase. High strength bioceramics, such as aluminia and zirconia are also used for load-bearing applications, but like metals, these ceramics are "bioinert" and could form non-adherent fibrous capsule *in vivo*, leading to loosening of implants. Bioactive ceramics (such as HA) interact with the surrounding tissues and form strong interfacial bonds. They are composed of ions commonly found in physiological environments, which make them highly biocompatible, moreover they are resistant to microbial attack, pH changes and are stable during temperature changes. On the other hand, these ceramics exhibit poor mechanical strength and low crack growth resistance, which limit their uses to non-load-bearing applications (Zhou H and Lee J, 2011). Calcium phosphate can

be used in permanent implants or as biodegradable artificial scaffolds due to its osteoconductive and osteoinductive properties as well as mechanical compatibility with native bone.

Tissue engineering has provided an alternative medical therapy using implants of polymeric scaffolds, with or without living precursor cells, as opposed to various transplants. Different polymers can be used as scaffolds to promote cell adhesion and maintenance of differentiated cell functions without hindering proliferation, in fact compared to metallic and ceramic materials, in polymeric scaffolds it is easy to chemically incorporate moieties that regulate cellular functions. Synthetic polymeric materials have been widely used in medical disposable supplies, prosthetic and dental materials, implants, dressings, extracorporeal devices, encapsulants, polymeric drug delivery systems, tissue engineered products and in orthopaedics (Tschon M, et al.,2007). Synthetic polymers can be made to exhibit predictable and reproducible mechanical and physical properties, such as tensile strength, elastic modulus and degradation rate, by fine controlling their chemical synthesis and processing, moreover, compared to metal and ceramic, they are easy to be fabricated into various shapes, with easy secondary processability and reasonable cost. Synthetic polymers have the advantage to be tailored to give a wide range of properties and more predictable uniformity, and they are generally free from the problems of immunogenicity, which can be a concern for naturally derived materials; moreover, synthetic polymers may contain low levels of chemical impurities (Gloria A, et al., 2010).

In connection with biomedical polymers and depending on their behaviour after an implant or when in contact with biological fluids, polymers can be classified as biostable (do not degrade *in vivo*), and biodegradable types. The use of biostable polymers avoids the issue of matching the implant degradation rate with tissue regeneration, the biodegradable ones have the potential to produce an implant that, with time, is substituted by the living tissue. Biodegradable synthetic

polymers are widely studied and used in bone regeneration, they must degrade at a rate corresponding to the kinetics of neo-tissue formation and have gained preference over erstwhile popular synthetic polymers such as polymthylmethacrylate (PMMA) and polyethylene (PE).The most widely studied and most commonly used synthetic biodegradable polymers, for bone applications, are the polyesters poly(lactic acid) (PLA), poly(glycolic acid) (PGA) and poly(ε-caprolactone) (PCL) all of which have their own advantages and disadvantages when used in bone applications (Table 4). Linear aliphatic polyesters are amongst the most popular materials for tissue fabrication, with a controlled degradation and the ability to entrap various drag molecules and yield materials of different strength. Polyglycolic acid (PGA) is a hydrophilic polymer with very fast degradation rate. It is a rigid thermoplastic material with high crystallinity (46-50%) and its degradation product is glycolic acid that is a natural metabolite. Because of the bulk degradation of PGA, there is a sudden loss of mechanical properties.

Polylactic acid (PLA) is hydrophobic and persists for over a year *in vivo*. PLA exists in three forms: PLLA (L isomer), PDLA (D isomer) and racemic mixture (PDLLA) and the D isomer degrades more rapidly that the L isomer. PLA degrades to form lactic acid which is normally present in the body, entering in the Krebs cycle and excreting as water and carbondioxide. PLA is more hydrophobic than PGA and is more resistant to hydrolytic attack than PGA. PLA and PGA polymers and copolymers since 1970 are good candidates as fixation devices, scaffolds for tissue engineering, and for ligament and tendon reconstruction (Rezwan K, et al., 2006).

Polycaprolactone (PCL) is a semicrystalline polymer that degrades at a much lower rate than PLA, indeed the homopolymer has a degradation time of the order of two to three years, it is non toxic with a tissue compatible material and has a propensity to form blends with a wide variety of

polymers. For this reason, PCL is used for developing long-term implantable materials (Salerno A, et al., 2009).

Tab.4. Most important polymeric materials in bone tissue engineering. Biocompatibility, disadvantages and applications.

POLYMERS	BIOCOMPATIBILITY	DISADVANTAGES	APPLICATIONS
Poly (lactic acid)	Minimal cytotoxicity, Mild foreign body reaction, Minimal inflammation	Local inflammation, random chain hydrolysis	Skin; cartilage; **bone**; ligaments; tendons; vessels; nerves; bladder; liver
Poly (glycolic acid)	Minimal cytotoxicity, Mild foreign body reaction, Minimal inflammation	Local inflammation, random chain hydrolysis	Skin; cartilage; **bone**; ligaments; tendons; vessels; nerves; bladder; liver
Poly (caprolactone)	Minimal cytotoxicity, Mild foreign body reaction, Minimal inflammation	Hydrophobic	Skin; cartilage; **bone**; ligaments; tendons; vessels; nerves

By blending these polymers in different ratios, materials with customized biological properties can be synthesized and another important advantage is the vast amount of chemical modification that can be applied to these polymers to get desired biocompatibility and cell-material interactions.

To date a wide range of materials has been developed for fixation, repair and regeneration of tissues; depending on the applications and the tissue requirements, there are some cases where it is difficult to achieve all targeted properties from a single material. Consequently, great opportunities exist in the development of hybrid materials, which include more than one type of materials, often with the incorporation of a synthetic polymer component. Thus, the creative combination of natural and synthetic biopolymers, ceramics, and inorganic materials offers a convenient bridge between chemical and biosynthetic approaches (Gentile P, et al., 2011).

Composite scaffolds have been widely used in various medical applications and devices because regenerative medicine is a new filed with new requirements for smart materials, where composites have a strong role to play. Even though each individual scaffold has advantages for bone tissue engineering applications, each scaffold has disadvantages in various properties including the brittleness of calcium phosphate and the inferior mechanical properties of natural and synthetic polymers. The combination of different materials to form composites has led to overcome the disadvantages of any one particular scaffold. In fact, composites are considered to be materials consisting of two or more chemically distinct constituents that differ in form and chemical composition and are insoluble in each other, having a distinct interface that separates the constituents, and they are composed of one or more discontinuous phases embedded within a continuous phase. The discontinuous phase is usually harder and stronger and it is called the reinforcement or reinforcing material, while the continuous phase is termed the matrix (Gelinsky M, et al., 2007).

They offer a variety of advantages over metals, ceramics and polymers, as they can incorporate the desirable properties of each of the constituent materials, while mitigating the more limited characteristics of each component. The properties depend upon the shape of the heterogeneities, upon the volume fraction occupied by them, and upon the interfaces among the constituents. The main benefit of using composite scaffolds is the ability to tailor their properties as per need, providing significant advantage over homogeneous materials (Simchi A, et al., 2011).

4.2 CHEMICAL AND PHYSICAL SCAFFOLD PROPERTIES

Besides biological characteristics, the scaffolds may be bioactive because of the appropriate chemical and physical (topography and microstructure) properties.

The way in which cells integrate with a scaffold is a more important property in tissue engineering applications and it is well established that cells interact with their environment through a number of sensors known as receptors, that may be transmembrane or intracellular and are coded to bind to specific molecules or ligands which mediate a specific intracellular response, such as proliferation, differentiation, gene expression, collagen synthesis or ion channels regulation. This phenomenon is known as cell signaling, where signaling molecules include ions, peptides or tissue or implant surface. The sequential process, initiated by binding of a signaling molecules, is known as signal transduction. Another form of cell interaction occurs through cell adhesion molecules (Nathan AS, et al., 2011).

The chemical and physical properties of scaffolds are very important for processing and performance, as they are directly related to the mechanical and biological properties of the scaffolds. The nature of a scaffold's surface determines its interaction with the body fluids, which contain several different kinds of proteins and this interaction leads to cascades of reactions, comprising the body's response to the implant, determining the development of the tissue-implant interface and long-term survivability. The surface properties of implant are important in order to address biocompatibility issues and the development of designs.

Because it is difficult to produce scaffolds that possess the necessary bulk properties with a biocompatible surface, a scaffold's surface can be modified in such a way so as to enhance its bioactivity, without sacrificing its bulk material properties. Many methods have been explored to modify the surfaces of scaffolds and all of them include some alterations of the chemical or

physical characteristics of the surface and can be accomplished by various means, such as ion beam processing, plasma surface modification, biochemical immobilization of biological molecules on the scaffold surface, or direct alteration methods such as etching or introduction of pores during fabrication of the scaffold. Modifying the chemical character of the surface often involves the changing of its hydorphobicity (Hutmacher DW, et al., 2007).

Surface chemistry is a major component of the cell response to a scaffold surface. Surface chemistry modification, the physical coating of surface and the surface functionalization are readable by cells and tissues because all these methods modify the adsorption of proteins from biological fluids that intermediate with cells. The main approach currently used to control the surface chemistry is based on the coating of surfaces with a controlled materials layer of variable thickness going from several nanometers to several tenths to a lot of various chemical or physical deposition methods. Moreover, a surface could be functionalized by adsorption, grafting of peptides of biomolecules, deposition of layer-by-layer or polymer brushes.

It is clear that optimizing the chemistry of a scaffold will greatly enhance the changes of a successful clinical outcome. It is believed that the surface chemistry of the scaffold dominates behaviour, through either the influence of its charge density and anatomic array on adherent or passing cell populations. In this regard, it is demonstrated that HA addition in the scaffold increases osteoblast proliferation and differentiation and reduces fibrous tissue encapsulation of implants exhibiting micromotion (Figure 12) (Borsari V, et al., 2005).

Chemical composition of scaffold surface, may not only act directly on the bone or cells but may act influencing events such as angiogenesis prior to ossification or producing specific cytokines or signal molecules.

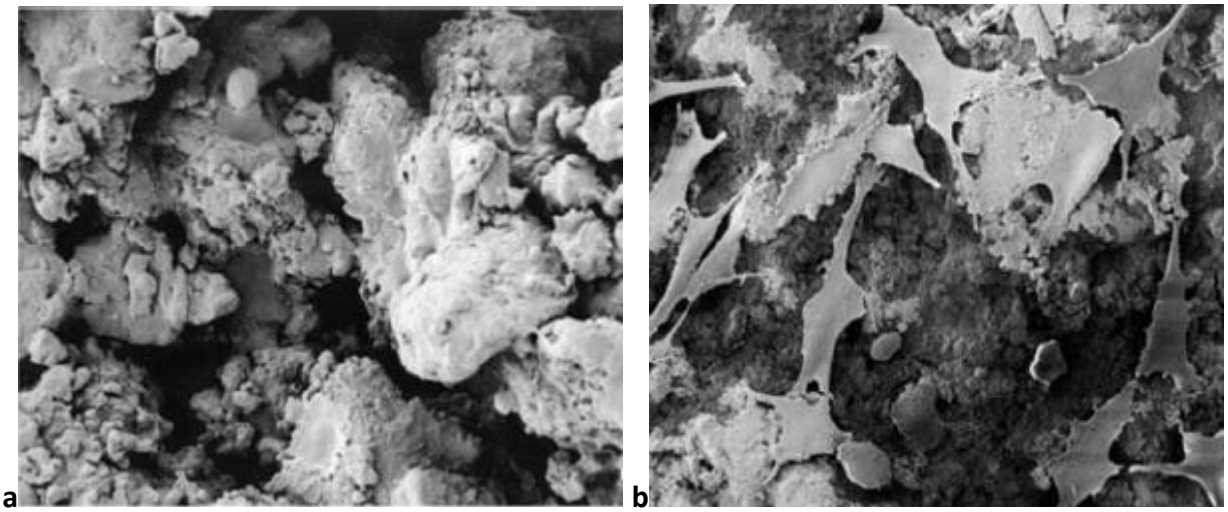

Fig.12. Example of chemical surface on osteoblast morphology. a) Ti surface; b) the same Ti surface covered with HA. (Images from Borsari V, et al., 2005).

The sensitivity of bone cells and matrix proteins is not limited to chemical phenomena; bulk geometry, surface geometry and topography also influence the process of osteogenesis through mechanical and physical considerations that promote or screen the osteoconductive potential of a material. Geometrical structural features such as the volume fraction, size, shape and degree of interconnectivity of the pores that characterized the scaffold, and even the density or rigidity of the scaffold struts, have been found to influence the biological response. A shape memory behaviour has been helpful for scaffolds use in biomedical applications, because it improves mechanical, chemical and biological properties, which include the capability of resistance against *in vivo* degradation, decomposition and corrosion. It is also important that a scaffold should be easily and reproducibility processed into a desired shape and structure, which can be maintained after implantation, thus defining the ultimate shape of the regenerated tissue and, among materials, polymers show the higher capability (Hing KA, 2004).

The roughness amplitude (or roughness height) should have intuitively a strong influence on cell response, but different if roughness amplitude is at the nano- or at the micro-scale. The roughness organization and morphology influence short-term and long-term adhesion, and proliferation

capacity of cells, on the other hand, cells are able to identify and respond differently to surfaces exhibiting different morphologies; for example disordered surfaces can stimulate MSCs differentiation in bone cells. The osteoinductivity of a scaffold is linked to the precise shape of surface concavities and this osteoinductivity occurs as a result of a concentration of some proteins such as BMPs within the surface concavities. On a smaller scale, surface texture has also been demonstrated to influence cell response to a material. Tissue differentiation and bone ingrowth are accelerated when the surface of the implant is coated with bioactive materials or through chemical and thermal treatments applied that convert the smooth to rough bioactive surface (Otsuki B, et al., 2006). Biocomposites, where one of the phases consists of inorganic particles, present a certain type of surface texture owing to the presence of these particles that may be fully embedded in the matrix or partially exposed in the material surface, generating specific surface topography depending on the geometry, dimensions and percentage of the inorganic phase. Although both micro- and nanotopography appear to have an important effect on protein adsorption and subsequent cell events, the complete picture and understanding of the relationship between micro- and nanotopography and cell response must be evaluated. An increase in cell number and attachment force has been reported on textured polymer substrates. A higher percentage of osteoblasts is inclined to attach to the rough surface, to synthesize extracellular matrix and mineralize. However, when the roughness level is greater than cell dimension it does not enhance cell response (Nathan AS, et al., 2011).

Other physical properties, such as density, absolute density, porosity, microstructure, crystal structure and degree of cristallinity, specific heat, melting point and boiling point, are directly related to mechanical properties such as tensile strength, bending strength, compressive strength and hardness (Yu H, et al., 2008).

Evaluation of mechanical properties of scaffolds is important for matching material properties to the *in vivo* environment and this feature requirements are tied to specific applications. As about polymers, the poor mechanical strength of PLA, PGA and their copolymers has still been a bottleneck in creating load-bearing implants, although these materials are well known for their bioactivity and bioresorbability. By comparing the mechanical properties of the porous composites to those of porous polymeric scaffolds, a slight increase of mechanical properties is revealed. Dynamic mechanical tests are performed to determine time-dependent viscoelastic behaviour of polymeric scaffolds and mechanical properties, such as Young's modulus, specific modulus, tensile strength, compressive strength, shear strength, yield strength, ductility and Poisson's ratio, are critical to be evaluated before scaffold design and fabrication. It is well known that bone is functionally adaptive, i.e. that it responds to external mechanical stimuli to either reduce or increase its mass as required. Mechanical forces regulate many cell types, including both osteoblasts and osteocytes, through a process known as mechano-transduction that loosely describes the chain of molecular events that enable mechanical stresses to be converted into biological signals and physiological responses. Mechanical stimulation has been shown to stimulate osteoblastic differentiation of osteoprogenitor cells and it is possible to see how variation of local strain in scaffold struts, as a result of porosity variation, may induce or inhibit bone formation. Moreover, the evaluation of mechanical properties is important for the development of a temporary scaffold for tissue engineering purposes because the material must keep its crucial integrity during the first stages of the new tissue formation and undertake a progressive and gradual degradation (Sanz-Herrera JA, et al., 2010). The rate of degradation of the scaffolds must be balanced with the rate of tissue regeneration to maintain the integrity of the scaffold throughout its lifetime. The architecture of scaffold constructs, for tissue regeneration,

plays a very important role in cell in-growth, migration, maintenance and further structure of the new tissue. Pore distribution, interconnectivity and size distribution are key issues and scaffolds, that present a highly interconnected porous network, formed by a combination of macro, micro and even nanopores, enable proper tissue vascularization, nutrient diffusion and waste release (Armatas GS, 2006).

4.2.1 Porosity

Scaffold design and porosity (Figure 13) are key components for the success of an implanted device. For tissue engineering applications, an important aspect, in the design of scaffolds, is their required 3D porous architecture because porosity is important for the development of new tissue. Porosity is defined as the percentage of void space in a solid, is a morphological property independent of the material, plays a dominant role in the biomechanical characteristics, initial cell attachment and subsequent tissue regeneration and influences the bioactivity of a material because of the structure's permeability. A scaffold should provide an open porous network to assure an uniform cell distribution and tissue regeneration, an appropriate transport of soluble signaling molecules, as well as nutrients and oxygen, and metabolic waste removal (Salerno A, et al., 2007), and this aim is reached by the combination of different pore sizes. Pores are necessary for bone tissue formation because they allow migration and proliferation of osteoblasts and mesenchymal stem cells, as well as vascularization. A porous surface improves mechanical interlocking between the implanted scaffold and the surrounding natural bone, providing greater mechanical stability at this critical interface (Hutmacher DW, et al., 2007). Although macroporosity (pore size>50 μm) has a strong impact on osteogenic outcomes, microporosity (pore size<10 μm) and pore wall roughness play an important role, contributing to higher bone-inducing protein

adsorbtion. It is observed a greater degree and faster rate of bone penetration with increasing macroporosity because any new bone formation is strongly influenced by the degree of macroporosity.

Microporosity has clearly been shown to have a significant impact on bioactivity with evidence to suggest that bioactivity is enhanced, not only through a combination of angiogenesis and cell adhesion, but also through the entrapment and adsorption of adhesion proteins or GFs within the micropores (Kilpadi KL, et al.,2004). Small pores favor hypoxic conditions and induce osteochondral formation before osteogenesis occurs. In contrast, larger pores rapidly become well-vascularized and lead to direct osteogenesis. Pore sizes of >300 μm and adequate porosities (80% for spinal fusion down to 60% for implant grafting in revision hip surgery) are best suited for successful regeneration of bone (Zhang C, et al., 2006). Although controversy, regarding optimal pore sizes for tissue engineering scaffold, exists a pore size of 200-600 μm is acceptable in most studies to provide adequate space for osteoblasts and vascular tissue ingrowth.

A key feature for a porous scaffold is interconnecting porosity, which allows the cells to invade the scaffold, subsequently to proliferate and form extracellular matrix and to migrate throughout the entire scaffold. It is essential that the solid struts have an associated interconnecting micro/macro scale porosity for an optimized biological response (Bonfield W, 2006).

Interconnected pores permit tissue and bone ingrowth, preventing loosening and retaining dynamic strength of implants.

There is a need for controlled porosity, that would be the most suitable from a biological standpoint and this requirement must be balanced by the need to have an adequate compressive strength before the process takes place. The desire for high porosities must be tempered by the

need to maintain suitable mechanical properties within the scaffold throughout its lifetime (Hing KA, 2004).

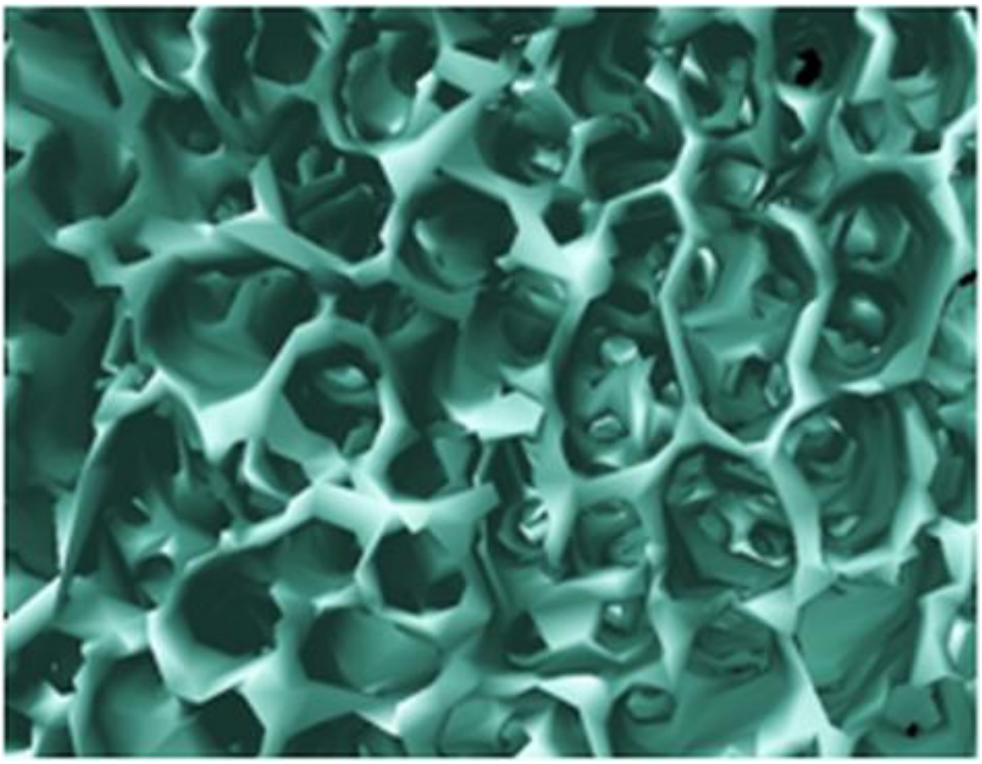

Fig. 13. Microtomographic image of a porous scaffold. (Image from laboratory of Preclinical and Surgical Studies-IOR).

5. AIM OF THE PROJECT

Tissue engineering is a promising strategy to overcome the need to restore or regenerate tissues. In orthopaedic surgery, the autologous bone graft is widely recognized as the first choice material because its ability to promote osteogenesis, osteoconduction and osteoinduction in the site of injury and its absolute and complete biocompatibility. Bone tissue, widely damaged by injury or disease, might also be replaced using constructs based on biocompatible materials and cells (Sundelacruz S and Kaplan DL, 2009). Recent advances in synthetic scaffold research give to us the possibility to investigate new solutions in the field of bone substitutes. Synthetic scaffolds, due to their non-biological origin, have no cross contamination risk, but there is the stringent need to study their biocompatibility and clinical behaviour (Weigel T, et al., 2006). Among synthetic materials, in recent years, studies of scaffold composite materials have been performed as to successfully reproduce the microenvironment required to support and improve the molecular interactions which occur within tissues, between cells and within the mineralized extracellular matrix. To date, polymer matrices reinforced by ceramic fillers such as hydroxyapatite represent a promising composite material, able to mimic the collagen/hydroxyapatite micro/macromorphology of “native bone material” (Frantzl P, 2007; Moroni L, et al., 2008).

Scaffold design, porosity and early cell colonization are key components for the success of the implanted materials. It is well known that the scaffold architecture plays a crucial role in initial cell attachment and subsequent migration into and through the matrix and in the mass transfer of nutrients and metabolites, providing sufficient space for development and later remodeling of the organized tissue. Defined morphological features (i.e. pore size) are required to ensure cell adhesion, molecular transport, vascularization and osteogenesis and in order to study the scaffold

architecture and the 3D cellular distribution inside, among the best known techniques, microtomographic approach was validated in recent years (Takemoto M, et al., 2006).

The aim of the present thesis was to comparatively investigate the *in vitro* and *in vivo* biological behaviour of new μ-bimodal polymeric, Poly ε-caprolactone (PCL), and composite, poly ε-caprolactone/hydroxyapatite (PCL/HA), scaffolds for the treatment of bone defects.

The scaffolds, fabricated with two different methods, gas foaming (GF) and selective polymer extraction (PE) from co-continuous blends (Salerno A, et al., 2009; Salerno A, et al., 2010), for PCL scaffold, and phase inversion/salt leaching for the composite PCL/HA scaffold (Guarino V, et al., 2008; Guarino V, et al.,2009), were characterized by a new porosity (μ-bimodal porosity) and pore interconnectivity.

During my PhD, at the Preclinical and Surgical Studies laboratory of Rizzoli Orthopaedic Institute of Bologna, microtomographic, *in vitro* and *in vivo* evaluations were performed, to assess the two scaffolds in terms of porosity, cell colonization of the scaffolds, biocompatibility, bioactivity, biofunctionality, biodegradability, and new bone formation.

More precisely, before *in vitro* and *in vivo* studies, tests were conducted with a new microtomographic approach (Micro-CT, SkyScan 1172) to evaluate the overall porosity, macroporosity and microporosity of these new kinds of scaffolds, at rest and after three different compression stages (1 mm, 3mm and at maximum compression of 222N).

Moreover, a visualization and a quantification of the distribution of cells through the entire PCL scaffold were evaluated with Micro-CT technique, after the seeding of cells (MG63) on the scaffold, because in literature, porous scaffolds with novel porous architecture should promote and guide the *in vitro* and *in vivo* adhesion, proliferation and 3D colonization of cells.

Subsequently, *in vitro* and *in vivo* tests, for the evaluations of cytotoxicity, biocompatibility, bioactivity, biofunctionality and biodegradability of the scaffolds were carried out with osteoblastic-like cells (MG63) and by implantation of the two scaffolds in rabbit bone defects.

The defect healing and the new bone growth were calculated with static and dynamic histomorphometric parameters.

6. TESTED SCAFFOLDS

In this thesis, for the regeneration of bone defects, the “in situ tissue regeneration” approach was taken into consideration and two scaffolds were investigated: a polymeric poly ε-caprolactone (PCL) and a composite poly ε-caprolactone/hydroxyapatite (PCL/HA) scaffold.

PCL and PCL/HA were manufactured by researchers from the Interdisciplinary Research Centre on Biomaterials, CRIB and the Institute of Composite and Biomedical Materials, National Research Council, respectively, from University of Naples Federico II. These research groups have also performed chemical-physical tests on the scaffolds (Salerno A, et al., 2009; Salerno A, et al., 2010; Guarino V, et al., 2008; Guarino V, et al., 2009).

6.1 PCL MANUFACTURE AND CHARACTERIZATION

The bio-inspired design of micro- and nano-structured materials for, tissue-engineered scaffolds, is strongly driven by the increasing demand to recreate an extracellular matrix–like three-dimensional (3D) substrate, facilitating more physiological growth of cells and final tissue regeneration.

However, the need to drive the biological events, that underpin the regenerative processes associated with therapy of tissue diseases, imposes constraints on the design of innovative scaffold materials. An essential attribute is the ability to encode the required biological signals within the scaffold, so that most of the processes involved in cell response (i.e., adhesion and cell migration, proliferation and differentiation) may be controlled.

Currently, such approaches mostly rely on the use of synthetic polymers such as poly(lactic acid) and PCL. They are used because of their ability to support, for long periods, the environmental stresses imposed on the pore walls by loads and the hydrostatic pressure of biological fluids

arising from the slow degradation kinetics found *in vitro* as well as *in vivo* (Guarino V, et al., 2007). Among polyesters, PCL has a long history in bone tissue engineering, mainly because it was shown to possess sufficient strength and stiffness to function for the period required by bone to heal.

The matrix made of PCL, a polymer hydrolytically degradable both via bulk and surface erosion, guarantees degradation kinetics slower than other aliphatic polyesters such as poly(glycolic acid) or poly(L-lactic acid), because of its strong hydrophobic nature, offering a valid mechanical support for long-term implantation (Guarino V, et al., 2007).

In this thesis, the μ-bimodal PCL scaffold was prepared by a combination of gas foaming (GF) and selective polymer extraction (PE) from co-continuous blends, as described by Salerno A (Salerno A, et al., 2009; Salerno A, et al., 2010).

As schematically illustrated in Figures 14, the GF–PE technique is characterized by three different steps:

(1) 3/2 (w/w) PCL (Mw=65 kDa and T_m 59°C-64°C) and thermoplastic gelatin (TG) co-continuous blend was prepared by melt mixing in an internal mixer (Rheomix® 600 Haake, Germany) at 60°C and 80 rpm for 6 min (Fig. 14A);

(2) the PCL/TG blend was subsequently gas foamed with a 4/1 (v/v) N_2/CO_2 blowing mixture, at a foaming temperature (T_F) of 44°C and with a pressure drop rate (PDR) of 700 bar s^{-1} (Fig. 14B);

(3) finally, the TG was selectively extracted from the foamed blend by soaking the sample in dH_2O at 38°C for 1 week (Fig. 14C).

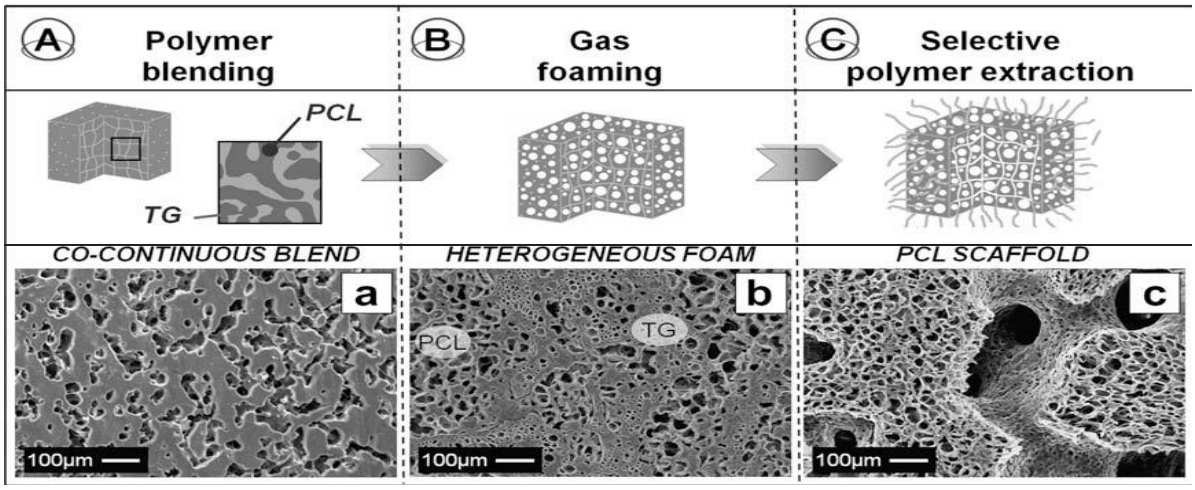

Fig. 14. Correspondence between the processing step and the microstructural evolution of PCL/TG system: (a) SEM micrograph of 3/2 (w/w) PCL/TG co-continuous blend after the selective extraction of the TG; (b) SEM micrograph of PCL/TG blend foamed with 4/1 (v/v) N_2/CO_2 blowing mixture, at T_F=44°C and PDR = 700 bar/s; (c) SEM micrograph of µ-bimodal PCL scaffold prepared by the selective extraction of the TG from the foamed PCL/TG blend. (Image from Salerno A, et al., 2009)

The most important microstructural and mechanical characterization, performed by Salerno A, et al., are summarized as follows:

- the morphology, porosity, mean pore size and pore size distribution of PCL were evaluated by scanning electron microscopy (SEM) (S440; LEICA, Germany) and image (Image J®) analyses. The scaffold was cross sectioned, gold sputtered and analyzed at an accelerating voltage of 20 kV. Than the SEM micrographs were converted to binary images and analyzed by the Image J software. The overall porosity was determined by the equation:

$$\%porosity=[1-(\rho_S/\rho_{PCL})]x100$$

where ρ_S is the apparent density of the scaffold calculated from mass and volume measurements. The mass was calculated by a high accuracy balance (10^{-3}g, AB104-S, Mettler Toledo, Italy), while the volume by geometrical calculation. The overall porosity results represent the mean value of five different porosity measurements. Image analysis was used to assess the volume fraction of the two different porosities by means of area

fraction measurements. The area fraction of the TG foamed phase provided the macroporosity volume fraction, while the difference between the mean overall porosity and the macroporosity amount yielded the microporosity volume fraction. Image analysis was also used to evaluate the mean pore size of the microporosity, based on the ASTM D3576 method;

- the static compression properties of PCL were determined using an Instron mechanical testing system (4204, Instron, Italy), working at a cross head of 1 mm/min and with a 1 kN loading cell. Five disc-shaped scaffolds were tested and the elastic compression modulus (E) and compression yield strength (σγ) were determined as the slope of the initial linear portion of the stress versus strain curve and the modulus slope at an offset of 1% strain, respectively;
- wettability tests were performed by a Contact angle System OCA20 (Dataphysics) to evaluate the effect of the microarchitecture of PCL on fluid perfusion. A 0.2 µL water drop was poured onto the scaffold and the wetting time (for complete fluid penetration) results were divided in 3 groups: FAST (wetting time <3 s), MIDDLE (from 3 to 10 s), and SLOW (higher than 10 s). Forty measurements were performed for the scaffold.

The process started from the preparation of a PCL and TG co-continuous blend, with a PCL weight fraction of 60%. After the extraction of the TG from the PCL-TG blend, the co-continuity of the gelatin phase was evident from SEM micrograph. Following the gas foaming process, due to the incompatibility of the PCL/TG blend and to the different foaming behavior of the 2 polymers, the microstructure of the PCL/TG foam was characterized by two different porous phases, with the PCL foamed phase characterized by a 40 µm mean pore size and a high degree of pore interconnection. The final removal of the TG from the foamed blend allowed the formation of an

additional porosity, characterized by elongated and highly interconnected macroporosity with a rounded and smaller microporosity induced by the GF step (Figure 15).

The value of overall porosity was about of 60%, uniformly distributed between the macroporosity (312 µm mean pore size), created by the selective extraction of the TG and microporosity (40 µm mean pore size), induced by the GF process.

The results of the mechanical characterization showed the typical stress-strain curve of porous materials, undergoing static compression testing, with an initial linear-elastic region followed by a short collapse plateau and, finally, the steep increase in the stress values. Moreover, the calculated average compression modulus and yield strength were 11.4 and 1.6 MPa, respectively. Nearly 80% of the wetting times measured was almost equally distributed in the FAST and SLOW ranges (mean wetting time=1.66±0.88 and 16.26±6.06 s, respectively), whereas the remaining 20% was in the MIDDLE range (Salerno A, et al., 2009; Salerno A, et al., 2010).

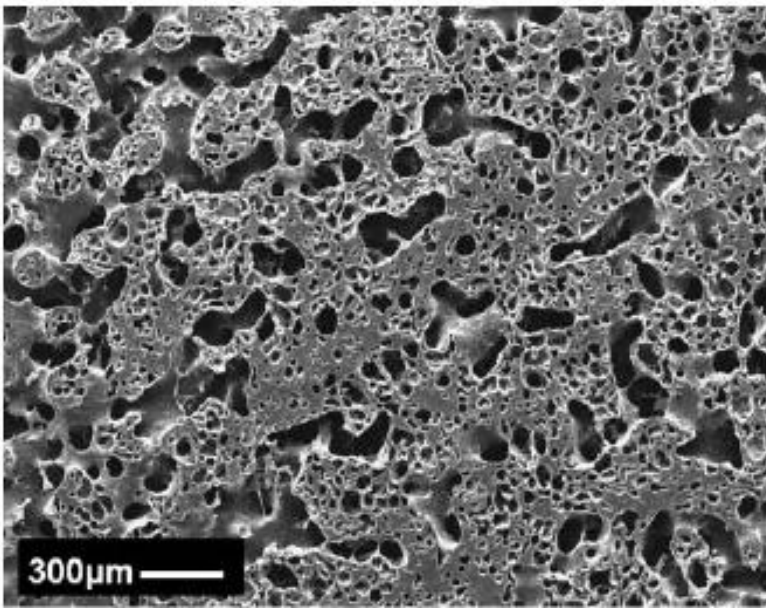

Fig. 15. Low magnification SEM micrographs of the µ-bimodal PCL scaffold. (Image from Salerno A, et al., 2010).

However, PCL alone is not adequate as a bone substitute, because it does not promote an osteogenic response, one of the main requirements in the designing an ideal bone analogue to

guide the cascade of biological events related to the formation of mineralized tissue (Ang KC, et al., 2007).

6.2 PCL/HA MANUFACTURE AND CHARACTERIZATION

Today, it is taking up the improvement in osteoconductivity through the employment of insoluble signals (bioactive phase) integrated with the degradable polymer matrix (Wang M, 2003).

The need for a mechanically functional material for bone substitution has generated numerous composites of calcium phosphate–reinforced polymers (Hutmacher DW, 2000). These act as reinforcement agents as well as osteoconductive signals, offering a valid compromise between the mechanical response and bioactivity of the scaffold. In particular, the challenging idea of designing ‘‘tissue-inspired composite materials” has moved towards the synthesis of ceramic/polymer composites with advantages over either pure ceramic or pure polymer (Catauro M, et al., 2006), resulting in superior materials for specific applications.

Traditionally, calcium phosphate-based ceramics have proved to be attractive bioactive materials for biological applications. It was proposed the use of calcium phosphates such as HA ($Ca_{10}(PO_4)_6(OH)_2$) with an atomic ratio of calcium to phosphorus (Ca/P) of 1.67 to stimulate a biochemical response from living tissues and to obtain a strong bond between the scaffold and the adjacent tissue with positive results.

As also reported by Khan et al. and Chim et al. the combination of calcium phosphate, which on its own is brittle and limited in its applications, and polymer is also well founded as the addition of the polymer can impart beneficial properties such as mechanical toughness, resistance to brittle failure, and formability to the calcium phosphate (Khan YM, et al., 2004; Chim H, et al., 2006).

In this thesis, PCL/HA scaffolds were developed with phase inversion/salt leaching method using NaCl crystals as porogen agent (Guarino V, et al., 2008). The scaffold of this thesis, showed a HA

relative volume fraction of 13% because it exhibited good mechanical performance than the other types, creating a good compromise between mechanical and bioactivity features, more important in the orthopaedic field.

Briefly, PCL pellets (M_W 65 kDa; Sigma Aldrich, Milan, Italy) were dissolved in a 20 wt % N-N-dimethylacetamide (J.T. Baker 06/2007) solution (5 g polymer in 20 ml solvent) by stirring for about 3 h at 58°C. Subsequently, NaCl crystals (sieved into specific size range of 212–300 μm) were homogeneously mixed to the polymer solution with a volume ratio of about 9/1, and the mixture was poured in the Petri dish and compressed by 0.127 N/mm^2 for 10 min, for a more uniform distribution of porogen agent into the polymer mixture. The mixture was then dipped in ethanol (3 ml each 20 min for three times) at room temperature and in bidistilled H_2O (Carlo Erba, Milan, Italy) for 7 days, with three changes a day. The HA powder was added to the PCL solution (29% w/w) before the solvent extraction. In particular, HA particles showed a three-modal dimension distribution ($d_{0.1}$ 0.42; $d_{0.5}$ 4.02 and $d_{0.9}$ 11.91 μm), with a specific surface area of 13.29 m^2/g and a theoretical density of 3.16 g/cm^3.

Some tests were performed, by Guarino V, et al. (Guarino V, et al., 2008), to assess the morphological and mechanical behaviour of the scaffold, and some of these techniques and results are summarized as follows:

- morphological investigation was studied by Scanning Electron Microscopy (SEM)/Energy Dispersive Spectroscopy (EDS) analyses. For SEM (Leica Stereoscan mod.420-Oxford Intsruments), scaffold was gold-coated using a sputter coater set at 15 mA for 20 min. EDS was performed (Oxford mod. INCA 200) to measure the energy and intensity distribution of X-ray signals generated by the electron beam striking the surface of the specimen. As

consequence, the elemental composition at a point, along a line, or in a defined area can be easily determined with a high degree of precision (nearly 0.1 wt%);

- thermogravimetric analysis (TGA) (TA instrument TGA model 2950) was used to verify the weight percentage of HA, using a nitrogen atmosphere with a temperature 20-500 °C;
- compressive mechanical properties were evaluated at room temperature on dynamometric machine (Instron 4204) with a 100 N load cell and a crosshead speed of 1 mm/min. The elastic modulus E was calculated by the initial slope of the stress-strain curve before the plateau region. Tensile properties were performed at room temperature by an Instron machine according to the ASTM 638/2a standard, using the same load cell and a crosshead speed of 1 mm/min. The elastic modulus E was evaluated by the slope of the stress-strain curve in the strain range of 0-0.1 mm/mm. The study was carried out through analysis of five samples of the scaffold;
- mercury intrusion porosimetry (Thermo Electron Pascal 140-240) was used for the evaluation of pore size distribution and it is based on the Washburn equation:

$$p.r = -2\gamma.\cos\theta$$

where p is the applied pressure, r is the radius of the pore, γ is the surface tension of the mercury, and θ is the contact angle between mercury and polymer. In this case, cylindrical shape of pores and constant pressure were assumed. A mercury surface tension of 480 mN/m and a contact angle of 141.38° were used for all measurements while p_{max} applied of 400 Pa and 200 KPa were chosen in connection with pore size analysis. This method provided simultaneously the total porosity, the average pore diameter, and the pore size distribution into 3D scaffolds. In addition bulk density, apparent density and specific surface were evaluated.

A typical bimodal porosity has been evidenced: a macroporosity (20-300 µm), due to the extraction of the sodium chloride crystals, and a microporosity (1-20 µm), ascribed to solvent/nonsolvent exchange, were observed (Figures 16). Since the PCL component underwent thermal degradation between 350 and 420°C, the effective HA weight percentage has been evaluated through residue determination at 500°C.

In particular, average residual products of 34.8 were found. The weight loss (%) is a function of temperature.

EDS confirmed the presence of stoichiometric HA (Ca/P atomic ratio=1.66) distributed in the 3D structure on the cross section of scaffold. The same value of Ca/P atomic ratio was achieved both on surface and cross-section.

With mercury intrusion porosimetry technique, an overall porosity of 92.12%, an average pore size of 129.3 µm, a bulk density of 0.134 g/cm^3 and a total specific surface area of 0.464 m^2/g were observed. The highest volumetric fractions of pores fall in the range of 20–200 µm.

As about mechanical properties, the tensile elastic modulus was about 1.31 MPa, with a Strain at maximum stress of 0.164 mm/mm and a maximum stress of 0.076 MPa. The compressive Toe region Elastic Modulus was of nearly 0.318 MPa. A PCL scaffold, used for comparison, showed an elastic modulus of 1.10 MPa, a strain at maximum stress of 0.160 mm/mm, a maximum stress of 0.060 MPa and a compressive Toe region Elastic Modulus of 0.258 MPa.

In another subsequent study, Guarino V, et al., compared PCL/HA 13% (the composite material used in my thesis) with pure PCL (Guarino V, et al., 2009).

The *in vitro* degradation mechanisms and kinetics of PCL and, especially, of the PCL added with HA, were evaluated by immersing materials in 3 different aqueous media, at 37°C: PBS at pH 7.5; 0.01 M NaOH solution; and SBF buffered at pH 7.5. For each degradation time (28 and 56 days), the

samples were recovered, washed with distilled water, vacuum-dried at room temperature, and weighed before being subjected to the various analyses.

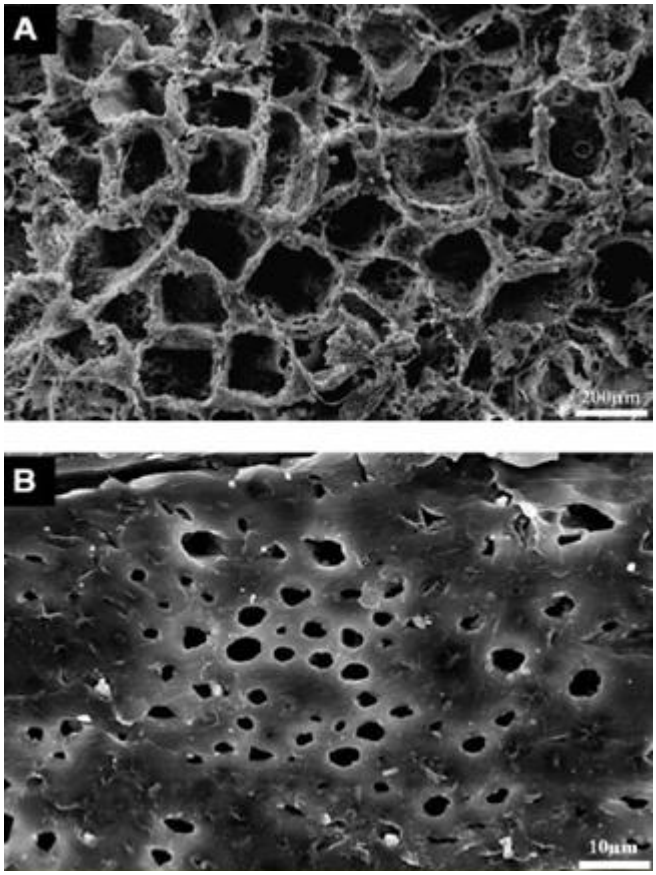

Fig.16. Bimodal porosity of the scaffold. A) Macroporosity due to the salt removal, B) microporosity due to the phase inversion mechanisms. (Image from Guarino V, et al., 2009).

The weight loss percentage of the samples was calculated according to the equation:

$$\% \text{ weight loss} = 100\ (\omega_0 - \omega_t)/\omega_0$$

Raman spectroscopy and thermal analyses were also performed. The Raman spectra of the untreated and *in vitro* degraded samples were recorded on a Jasco R1100 spectrometer with a 488 nm radiation from a Spectra-Physics argon ion laser source. The spectral resolution was 4 cm^{-1}, and laser power at the sample was nearly 40 mW. The thermogravimetry (TG) thermograms of the untreated and *in vitro* degraded scaffolds were performed using a Mettel TA-STAR, TGA/SDTA

851^{e} thermobalance, in air with a heating rate of 2°C/min, from 25 to 1000°C. The PCL content was evaluated through the weight loss in the 200-500°C range. The DSC Thermograms of the untreated and *in vitro* degraded samples, were performed with a Mettler TA-STAR, DSC 821^{e} calorimeter, covering 5-120°C. The samples were heated at 2°C/min and then cooled at -2°C/min.

Briefly, results showed that the polymer phase in the untreated (not degraded) PCL/HA scaffold appeared more crystalline than in the pure PCL sample. Specifically, an increase of crystallinity from 71% (PCL) to 74% (PCL/HA) was observed, with a lower amount of amorphous regions. In the case of PCL/HA, degradation proceeded more slowly compared to pure PCL, due to the higher values of crystallinity. However, the behaviour of PCL/HA 13% suggests that crystallinity cannot be the only parameter that determines the degradation kinetics of the composite. Although the PCL/HA 13% was characterized by a cristallinity quite similar to pure PCL, the net weight loss percentage of the composite, after 56 days of degradation in NaOH solution, was significantly lower than that of the pure PCL under the same condition, being 0.9% versus 15%, respectively. These results lead to the conclusion that the HA component plays a significant and complex role in the inhibition of degradation (Guarino V, et al., 2009).

7. MICROTOMOGRAPHY (MICRO-CT)

Before the explanation of the methodology for the scaffold microtomographic analyses, a brief description of the microtomography is reported.

Microtomography is based on the same principles of a normal X-ray tomography used in clinical medicine but avails itself of a microscopic level resolution. This type of equipment allows images to be obtained of the internal structure of a small object with high spatial resolution and high speed, without sample preparation or chemical fixation.

Typically, the spatial resolution of conventional medical CT-scanners is in the range of 1 - 2.5 mm, which corresponds to 1 -10 mm^3 voxel (volume element) size. Computerized X-ray microscopy and microtomography now give possibilities to improve the spatial resolution by seven to eight orders in the volume terms. The system “SkyScan 1172", used in this thesis, allows to reach a spatial resolution of 5 µm corresponding to near $1x10^{-7}$ mm^3 voxel size. As in the “macro" CT-scanners, the internal structure can be reconstructed and analyzed fully non-destructively (Ohgaki T, et al., 2006).

The SkyScan 1172 (Figure 17) is a high resolution X-ray Micro-CT system with an architecture in which both the sample stage and the X-ray camera are moveable. This allows a good combination of image resolution, sample size accommodation, scan speed, and sample throughput. The flexible scanner geometry is particularly advantageous over intermediate resolution levels, where scans are around ten times factor compared to previous scanners with a fixed source-detector design. Table 5 summarizes the main principal features of Skyscan 1172.

Micro-CT is extremely helpful when it comes to characterize devices in the preimplant phase and evaluating possible deformations and/or degradations after the explantation phase, moreover it is useful for the analysis of both tissue engineering scaffolds and bone tissue regeneration after the

preclinical application of innovative biomaterials and biocomposites (Stock SR, 2008). Micro-CT shows some advantages over the classical histology, such as the maintenance of the integrity of the analyzed specimen, the lower acquisition time and the higher number of analyzed sections than histology and the possibility to perform 3D studies. Moreover, Micro-CT possesses 3 stages, the cooling, the material testing or compression chamber and the micro-positioning stages (Figures 18). The first is useful for in-situ object scanning during specific temperature and it contains all necessary parts to cool down a sample, measure and stabilize the sample stage temperature. An object can be scanned in any selected temperature in the range of approximately +30°C to -20°C. The second is used for compression and tension tests and it permits to scan an object during mechanical tests, contains useful parts for compression and tension and permits to measure the load applied. The third, is applyed for the correct centering and positioning of more little specimens for the different phases of scan, acquisition and reconstruction.

Fig.17. Micro-CT Skyscan 1172.

a  b  c 

Fig.18. The three stages of Micro-CT: a) the cooling, b) the material testing or compression chamber and c) the micro-positioning stages.

Tab.5. Characteristics of Micro-CT Skyscan 1172.

	CAMERA 10 MEGAPIXEL
SPECIMENT MAX SIZE	6 cm Ø, ca 6 cm h
SPOT SIZE	<5µm@4W, 20-100KV, 0-250 µA
X-RAY SOURCE	sealed microfocus X-ray tube, air cooled,>10000h lifetime
RESOLUTION	5 µm
PIXEL SIZE (MAX.MAGNIFICATION)	<0.9 µm
N° OF PIXELS	4000X2300
RECONSTRUCTION TIME	6.8 sec per cross section 1024x1024 pixels
RECONSTRUCTION ALGORITHMS	Cone-beam volumetric reconstruction
OPERATION CONDITIONS	-10°C+50°C storage, 18°C-25°C operation, 70% humidity max
SMALLEST DETAIL DETECTABILITY	~1 µm

Briefly, in Skyscan 1172, the system obtains multiple X-ray shadow transmission images of the object from different angular views, as the object rotates on a high-precision stage (Acquisition step). From these shadow images, cross section images of the object are reconstructed by a modified Feldkamp cone-beam algorithm, creating a complete 3D representation of internal microstructure and density over a selected range of heights in the transmission images. For the reconstruction one can use a volumetric (cone-beam) reconstruction of one, several, or all cross sections or a region of interest (ROI) reconstruction. After the serial reconstruction, one can display the cross sections onto the screen as well as reconstruct a realistic 3D-image with possibilities to “rotate" and “cut" the object model. On this model the internal morphological parameters can be calculated. Moreover, it is also possible to create virtual 3D models of the analyzed samples, that are very useful for a complete visualization and understanding of inner and outer morphology of a scaffold. CT-analyzer (*CTAn*) is a dictate application for deriving quantitative parameters and constructing visual models from scanned datasets obtained with SkyScan Micro-CT instruments. Morphometric parameters are calculated by CT-analyzer either in direct 3D based on a surface-rendered volume model, or in 2D from individual binarized crossection images. Further, for both 3D and 2D measurements, there are two types of analyses. Firstly, all objects in the selected region can be analyzed together, and the integrated results can be calculated, such as total volume or surface of all objects, or mean thickness of all objects, etc. Secondly, individual “discreet” objects can be categorized, on the basis of being entirely surrounded by space either in 2D (on a single crossection only) or in 3D (for a selected volume comprising many crossectional levels). Morphometric parameters in 3D and 2D can be carried out on all the individual objects.

All calculations are performed over a selected region. Consistent and accurate selection of the regions or volumes of interest is fundamentally important to obtaining accurate and meaningful

data. Some clarification of terminology for this is useful. The term “region of interest”, or ROI, refers to a selected region of a single crossectional image and 2D analysis is performed within a ROI. The “volume of interest” (VOI) refers to the collective sum of all ROIs over a contiguous set of crossectional image slices, representing a selected 3D volume. In Figure 19 the Micro-CT working steps are summarized.

All measurements of morphometric parameters in 3D and 2D are performed on segmented or binarized images (Tables 6). Segmentation or “thresholding” must be done prior to morphometric analysis.. Parameter names follow two alternative nomenclatures, “General Scientific” or “Bone ASBMR”, the latter based on Parfitt et al. (1987). Parfitt’s paper proposed a system of symbols for bone histomorphometry, and the principles of Parfitt’s system are applied here to both the Bone (ASBMR) and the General Scientific parameter names (Parfitt AM, et al., 1987-A).

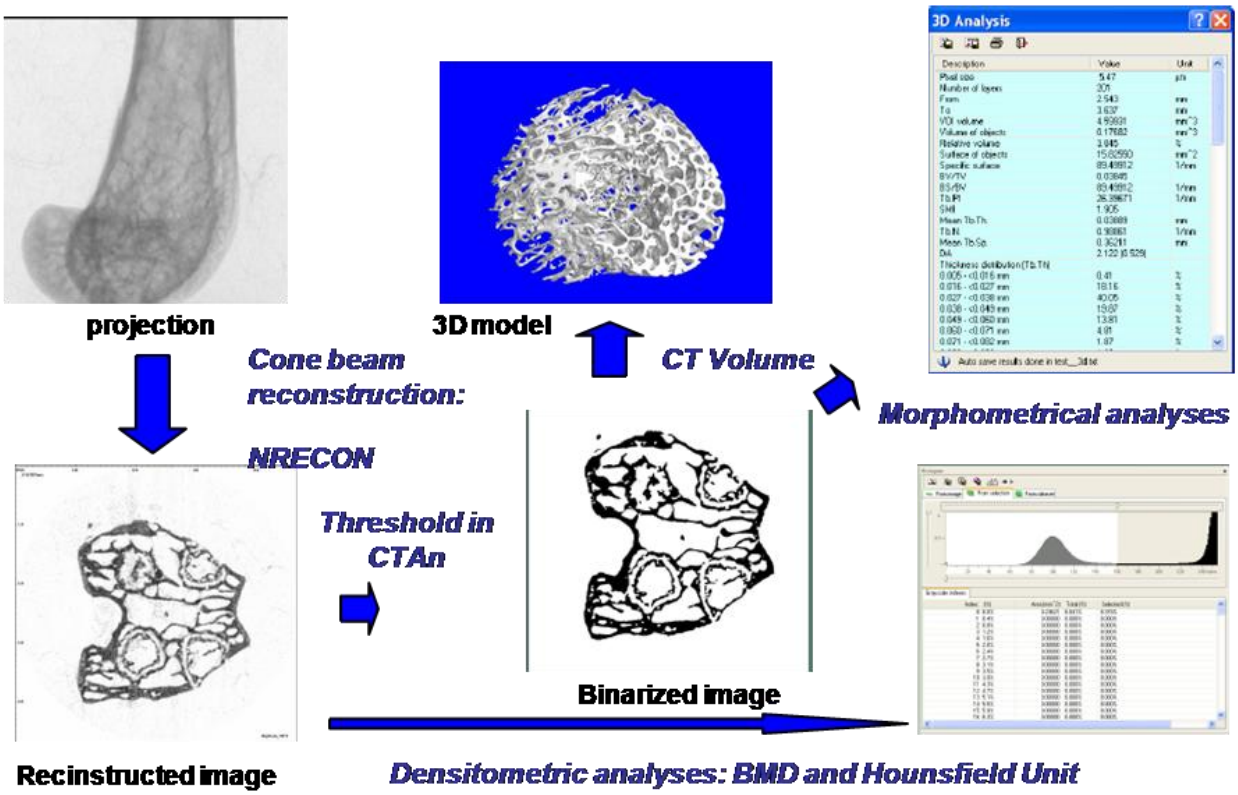

Fig.19. Scheme of Micro-CT working steps.

Tab.6. 2D and 3D parameters calculated by Micro-CT.

3D integrated analysis of all objects in VOI (all selected image levels)				3D individual analysis of all objects in the VOI (over all selected image levels)		
Parameter	*Symbol*	*Unit*		*Parameter*	*Symbol*	*Unit*
VOI volume	TV	mm^3		Object volume	Obj.V	mm^3
Object volume	Obj.V	mm^3		Object surface	Obj.S	mm^3
Percent object volume	Obj.V/TV	%		Volume of pores	Po.V	mm^3
VOI surface	TS	mm^2		Surface of pores	Po.S	mm^2
Object surface	Obj.S	mm^2		Porosity	Po	%
Intersection surface	i.S	mm^2		Number of pores	N.Po	
Object surface / volume ratio	Obj.S/Obj .V	mm^{-1}		Centroid x	Crd.X	mm
Object surface density	Obj.S/TV	mm^{-1}		Centroid y	Crd.Y	mm
Fragmentation index	Fr.I	mm^{-1}		Centroid z	Crd.Z	mm
Centroid (x)	Crd.X	mm				
Centroid (y)	Crd.Y	mm				
Centroid (z)	Crd.Z	mm				
Structure model index	SMI					
Structure thickness	St.Th	mm				
Structure linear density	St.Li.Dn	mm				
Structure separation	St.Sp	mm^{-1}				
Degree of anisotropy	DA					
Eigenvalue 1						
Eigenvalue 2						
Eigenvalue 3						
Fractal dimension	FD					
Number of objects	Obj.N					
Number of closed pores	Po.N(cl)					
Volume of closed pores	Po.V(cl)	mm^3				
Surface of closed pores	Po.S(cl)	mm^2				
Closed porosity (percent)	Po(cl)	%				
Volume of open pores	Po.V(op)	mm^3				
Open porosity (percent)	Po(op)	%				
Total volume of pores	Po.V(tot)	mm^3				
Total porosity (percent)	Po(tot)	%				

Default results filename	[prefix]_3D.txt/csv		Default results filename	[prefix]_i3D.txt/csv

2D integrated analysis of all objects in VOI (all selected image levels, line-by-line)				2D individual analysis of all objects in the ROI (from the single current image level only)		
Parameter	*Symbol*	*Unit*		*Parameter*	*Symbol*	*Unit*
VOI volume	TV	mm^3		Area	Ar	mm^2
Object volume	Obj.V	mm^3		Perimeter	Pm	mm
Percent object volume	Obj.V/TV	%		Form factor	FF	
VOI surface	TS	mm^2		Equivalent circle diameter	ECD	mm
Object surface	Obj.S	mm^2		Roundness	Rd	
Object surface / volume ratio	Obj.S/Obj .V	mm^{-1}		Euler number	EN	
Mean total crossectional ROI area	T.Ar	mm^2		Porosity	Po	%
Mean total crossectional ROI perimeter	T.Pm	mm		Extent	Ext	
Mean total crossectional object area	Obj.Ar	mm^2		Orientation	Or	°
Mean total crossectional object perimeter	Obj.Pm	mm		Eccentricity	Ecc	
Mean number of objects per slice	Obj.N			Centroid x		mm
Average object area per slice	Av.Obj.Ar	mm^2		Centroid y		mm
Average object equivalent circle diameter per slice	Av.Obj.E CD	mm		Moments of inertia x	MMIx	mm^4
Mean polar moment of inertia	MMI (polar)	mm^4		Moments of inertia y	MMIy	mm^4
Mean eccentricity	Ecc			Polar Moment of inertia	MMIp	mm^4
Crossectional thickness	Cs.Th	mm		Product of inertia	pI	mm^4
Structure thickness (plate model)	St.Th(pl)	mm		Minimum principal moment of inertia	MMI(min)	mm^4
Structure separation (plate model)	St.Sp(pl)	mm		Maximum principal moment of inertia	MMI(max)	mm^4
Structure linear density (plate model)	St.Li.Dn(p l)	mm^{-1}		Major axis	Ma	mm
Structure diameter (rod model)	Tb.Dm(rd)	mm		Minor axis	Mi	mm
Structure separation (rod model)	Tb.Sp(rd)	mm		Major diameter	d(max)	mm
Structure linear density (rod model)	St.Li.Dn (rd)	mm^{-1}		Minor diameter	d(min)	mm
Mean fragmentation index	Fr.I	mm^{-1}		Aspect ratio	AR	
Closed porosity (%)	Po(cl)	%		Mean Thickness	Av.Th	mm
Centroid (x)	Crd.X	mm				
Centroid (y)	Crd.Y	mm				
Centroid (z)	Crd.Z	mm				
Mean fractal dimension	FD					
Total intersection surface	i.S	mm^2				

Default results filename	[prefix]_2D.txt		Default results filename	[prefix]_3D.txt/csv

7.1 MICRO-CT EVALUATION OF SCAFFOLD POROSITY: MATERIALS AND METHODS

Three samples of each scaffolds (PCL and PCL/HA) with 5 mm in diameter and 5 mm in height, were used for the microtomographic evaluations of the morphological characteristics such as porosity and the behaviour of the scaffolds during biomechanical tests, evaluating the changes of porosity during compression steps.

The Micro-CT tests were divided into 2 steps:

The first step was to carry out an acquisition of the two scaffolds with the Micro-CT system Skyscan 1172, to evaluate total porosity, macroporosity and microporosity.

The acquisition of both scaffolds was made without using any metallic filter between the X-ray and the sample, with a source current of 167µA and a source voltage of 60kV. Both samples were rotated until 360 degrees with a rotation step of 0.30 degrees and a frame averaging of 3. The image pixel size was 3.60 µm. Moreover, the acquisition step had a duration of 1 hour.

The images, obtained from acquisition, were later reconstructed by the software NRecon (version 1.4.4) without any correction but with the specific post-alignment depended on acquisition and undersampling 1, with images dimension of pixel of 2.5 µm.

The images datasets were analyzed by CTAn (1.9.2.5. version) to evaluate 3D and 2D total porosity, macroporosity, microporosity and interconnectivity. The reconstructed images represented the entire volume of the sample.

In order to do that, a cylindrical volume of interest (VOI), totally enclosed in the scaffold, was considered, excluding lateral edges and some slices on the top and on the bottom of the scaffold. Then the images were binarized, considering the biomaterial plot as the object (white).

After binarization the 2D total porosity was calculated with the formula:

$$\frac{1}{N}\sum_{i}^{N}\frac{(T.Ar_i - Obj.Ar_i)}{T.Ar_i}$$

where N is the number of analyzed sections, T.Ar is the total Region of Interest Area and Obj.Ar is the object Area. The 3D porosity was calculated as the ratio between the total pore volume and the total volume of interest, whereas the interconnectivity was calculated as the largest volume of a single 3D pore detected, compared to the total pore volume.

The 2D distribution of pores and the number of pores throughout the entire volume of the sample were also evaluated. Using these data a count of macro and micro porosity for each scaffold was checked.

In the second step the mechanical tests of compression of both scaffolds were done.

The materials were positioned between the two plates of the compression chamber (Figure 18b) and a load started to be applied. After a displacement of 1mm, 3mm and at maximal compression, corresponding to 222N, the compression was temporarily interrupted to make acquisition.

The load was measured by an accurate tension/compression load cell. The sample should be put on the lower disc of the compression chamber, that is the part that will move up when the specimen is being compressed. The same values of acquisition and reconstruction of the first step were used and the graphs of load/displacement of the analyzed samples were recorded.

Also in this case, the obtained datasets of reconstructed images were analyzed by CTAn to evaluate the porosity and the same kind of VOI totally enclosed in the scaffold was used.

7.2 MICRO-CT SURFACE VISUALIZATION AND QUANTIFICATION OF CELLS ON THE PCL SCAFFOLD: MATERIALS AND METHODS

Micro-CT approach was used to observe cell-scaffold interaction in term of cell surface localization, visualization and colonization through the entire PCL scaffold and to make a direct comparison of the microtomographic sections with the Scanning Electron Microscopy (SEM) images of the surface.

Before cell seeding, cylindrical PCL scaffolds were divided into 2 equal pieces and sterilized by soaking in 70% ethanol (overnight), then in 1% antibiotic/PBS solution (2 hours). Finally, the materials were washed with PBS and pre-wetted in complete medium for 1 hour, to permit proteins adsorption, to promote material hydrophilicity and then cell adhesion onto PCL. A culture of MG63 was used and maintained in DMEM medium (SIGMA, St.Loius, MO), containing 10% fetal bovine serum (FBS), 2 mm L-glutamine, 100 units/ml penicillin and 100 µg/ml streptomycin in saturated atmosphere (5% CO_2/95% air), at 37°C. The cells were subcultured in flasks, detached by 0.25% trypsin/EDTA (GIBCO, Invitrogen, NY, USA) seeded dropwise in 20 µl of medium onto 0.25 cm^2 PCL surface, and placed in 24-well plates (Costar, NY, USA). This procedure allowed cell adhesion to the surface of the materials, infiltration into the porous structure and also prevented cell dispersion. After 1 hour, each scaffold was carefully removed into a new 24-well plate and covered with 1 ml of complete medium. Three samples of PCL scaffold were placed in replicate. The MG63 cell line was seeded at different densities: $1x10^5$ cells/cm^2, $2x10^5$ cells/cm^2 and $4x10^5$ cells/cm^2. Two different experimental times, 1 week and 2 weeks, were selected for the analysis of the MG63 colonization. Furthermore, PCL without cells was used as negative control, with the same culture conditions as the seeded constructs and the same endpoints.

The specimens were analyzed by Micro-CT before gold-coating and the subsequent SEM analysis. Cells haven't the intrinsic X-ray attenuation ability so they aren't seen with Micro-CT technique, thus it becomes necessary to use a contrast agent. Osmium tetroxide (OsO_4) was used because of its great affinity with lipids: it reacts with unsaturated lipids by forming black compounds containing hexavalent osmium that are visible by Micro-CT (Metsher BD, 2009).

Each specimen was scanned at a source voltage of 30 Kv and a source current of 175 µA, without filters. The samples were rotated to 180 degrees with a rotation step of 0.4 degrees and a frame averaging of 4. The pixel size was 2.5 µm and the scan duration was nearly 1 hour. The scanning dataset, obtained after the cone beam acquisition, consisted of approximately 500 images in 16-bit tiff format (4000 X 2096 pixels). The acquisition images were later reconstructed by the software NRecon (1.6.2.1. version) without corrections except for the specific misalignment for each acquisition and an accurate ring artefact reduction because of the small rotation step and the small pixel size. The image datasets in 8-bit jpg format (1000 images 4000 X 4000 pixels) were visualized with DataViewer software (1.4.3 version) to identify surface sections and to allow the direct comparison with SEM surface images.

The threshold value for image segmentation for quantification and relevant distribution of seeded cells was chosen according to attenuation histograms of the sample X-rays, i.e. scaffolds cultured with MG63 at 1 week and 2 weeks and scaffolds without MG63 at the same experimental times. The attenuation histograms of the samples referred to a cylindrical volume of interest (VOI) with a diameter of 4 mm and a height of 1.5 mm for each sample analyzed and placed within the scaffold. This VOI was placed so that it was included inside the sample and had the first section made of air outside the scaffold itself as its upper limit. For quantitative analysis of the cells the CTAnalyzer (1.11.8 version) software program was used. The cell volume within the total volume

of the scaffold was calculated in 3D and the result was expressed as 3D cell density in percent. Differences between groups were compared using analysis of variance (ANOVA) and post hoc testing with Gabriel's post hoc test.

For SEM evaluations, the same cell-scaffold constructs, used in the previous Micro-CT tests, were fixed for 2 hours in 2.5% glutaraldehyde in 0.1 M cocodylate buffer at pH 7.2, at 4°C and then, they were dehydrated in graded series of ethanol and in hexamethyldisilazane. After gold-coating, the samples were used for the SEM observation by Stereoscan200, Cambridge. The images, obtained by the backscattered electron (BSE) technique were performed at 30 KV.

7.3 MICRO-CT EVALUATION OF SCAFFOLD POROSITY: RESULTS

The μ-bimodal PCL and PCL/HA overall porosity, macroporosity, microporosity and interconnectivity before the compression tests are summarized in Table 7. It was highlighted that the scaffolds were characterized by high interconnectivity and good mechanical responses.

Tab.7. Overall porosity, macroporosity, microporosity and interconnectivity of the two scaffolds.

	PCL	PCL-HA
OVERALL POROSITY (%)	**45.3 ± 2.5**	**51.9 ± 2.5**
MACROPOROSITY(%)	**49.7±1.2**	**67.3±2.3**
MICROPOROSITY (%)	**50.3±0.7**	**32.7±3.4**
INTERCONNECTIVITY (%)	**99.7±0.12**	**98.5±0.15**

The variation of overall porosity of the polymeric scaffold, submitted to the mechanical tests, was evaluated by plotting the percentage of porosity for each slice through the volume for every step of compression analyzed, as depicted in Figure 20.

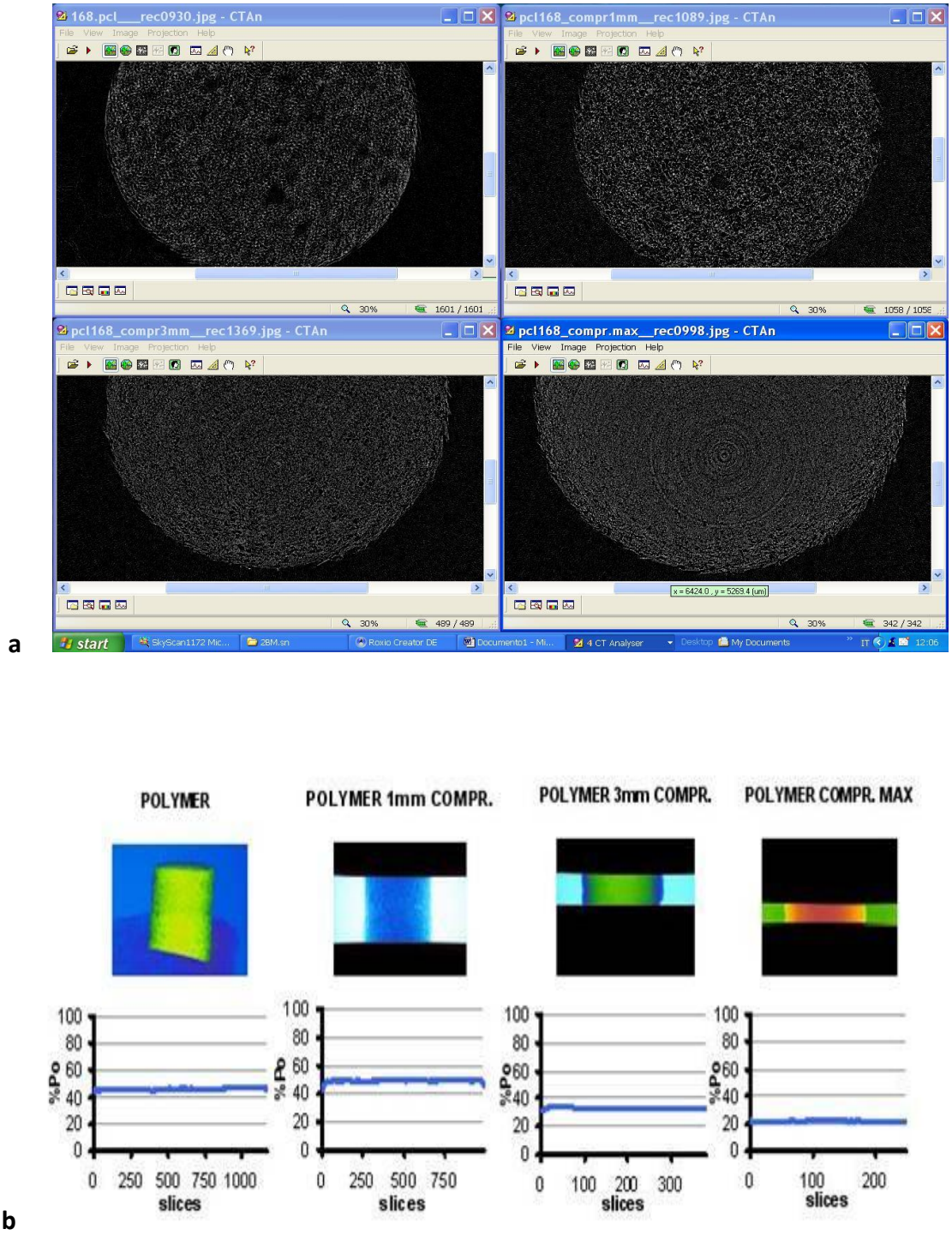

Fig.20. a) The 2D Micro-CT images of the PCL scaffold and b) the percentage of porosity through the volume for every analyzed compression steps.

It was noted a slight improvement in porosity in the first phase of compression due to an initial expansion of pores and then a progressive loss.

Nearly the same results were obtained with the PCL/HA composite, as depicted in Figure 21.

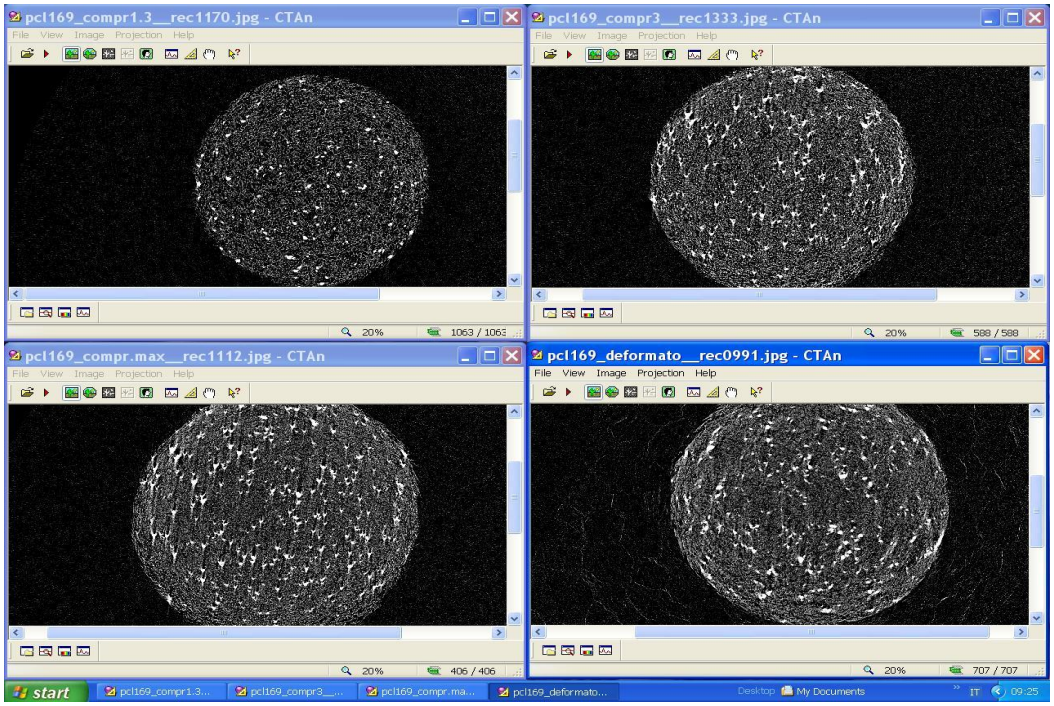

a

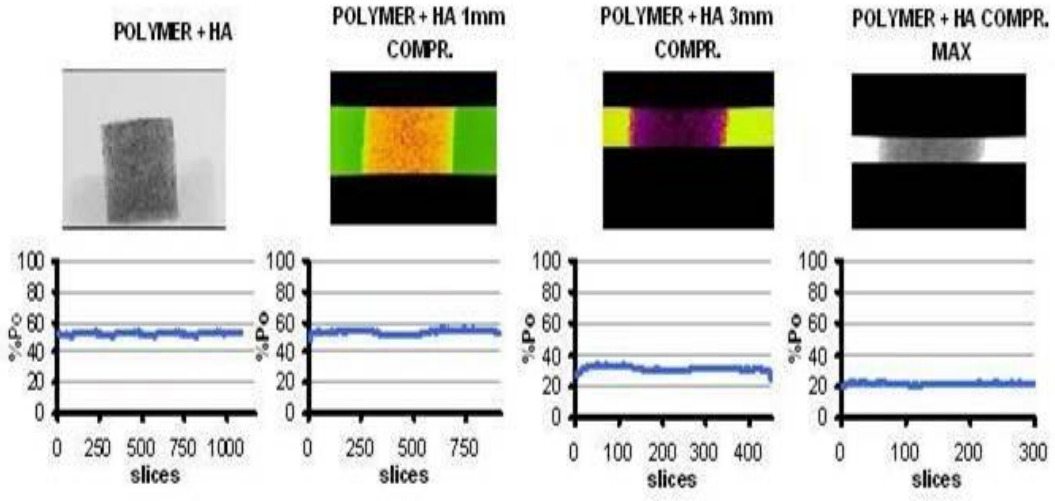

b

Fig.21. a) The 2D Micro-CT images of the PCL/HA scaffold. HA particles appeared like light grey dots. b) The percentage of porosity through the volume for every analyzed compression steps.

Moreover, the 3D and 2D analyses of overall porosity, at rest and after maximum compression, for both scaffolds were evaluated and the values are summarized in Table 8.

Tab.8. 3D and 2D overall porosity of the two scaffolds at rest and after maximum compression.

Sample	3D porosity (%)	2D porosity (%)
PCL	**45.3±2.5**	**44.5±0.3**
PCL max compression	**21.7±0.8**	**21.2±0.7**
PCL/HA	**51.9 ± 2.5**	**49.8±1.2**
PCL/HA max compression	**21.8±1**	**21.3±1.3**

The distribution of 2D size of pores, comparing the decrease of pore dimension in the samples after compression, is observed in Figure 22.

An improvement in the microporosity after the compression, in spite of an all-in loss of porosity was noted.

The graphs of load/displacement obtained, gave us information on some of the mechanical properties of the materials and it was noted that adding HA there was no significant effect on the elasticity of the polymeric scaffold. The graphs are shown in Figure 23, where the red points represent every steps of compression in which Micro-CT evaluations were done.

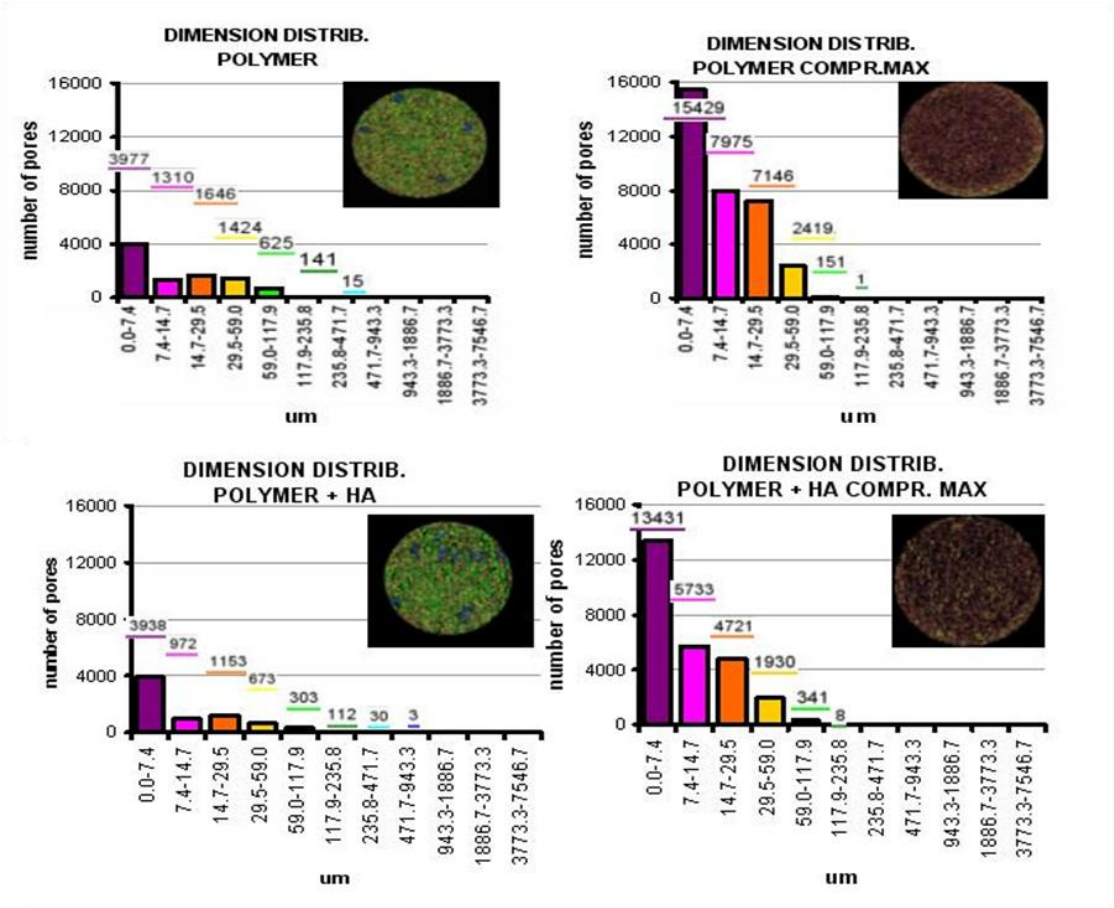

Fig.22. Istograms of the distribution of 2D size of pores for PCL and PCL/HA scaffolds, before and after maximum compression.

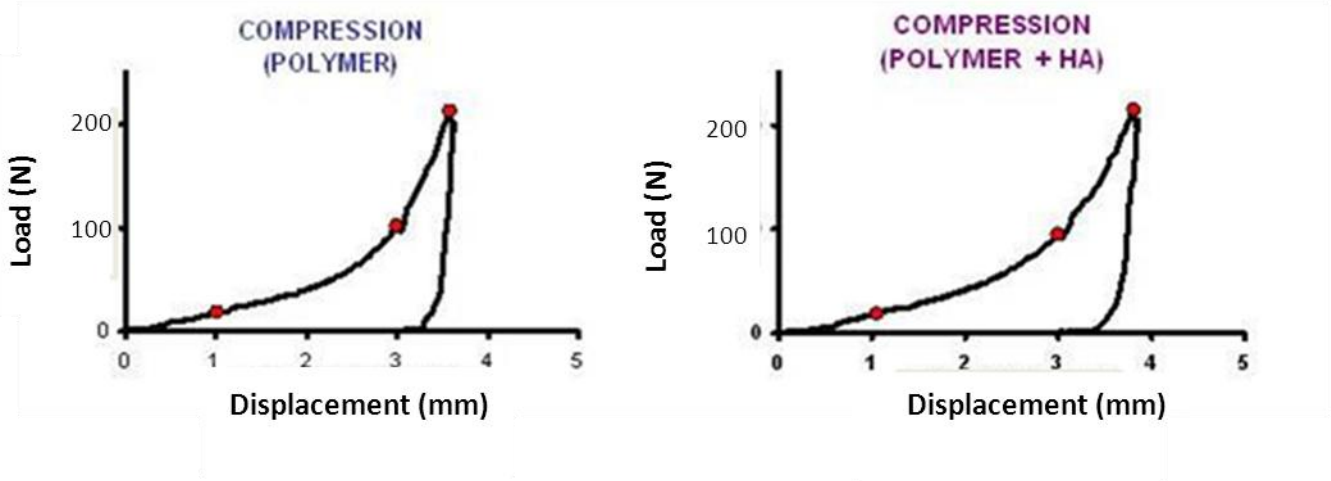

Fig.23. The load/displacement graphs for PCL and PCL/HA scaffolds. Red points represent every steps of compression in which evaluations were done.

7.4 MICRO-CT SURFACE VISUALIZATION AND QUANTIFICATION OF CELLS ON THE PCL SCAFFOLD: RESULTS

SEM and Micro-CT images of the seeding surface of the cell/scaffold constructs are reported in Figures 24. As shown, the cells proliferated and almost uniformly colonized the surface of the scaffold. Furthermore, differences in cell proliferation were observed as a function of the starting seeding density. In particular both at 1 week and at 2 weeks after seeding, the grey level contrasts were stronger with a cell density of $1x10^5$ cells/cm^2 and $4x10^5$ cells/cm^2. Conversely, the images obtained from the $2x10^5$ cells/cm^2 seeding were less bright. Moreover, the distribution of the grey level contrasts was well defined and the cells, or the cell clusters, appeared as pointed shape.

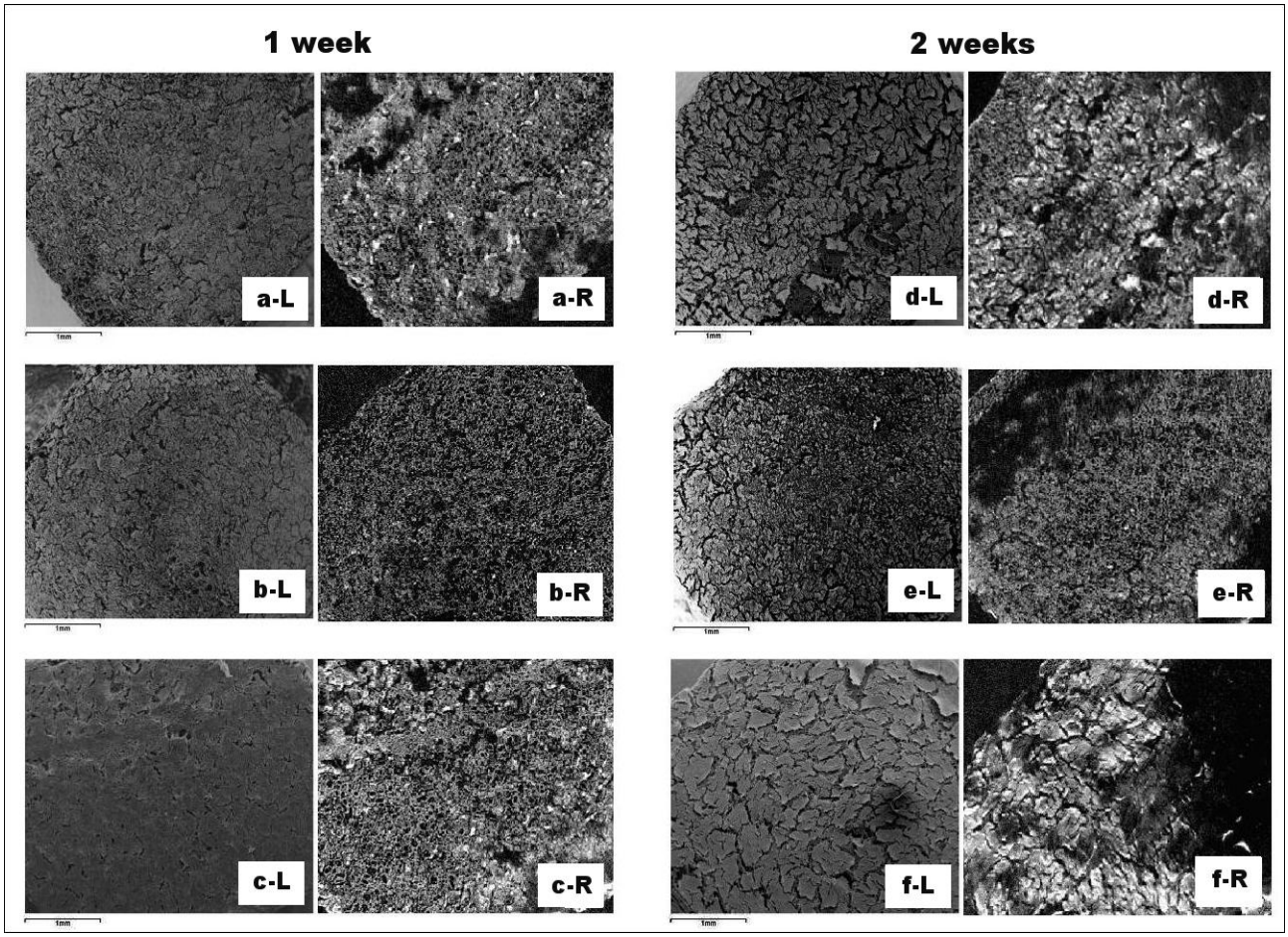

Fig.24. Images of samples surfaces seeded with MG63 cells at 1 week and at 2 weeks. L are SEM images, whereas R are Micro-CT sections. a,d: cell density of $1x10^5$ cells/cm^2. b,e: cell density of $2x10^5$ cells/cm^2. c,f: cell density of $4x10^5$ cells/cm^2.

The 3D results of cell density within the scaffold, expressed as ratio between the volume of cells detected and the total volume of the scaffold, showed an increase over time for all concentrations of seeded cells. At 2 weeks, the cell volume values increased significantly by 91% for scaffolds seeded with $1x10^5$ cells/cm^2, 178% for scaffolds seeded with $2x10^5$ cells/cm^2 and 119% for scaffolds seeded with $4x10^5$ cells/cm^2. Significant differences were found at 2 weeks between cell proliferation of the scaffolds seeded with $1x10^5$ cells/cm^2 and $2x10^5$ cells/cm^2 (p<0.05) (Figure 25).

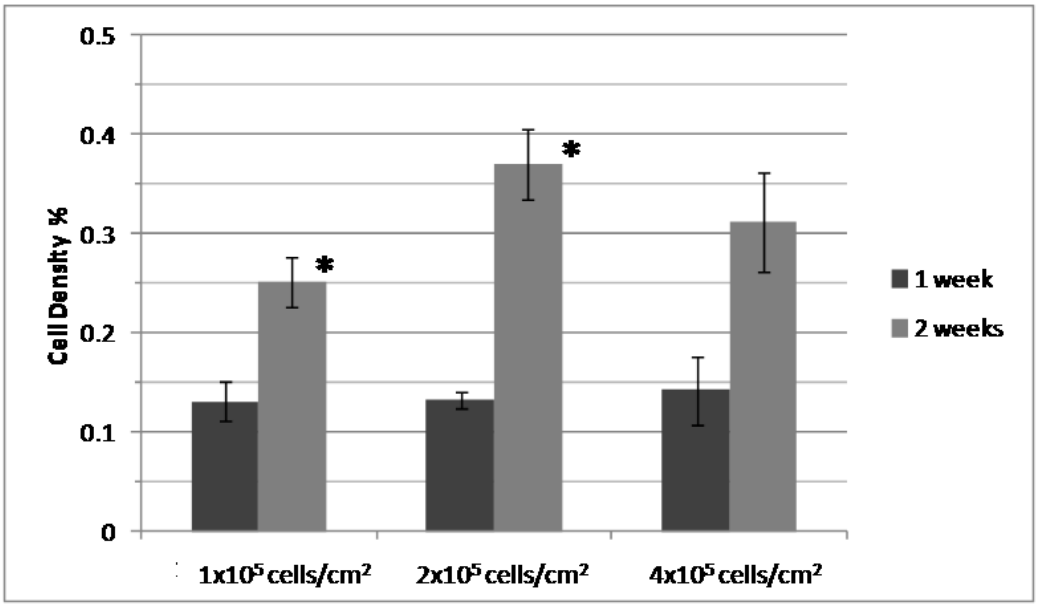

Fig.25. 3D cell density (%) of MG63 cells seeded on PCL scaffolds at different concentrations and different experimental times.* means statistical difference between scaffolds at the same experimental time (p<0.05).

The picture of the 3D models also showed the spatial distribution of cell colonization of the scaffold and provided a vision of the cell proliferation trend over time. The increase in cell number, shown by the increase in cell density within the scaffold, was thus detected more at the surface in scaffolds seeded at concentrations of $1x10^5$ cells/cm^2 and $4x10^5$ cells/cm^2, whereas seeding at a concentration of $2x10^5$ cells/cm^2 on the PCL scaffold was less evenly spread over time (Figure 26).

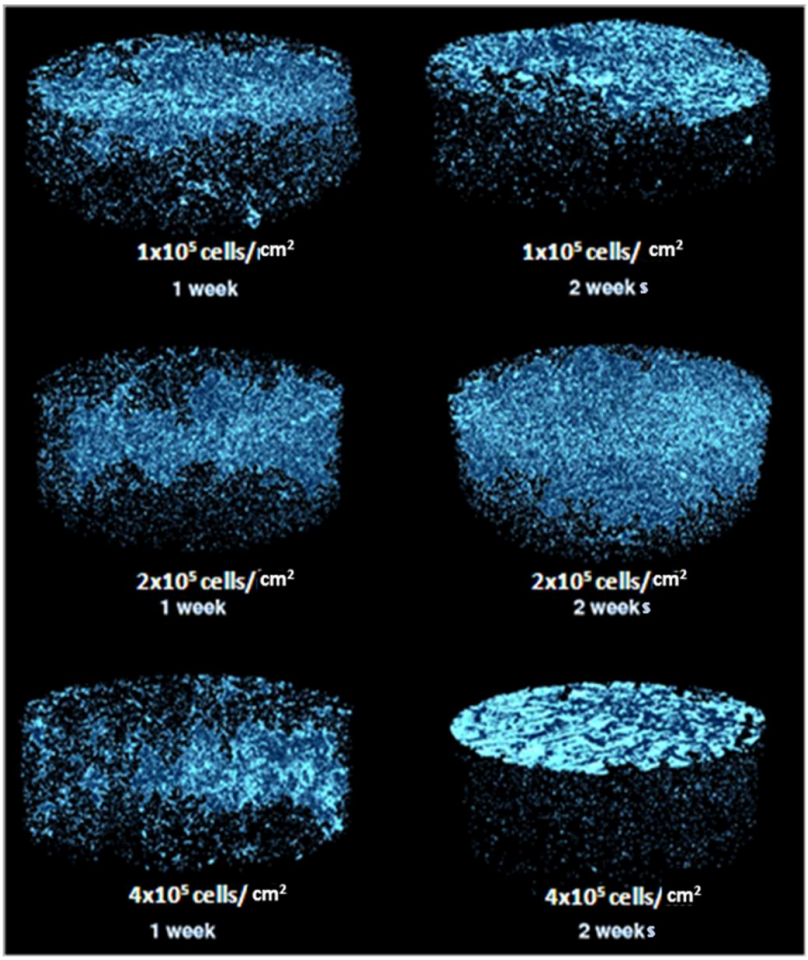

Fig.26. 3D models of PCL scaffolds seeded with different concentrations of MG63 cells at 1 week and 2 weeks after seeding.

At 2 weeks, cells seeded with an initial density of $2x10^5$ cells/cm^2, were observed more inside the scaffold than on surface, confirming the previous results of SEM and Micro-CT surface images.

8. *IN VITRO* STUDY

Based on the different kind of tissues in which the device will be implanted, there are different models for the biocompatibility evaluation (UNI EN ISO 10993-1:2010). Among the first biocompatibility evaluation tests, cytotoxicity studies are developed to determine the *in vitro* biological response, using appropriate biological parameters (UNI EN ISO 10993-5:2009).

8.1 MATERIALS AND METHODS

In the present study, all materials, were tested as cylinders (6 mm diameter x 2 mm height) and a human osteoblast-like cell line (MG63) was used. Before *in vitro* tests, materials were sterilized by γ-rays at 25 KGy (Gammarad, Bologna, Italy). Cells were cultured in sterile DMEM (with 10% foetal calf serum, 100 U/ml penicillin and 100 µg/ml streptomycin) at 37°C in a 95% air/5% CO_2 atmosphere. Cells at confluence were released with 0.05% (w/v) trypsin and 0.02% (w/v) EDTA, and counted with Trypan Blue exclusion dye (Sigma) in an Neubauer counting chamber. Briefly, cells were centrifuged at 1100 rpm for 5 minutes and then resuspended in 1ml of medium. Ten µl of cell suspension were added to a solution of 50 µl of 0.4% Trypan Blue and 40µl of NaCl 0.9% and subsequently, ten µl of this solution were transferred in the Neubauer chamber and cells were counted under light microscope at 10x of magnification in four squares of the chamber. Died cells appeared blue, while viable cells were colourless. The viable cell number was obtained by the following equation:

$$\text{Viable cells} = \text{cell count/squares} \times \text{dilution factor} \times 10^4$$

where the dilution factor is 10 and 10^4 is the chamber area.

A cell concentration of $1x10^5$ cells /ml was seeded, in triplicate, in three 24-wells plates, on sterile materials to be tested (3 PCL and 3 PCL/HA materials for each plates).

The same amount of cells was seeded in empty wells as negative control (CTR). One ml of DMEM was added to all the wells. Plates were cultured in standard conditions, at 37°C with 95% humidity and 5% CO_2 for 24 hours, 7 and 14 days (3 experimental times) and the medium was changed twice a week. At 24 h, medium was changed with DMEM additioned with β-glicerophosphate (10^{-8} nM) and Ascorbic acid (50 mg/ml) to activate osteoblasts. For the production of osteocalcin the culture medium was enriched with $1,25(OH)_2D_3$, 48 h before end of the experimental times. At 4 and 24 hours, early evaluations of cell adhesion and morphology (neutral red staining), were tested, respectively. The Lactate dehydrogenase release (LDH), also evaluated at 24 hours, is an indirect cytotoxicity parameter, because the release of this enzyme is an index of the irreversible lysis of cellular membranes. At the end of experimental times the supernatants were collected and centrifuged to remove particulates, if any. Aliquots were dispensed in Eppendorf tubes for storage at -20°C for following quantitative tests: Bone-specific alkaline phosphatase activity (BAP), Osteocalcin (OC), Type I pro-collagen production (CICP) and Transforming growth Factor β1 (TGF-β1), Tumor Necrosis Factor α (TNF-α) and Interleukin 6 (IL-6) release. All the measured concentrations were evaluated at 7 and 14 days and normalized by Total Protein (TP, Total Protein micro-Lowry kit, SIGMA). At 24 hours, 7 and 14 days, WST-1 proliferation test was performed to assess cell proliferation rate and a reduction of the vitality more than 30% than control is an index of cytotoxicity.

8.1.1 Cell adhesion and morphology

- Cell adhesion: After an incubation of 4 hours, to let the cells to adhere to the substrate, the medium with the non- adherent cells was collected. The cells in suspension were counted and the results were given as percentage:

$$\text{Adherent cells} = (\text{seeded cells} - \text{non-adherent cells}) \times 100$$

-Cell morphology: A 0.033% solution of Neutral Red staining (Sigma, lot 57H2326) was added to culture medium of all wells for 90 min. Cultures were examined by microscopy (Olympus mod.1X71) at 10 and 4 x of magnification for the evaluation of cell morphology and explanatory images were selected. The cell morphology was evaluated by the following qualitative score (Qualitative morphological grading cytotoxicity-ISO 10993-5:2009 E) in Table 9.

Tab.9. Qualitative morphological grading of cytotoxicity

Grade	Reactivity	Conditions of all cultures
0	None	Discrete intracytoplasmatic granules, no cell lysis, no reduction of cell growth.
1	Slight	Not more than 20% of the cells are round, loosely attached and without intracytoplasmatic granules, or show changes in morphology; occasional lysed cells are present; only slight growth inhibition observable.
2	Mild	Not more than 50% of the cells are round, devoid of intracytoplasmatic granules, no extensive cell lysis; not more than 50% growth inhibition observable.
3	Moderate	Not more than 70% of the cell layers contain rounded cells or are lysed; cell layers not completely destroyed, but more than 50% growth inhibition observable.
4	Severe	Nearly complete or complete destruction of the cell layers.

8.1.2 Cell proliferation and viability

At 24 hours, 7 and 14 days, the Cell Proliferation Reagent WST-1 (Roche Diagnostics, GmbH, Mannheim, Germany) test was performed to assess cell proliferation and viability. WST-1 reagent contains tetrazolium salts that are cleaved to colored formazan by mitochondrial enzymes of cells (Berridge MV, et al., 1996). An expansion in the number of viable cells results in an increase in the overall activity of mitochondrial dehydrogenases in the sample. This augmentation in enzyme activity leads to an increase in the amount of formazan dye formed, which directly correlates to the number of metabolically active cells in the culture.

Briefly, 100 µl of WST-1 solution and 900 µl of medium (final dilution 1:10) were added to the cell monolayer, and the multi-well plates were incubated at 37°C for further 4 hours. Supernatants were quantified spectrophotometrically at 450 nm with a reference wavelength of 640 nm. Results of this test were reported as optical density (OD).

8.1.3 Lactate dehydrogenase release (LDH)

LDH reagent (Sigma Diagnostic, St Louis, MO) was used for the quantitative determination of LDH in the 24 hours supernatants. The reagent catalyzes the oxidation of lactate to pyruvate with simultaneous reduction of nicotinamide adenine dinucleotide (NADH) (Heffner J, et al., 1997). The formation of NADH results in an increase in absorbance measured at 340 nm. The rate of increase in absorbance is directly proportional to LDH activity in the sample. This test is a marker of cytotoxicity because only non-viable cells, with disrupted cellular membranes, release LDH.

8.1.4 Bone-specific alkaline phosphatase activity (BAP)

The skeletal, or bone-specific isoform of alkaline phosphatase is a tetrameric glycoprotein found on the cell surface of osteoblasts. BAP is an early differentiation marker of osteoblasts and it is involved in preparing the extracellular matrix for the ordered deposition of mineral component of bone (Price CP, 1993; Whyte MP, 1994). BAP immunoassay (Quidel Corporation, San Diego, CA, USA) was performed and provided a quantitative measure of BAP activity of MG63 cultured on both scaffolds and CTR. The concentration was evaluated at 405 nm in a microplate reader, using a standard curve.

8.1.5 Osteocalcin measurements (OC)

OC is found exclusively in bone tissue, is the most abundant noncollagenous protein of the extracellular bone matrix, is a highly-specific late osteoblast marker, and may be useful as a biochemical indicator of bone turnover.

It is a 5800 molecular weight protein produced by osteoblasts; it contains three gamma-carboxyglutamic acid residues that are thought to be involved in calcium ion and hydroxyapatite binding (Puchacz E, et al., 1989). The OC quantitative determination was assessed by the OC immunoassay (Quidel Corporation, San Diego, CA, USA) on collected supernatants. The OC concentration was evaluated at 405 nm in a microplate reader, using a standard curve.

8.1.6 Type I pro-collagen production (CICP)

Type I collagen is the primary organic constituent of bone: it forms about 90% of the organic material in bone matrix and bone hydroxyapatite crystals attach to the collagen fibrils in relation to the forces applied to bone. Its levels have been linked to bone growth and formation (Parfitt AM, et al., 1987-B). It is a triple-helical molecule, which forms the fibrous framework of all connective tissues and is synthesized as procollagen, a larger precursor molecule. Procollagen consists of mature collagen with extension peptides at both the amino and carboxy termini. These extension peptides, or propeptides, are cleaved from the collagen molecule by specific proteases prior to incorporation of collagen into a growing collagen fibril. The release of these peptides into the circulation provides a stechiometric representation of the production of collagen. Levels of CICP are indicative of collagen production *in vivo*. The determination of type I collagen production was based on the amount of CICP present in the cell supernatants and measured using a specific enzyme-linked immunoassay (Quidel Corporation, San Diego, CA, USA). The concentration was evaluated in a microplate reader at 405 nm, using a standard curve.

8.1.7 Transforming growth factor β1 release (TGF-β1)

TGF-β1, a member of the bone morphogenetic protein superfamily, is synthesized, with only few exceptions, by virtually all cells, enhances the deposition of extracellular matrix through promotion of synthesis and inhibition of degradation.

It plays critical roles in growth regulation and development, inhibits proliferation of most cells, but can stimulate the growth of some mesenchymal cells and can exert immunosuppressive effects. Moreover, it is inhibitive to T-and B- cell proliferation as well as to maturation and activation of macrophages, inhibits activity of natural killer cells and lymphokine activated killer cells and blocks production of cytokines. In the bone tissue, TGF-β1 is reported to increase preosteoblastic cell proliferation, to promote osteoblast differentiation and to stimulate extracellular matrix production (Barnes GL, et al., 1999). TGF-β1 was measured using the assay (Quantikine Human TGF-β1, R&D Systems, CA, USA) in cell culture supernatant by employing a quantitative sandwich enzyme immunoassay technique. The concentration was evaluated at 450/540 nm in a microplate reader, using a standard curve.

8.1.8 Tumor necrosis factor α release (TNF-α)

It is a polypeptide cytokine, produced by monocytes and macrophages and it acts as a multipotent modulator of immune response and further as a potent pyrogen. TNF-α activates neutrophils, altering the properties of vascular endothelial cells, regulating metabolic activities of other tissues, as well as exhibiting tumoricidal activity. Its production is mediated by the action of lymphokines and endotoxins on the macrophage and it may play a significant role in the pathogenesis of inflammatory disease of the joints and other tissues. It is a pleiotropic cytokine that plays a central role in inflammation and apoptosis. It is reported that TNF-α promotes inflammatory cell infiltration, serves as chemotactic agent for monocytes and activates phagocytic mechanisms (MacEwan DJ, 2002). TNF-α regulates, also, the differentiation of hematopoietic stem and progenitor cells: in bone tissue, it induces bone resorption by stimulating the production of osteoclasts and by increasing the bone-resorbing activity of formed osteoclasts.

A quantitative sandwich enzyme immunoassay against human TNF-α (R&D Systems, CA, USA) was performed and its concentration was evaluated at 450/540 nm in a microplate reader, using a standard curve.

8.1.9 Interleukin 6 release (IL-6)

While a number of interleukins are seemingly pleiotrophic in their effects, IL-6 may be considered the prototypic pleiotrophic cytokine. It is a variably glycosylated, 22-27 kDa secreted glycoprotein that serves as a prototype for a family of molecules that includes leukemia inhibitory factor (LIF), oncostatin M (OSM), ciliary neurotrophic factor (CNTF), cardiotrophin-1 (CT-1) and IL-11. Cells, known to express IL-6, include CD8+ T cells, fibroblasts, synoviocytes, adipocytes, osteoblasts, megakaryocytes, endhotelial cells, sympathetic neurons, cerebral cortex neurons, cromaffin cells of the adrenal medulla, retinal pigment cells, mast cells, keratinocytes, Langerhans cells, fetal and adult astrocytes, neuthophils, monocytes, eosinophils, colonic epithelial cells, B1 B cells, and pancreatic islet beta cells (Kishimoto T, et al., 1995). IL-6 production is generally correlated with cell activation and it can be found in the blood of normal individuals in the 1 pg/ml range, with modest elevations in certain cancers (melanoma) (10 pg/ml), and large elevations after surgery (30-430 pg/ml). IL-6 has been described as a pro-inflammatory molecule, a modulator of bone resorption, a promoter of hematopoiesis, and an inducer of plasma cell development. It also has been shown to influence IL-4 production. The various activities of IL-6 suggest that this factor will have a major role in the mediation of the inflammatory and immune responses initiated by infection or injury. Particularly, it is considered a marker of the low tolerance of a biomaterial both *in vitro* and *in vivo* and is a modulator of bone resorption. It was measured using the assay (Human IL-6 Immunoassay kit, R&D Systems, CA, USA) in cell supernatant by employing the

quantitative sandwich enzyme immunoassay technique. The concentration was evaluated at 450/540 nm in a microplate reader, using a standard curve.

8.1.10 Total protein quantification

The method of Lowry has been, for decades, the procedure of choice for quantification of soluble proteins due to its sensitivity, simplicity and precision. The procedure, used in this thesis, was based on Peterson's modification of the micro Lowry method and used sodium dodecylsulfate, to facilitate the dissolution of relatively insoluble lipoproteins. The procedure is based on two chemical reactions. The first is the biuret reaction, in which the alkaline cupric tartrate reagent complexes with the peptide bonds of the protein. This is followed by the reduction of the Folin & Ciocalteu's phenol reagent, which yields a purple color (Peterson GL, 1977). Absorbance of the colored solution was red at a suitable wavelength between 500 nm and 800 nm.

8.2 STATISTICAL ANALYSIS

Statistical evaluation of data was performed using the software package SPSS/PC^{+} Statistics ^{TM} 10.1 (SPSS Inc., Chicago, IL USA). Data are reported as mean ± standard deviations (SD) of triplicate at a significance level of $p<0.05$. After having verified normal distribution and homogeneity of variance, a one-way ANOVA was done for comparison between groups. The Scheffé's post hoc multiple comparison tests were performed to detect significant differences between groups.

8.3 RESULTS

8.3.1 Cell adhesion and morphology

-The results of adhesion, for MG63 cells, grown on tested materials, are summarized in Table 10. MG63 adhesion, after 4 h of incubation, on PCL and PCL/HA was normalized to that of CTR (100%), and no significant differences were found among the two scaffolds.

Tab.10. Results of MG63 adhesion on PCL and PCL/HA (n=3). Results are reported as mean ± standard deviation (SD).

MATERIAL	ADHESION
PCL	85 ± 2.3%
PCL/HA	89 ± 3.0%

-The cells, grown on both scaffolds, appeared well stained with a normal morphology (0 degree) as cells of control group. The cells appeared spindly with well defined cellular membranes and without lysis or reduced proliferation, in comparison to the control (Figures 27).

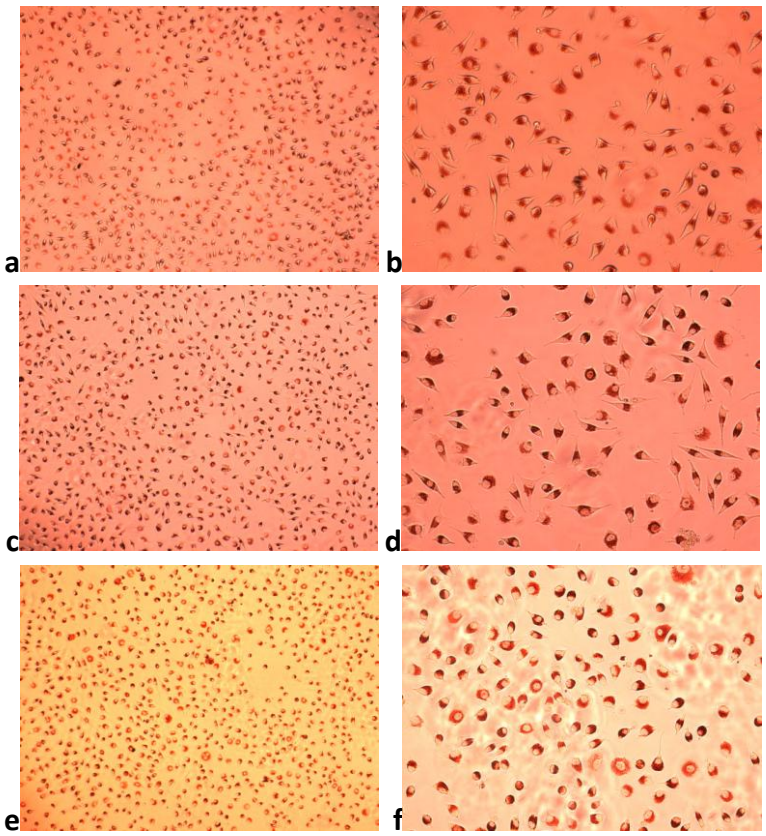

Fig.27. Neutral red staining. a, c, e magnification 10x; b, d, f magnification 4x. MG63 a, b) seeded on PCL; c, d) seeded on PCL/HA and e, f) in empty wells (control). (Images from Laboratory of Preclinical and Surgical Studies-IOR).

8.3.2 Cell proliferation and viability

In Figure 28, the WST-1 viability test highlighted that cells, seeded onto the two scaffolds, at 24 hours, proliferated well as control, without significant differences. At 7 days cells, on PCL/HA scaffold, proliferated significantly less than on PCL and control (CTR); at 14 days differences of viability between the two scaffolds were not observed, while cells grew significantly less on both two scaffolds than in empty wells (CTR). Moreover, cells seeded on both materials and CTR significantly increased proliferation between 24 hours and 7 days, while not between 7 and 14 days.

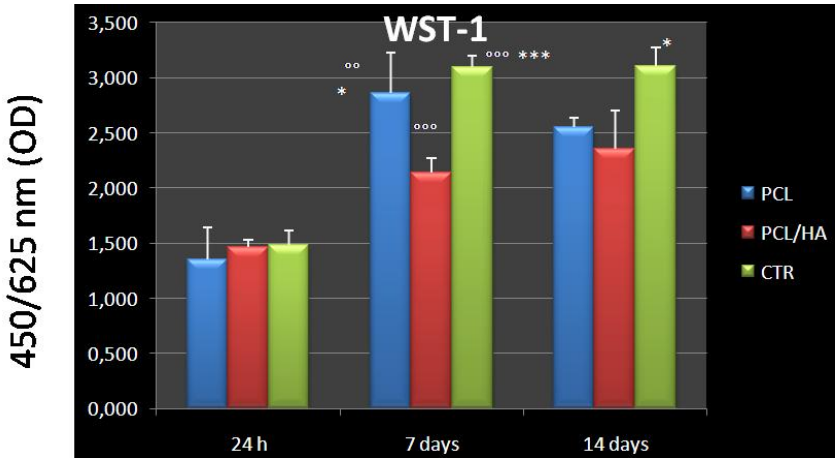

Fig.28. At 24 hours, no significant differences among materials and control were observed.
At 7 days, *** p<0.0005: CTR *Vs* PCL/HA; *p<0.05: PCL *Vs* PCL/HA. At 14 days, *p<0.05: CTR *Vs* PCL/HA and PCL. °°p<0.005: 7 days *Vs* 24 hours (PCL); °°°p<0.0005: 7 days *Vs* 24 hours (PCL/HA and CTR).

8.3.3 Lactate dehydrogenase release (LDH)

LDH release did not show significant differences among the two scaffolds and control (Figure 29).

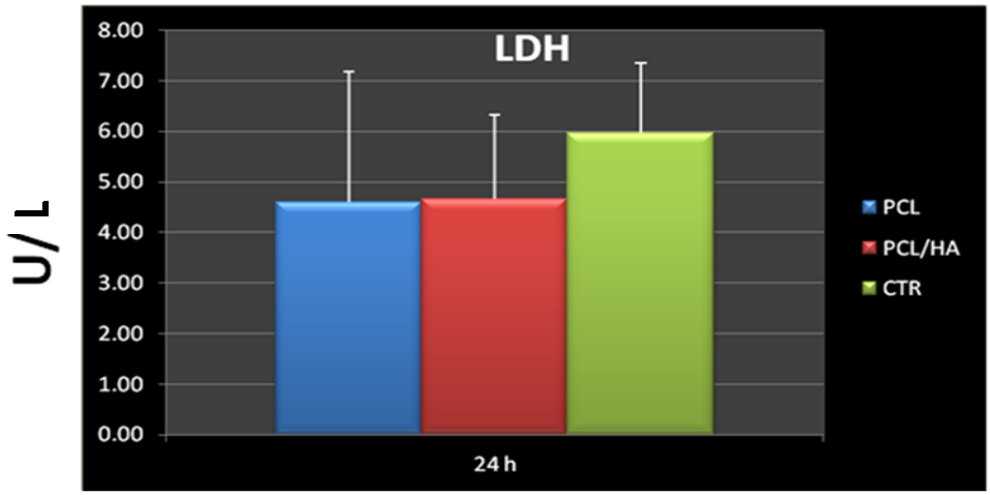

Fig.29. No significant differences were observed among the scaffolds and control.

8.3.4 Bone-specific alkaline phosphatase activity (BAP)

As far as the differentiation markers were concerned, BAP values (Figure 30), an early marker of osteoblast differentiation, were significantly higher at 7 days for PCL/HA as compared to PCL and control, while at 14 days, for PCL/HA as compared only to control. No significant differences were observed between the two experimental times.

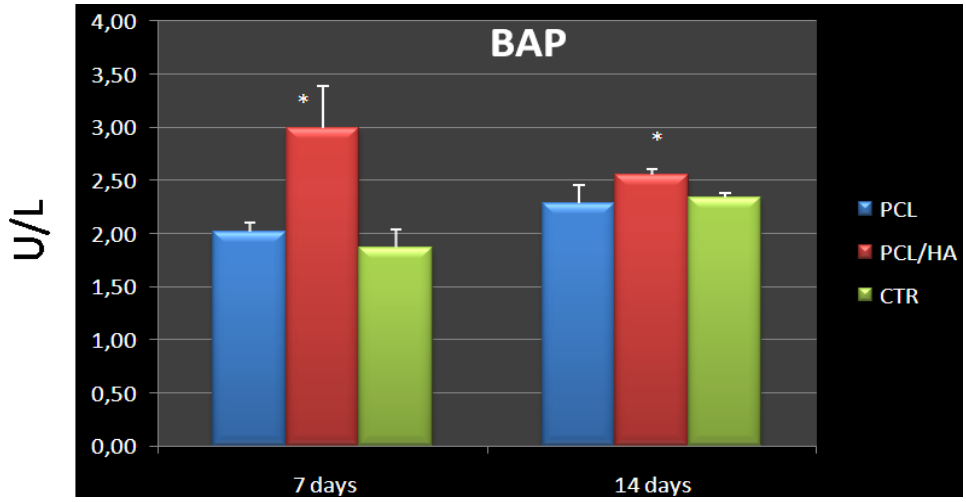

Fig.30. At 7 days, *p<0.05: PCL/HA *Vs* CTR and PCL. At 14 days, *p<0.05: PCL/HA *Vs* CTR. No significant differences between the two experimental times were observed.

8.3.5 Osteocalcin measurements (OC)

The levels of OC, a late marker of osteoblast differentiation, were significantly higher only on PCL/HA as compared to PCL, at 7 days. Moreover, its production significantly increased on both scaffolds and control between 7 and 14 days (Figure 31).

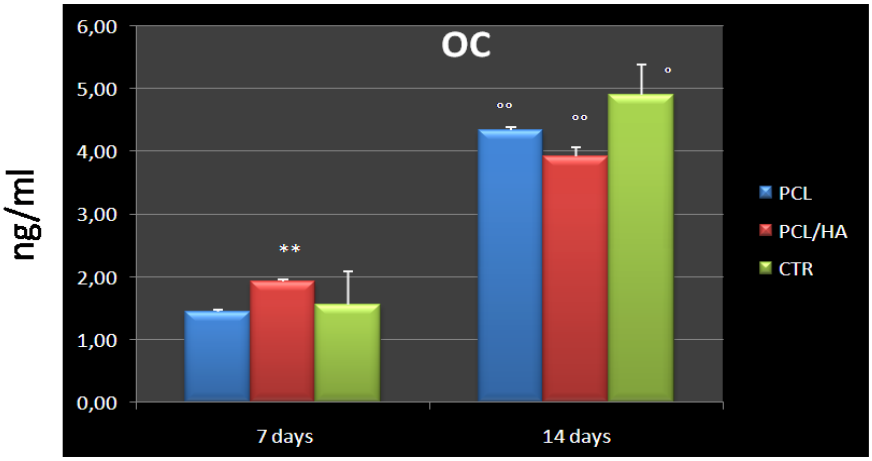

Fig.31. At 7 days, ***p*<0.005: PCL/HA *Vs* PCL. °*p*<0.05:14 days *Vs* 7 days (CTR); °°*p*<0.005:14 days *Vs* 7 days (PCL and PCL/HA).

8.3.6 Type I pro-collagen production (CICP)

In the CICP secretion (Figure 32), it could be observed that, at 7 days, cells seeded on PCL/HA scaffold produced significantly higher value than on PCL. No significant differences were observed among scaffolds and control at 14 days and between 7 and 14 days for all the scaffolds and control.

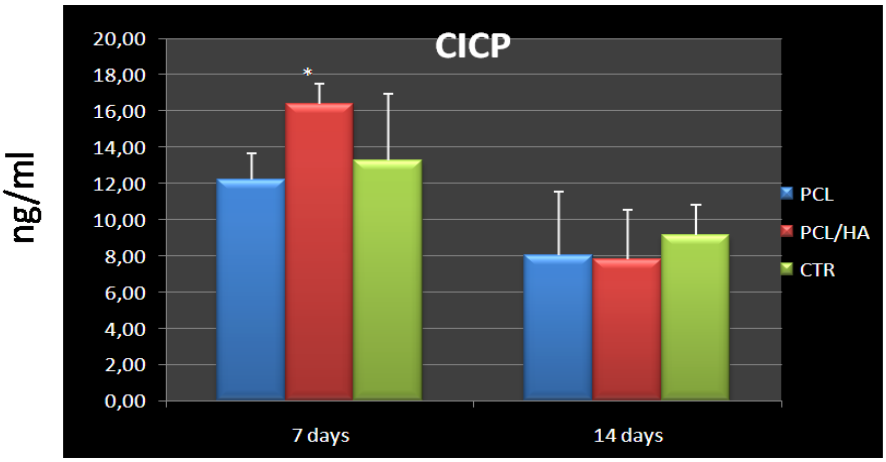

Fig.32. At 7 days, **p*<0.05: PCL/HA *Vs* PCL. No significant differences were observed at 14 days and between the two experimental times.

8.3.7 Transforming growth factor β1 release (TGF-β1)

As observed in Figure 33, cells cultivated on both scaffolds and control at both experimental times produced TGF-β1 without significant differences. Moreover no significant differences were noted between the experimental times for all the scaffolds.

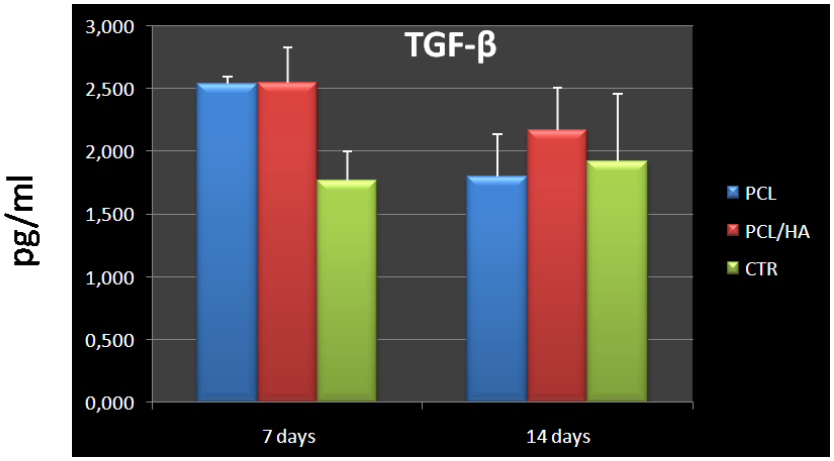

Fig.33. No significant differences were observed among the two scaffolds and control, at 7 and 14 days, and between the two experimental times.

8.3.8 Tumor necrosis factor α release (TNF-α)

TNF-α levels showed no significant differences among scaffolds and control at 7 and 14 days. Moreover, its production, on PCL/HA, was significantly lower at 14 days as compared to that at 7 days (Figure 34).

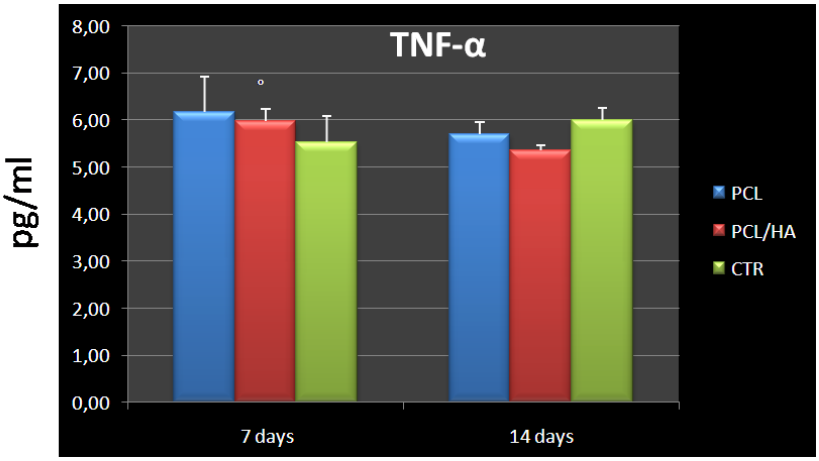

Fig.34. No significant differences were observed among the two scaffolds and control at 7 and 14 days. °p<0.05: 7 days *Vs* 14 days (PCL/HA).

8.3.9 Interleukin 6 release (IL-6)

No significant differences were observed among scaffolds and control at 7 and 14 days and between the 2 experimental times (Figure 35).

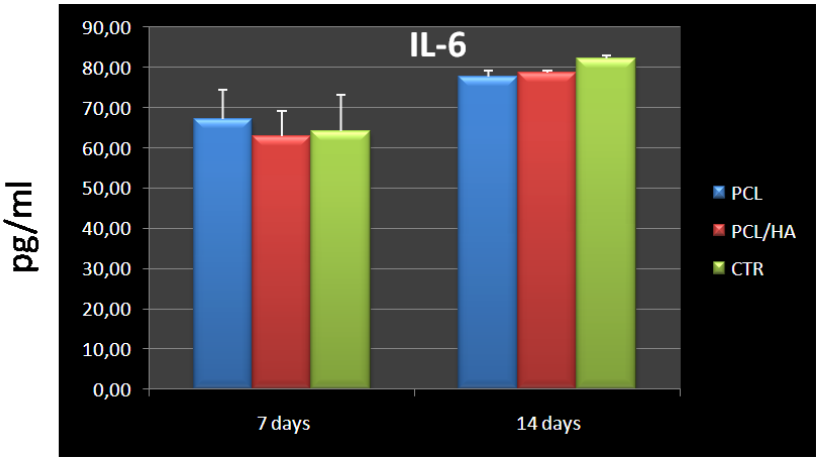

Fig.35. No significant differences were observed among the two scaffolds and control at 7 and 14 days and between the two experimental times.

9. *IN VIVO* STUDY

A biological response to a scaffold, implanted in a human host, is characterized by physiological effects from surgery trauma, the presence of the implant, the subsequent inflammatory reaction and the remodeling of the nearly tissue. All these factors might be evaluated by *in vivo* animal models, because the pre-clinical efficacy of every innovative therapies, based on the implant of bioactive or engineered materials, requires a preclinical evaluation (Fini M, et al., 2006).

This phase is performed according to European and Italian legislation on animal experimentation: Law by Decree January 27, 1992, No.116. and the ethical principles state in the "Guide for the Care and Use of Laboratory Animals". Briefly, in this thesis, the experimental animal protocol was sent and approved by the Scientific Ethical Committee, responsible public authorities of Rizzoli Orthopaedic Institute and the Italian Ministry of Health. Following laws on animal experimentation, animals were acquired from authorized farms, submitted to a quarantine period (10 days) before the utilization and to a standard and controlled diet. All surgical procedures were performed under general anaesthesia, with the control of animal welfare by a veterinarian and with post-operative analgesic therapy in order to avoid pain and suffering. In order to reduce the species variability, a sufficient number of animals per group, homogeneous for sex, age, nutrition and environment, was chosen (Buma P, et al., 2004).

9.1 MATERIALS AND METHODS

Fourteen skeletally mature, adult male New Zealand rabbits (Charles River, Calco, Lecco, Italy), with a body weight of 2.7 ± 0.3 Kg, were housed under controlled conditions (room temperature 22±0.5 °C; relative humidity 55±5%; 12 h of light and 12 h of darkness) and were supplied with standard diets and water ad libitum. At time of surgery, a general anaesthesia was induced with an intramuscular injection of 44 mg/kg Ketamine (Imalgene 1000, Merial Italia S.p.A, Assago-Milano, Italy) and 3 mg/kg Xylazine (Rompun Bayer AG, Leverkusen, Germany), and assisted ventilation (O_2:1 l/min; Air: 0.4 l/min; Sevorane: 2.5–3%). In sterilized conditions, after shaving, disinfection and sterile draping of the operation site, a 2-cm skin incision was made on the lateral aspect of distal femoral condyles of both legs. Bilateral confined cancellous defects were drilled in both limbs with a growing diameter drill (from 3.2 mm to 5 mm in diameter), obtaining a defect with 5 mm in diameter and 10 mm in depth (Figures 36). All the defects were carefully rinsed with Ringer's solution and cleaned out, so that any abraded particles, formed during drilling, were removed.

In all fourteen rabbits, the left defect was treated with PCL/HA scaffold, while the right one with PCL (cylinders of 5 mm in diameter and 10 mm in height). Seven rabbits were euthanized after 4 weeks (Group 1) and the others after 12 weeks (Group 2). Eleven and four days before euthanasia, the animals received two intramuscular injections of oxytetracycline (30 mg/Kg). This antibiotic bounds selectively to new-formed bone tissue and is visible with fluorescence techniques. At the end of the experimental times, under general anaesthesia, the animals were pharmacologically euthanized with intravenous injection of 1 ml Tanax (Hoechst AG, Frankfurt-am-Mein, Germany). Femurs were removed, stripped of soft tissues and, after macroscopic observation, were processed for histological and histomorphometric evaluations.

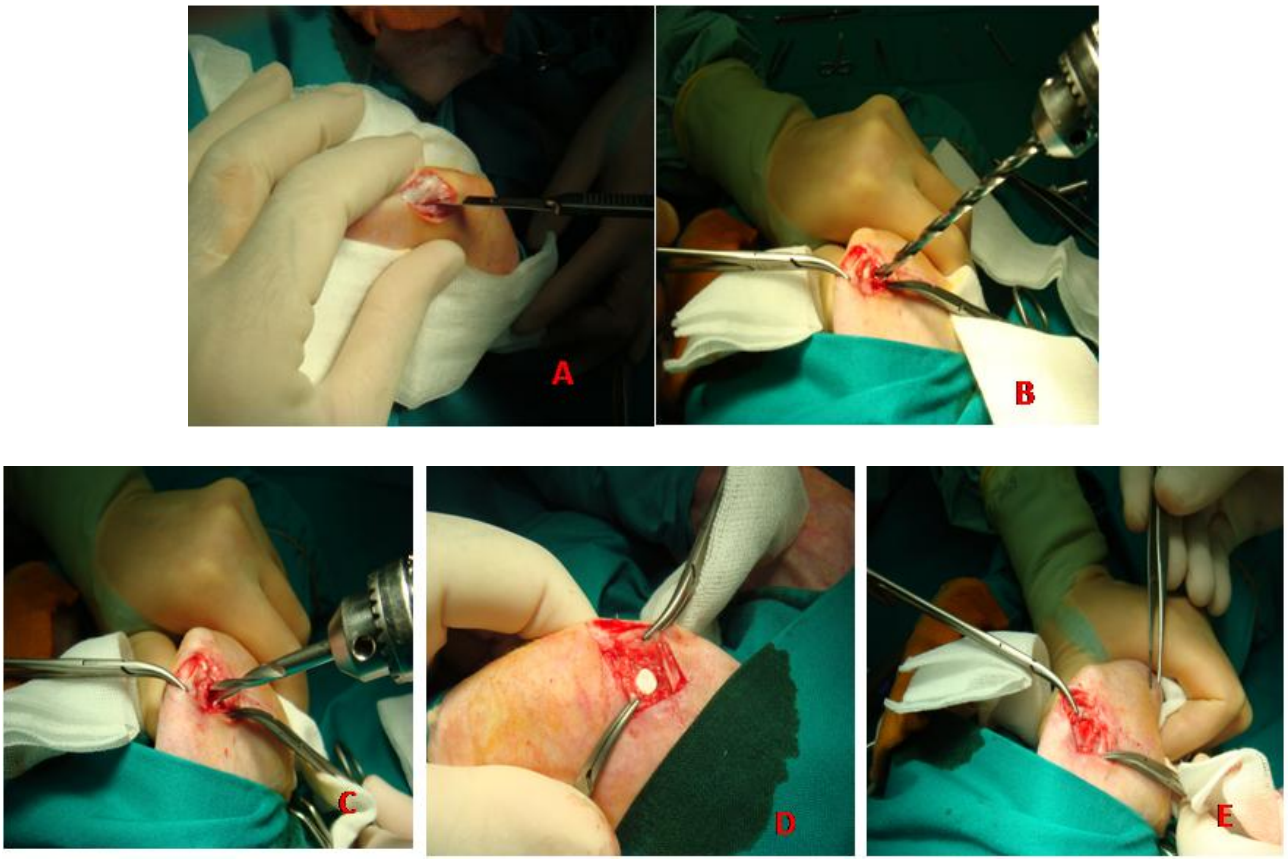

Fig.36. A: skin incision; B-C-D-E: utilize of drills with growing diameters to obtain a bone defect of 5 mm in diameter and 10±0.5 mm in depth. (Images from Laboratory of Preclinical and Surgical Studies-IOR).

9.1.1 Histology and histomorphometry

The femoral condyles of rabbits were fixed in 4% para-formaldehyde for 48 h for undecalcified bone processing; the samples were then dehydrated in graded series of alcohols for 24h, respectively (50°, 75°, 95° twice and 100° twice). After a 24h-infiltration period in methylmetacrilate, they were finally embedded in poly-methylmetacrilate (Merck, Schuchardt, Hohenbrunn, Germany). Femur blocks were sectioned along a plane parallel to the longitudinal axis of femour with Leica 1600 diamond saw microtome (Leica SpA, Milan, Italy), obtaining a series of sections of 100±10 µm in thickness.

Subsequently these sections were thinned and polished (Struers Dap-7, Struers Tech, Denmark) to a thickness of 30 ± 10 µm.

Histology and Static histomorphometry

A total of three consecutive sections for each sample were obtained, stained with Toluidine blue, Acid fuchsin and Fast Green and analyzed for histological and histomorphometric evaluations. Toluidine Blue is a basic stain, that bounds to electrically negative structures (nucleic acid) and especially to glycosaminoglycans and proteoglycans (cartilage fundamental substance), making cartilage blue. Fast green contains acrylic groups, bounding to bone structure, making this tissue green. Acid fuchsin is an organic stain, used in association with the other stains. All of them, combined, represent the routine staining for the bone and cartilage tissues. Histological and histomorphometric analyses were performed by means of a light optic Olympus BX41 microscope (Olympus Italia Srl, Milano, Italy) at different magnifications and the QWIN image analysis software (Leica Imaging Systems Ltd, Cambridge; England). Histological evaluation was performed at different magnifications (1.25x, 2x, 20x and 40x).

For static histomorphometry, three parameters were evaluated:

- BONE HEALING RATE (BHR, %): represents the healing of the bone defect in terms of decrease of its area. It was calculated by the ratio of decreased bone defect area, after scaffolds implantation, with the initial area of the defect (initial defect area=19,6 mm^2) expressed as percentage. For BHR evaluations, the area of the defect was manually measured with Leica QWIN software at 1.25x of magnification.
- BONE AREA: the new bone was measured outside (BAr/TAr) and inside (BAr/TAr_{int}) the implanted scaffolds and it was expressed as percentage of newly formed bone divided by the area of the entire analyzed region. Briefly, 4 region of interests (ROIs), at 20x of magnification, were selected to cover the entire condyle defect. The ROIs were binarized, by means of the Leica QWIN software.

Dynamic histomorphometry

Subsequently, other 3 sections for each specimen were observed with fluorescent microscopy (Olympus Italia Srl, Milano, Italy) at 20x of magnification and the following parameters were calculated:

- MINERAL APPOSITION RATE (MAR, μm/day): the rate of progression of the mineralization front labeled twice as index of osteoblast activity. It was calculated with the following equation:

$$MAR = \frac{\sum x}{n} \cdot t \cdot \frac{\pi}{4}$$

Σx= sum of all the measurements between double labels, π/4= the obliquity correction factor, n=(10) the total number of measurements and *t*= the time interval of the oxytetracycline administration (7 days). The measurement is the distance between two parallel fluorescent labeled trabecolae (Giavaresi G, et al., 2010).

- BONE FORMATION RATE (BFR/B.Pm or BFR) ($\mu m^2/\mu m$/day): the quantity of mineralized bone expressed per unit of bone perimeter per day. This value is calculated as:

BFR= MAR*(1/2 sL.Pm/B.Pm+dL.Pm/B.Pm).

sL.Pm= perimeter of single labeled trabecolae, B.Pm=perimeter of trabecolae; dL.Pm= perimeter of double labeled trabecolae (Giavaresi G, et al., 2010).

9.2 STATISTICAL ANALYSIS

Statistical evaluation of data was performed by using SPSS v12.1 software (SPSS Inc.). Data are reported as Mean±SD at a significant level of $p<0.05$. Two-way (scaffold, experimental time) ANOVA, followed by Bonferroni's t test, was applied to compare histomorphometric data.

9.3 RESULTS

9.3.1 Histology and histomorphometry

Histological evaluations at 4 weeks, revealed an initial presence of thin, new bone trabeculae from preexistent bone, that progressively occupied the peripheral zones of the defect (Figures 37 a, b), till 12 weeks, when the new bone was formed inside the porosity, also in the central portion of the both scaffolds (Figure 37 c). New bone trabeculae were recognized because are thin than the preexistent old bone and were present inside and outside the scaffolds (Figures 37 a, b, c). At 12 weeks, for all the scaffolds, the new bone trabeculae, outside the scaffolds, appeared more dense than at 4 weeks, that instead were thin and rarefied, as observed in Figure 37 b, c. Inside the outer new trabeculae, it was revealed the presence of lacunae with osteocytes and osteoblasts along the perimeter (intense blue staining) (Figure 37 c). In the peripheral parts of the implanted scaffolds numerous fibroblasts, fundamental cells of connective tissue with their fusiform aspect, few macrophages and few leukocytes were observed (Figure 37 d) and no fibrous capsule, between the scaffolds and outer bone, was noted for both scaffolds at both experimental times (Figures 37). Moreover, at 12 weeks the new bone was more than at 4 weeks, especially in case of PCL/HA. Figure 38 clarifies the presence of new bone trabeculae inside the scaffolds at 12 weeks, where the material was still visible and it was only partially degraded.

Figures 39 show images of the two scaffolds at the two experimental times at 1,25x of magnification and confirm the above mentioned observations.

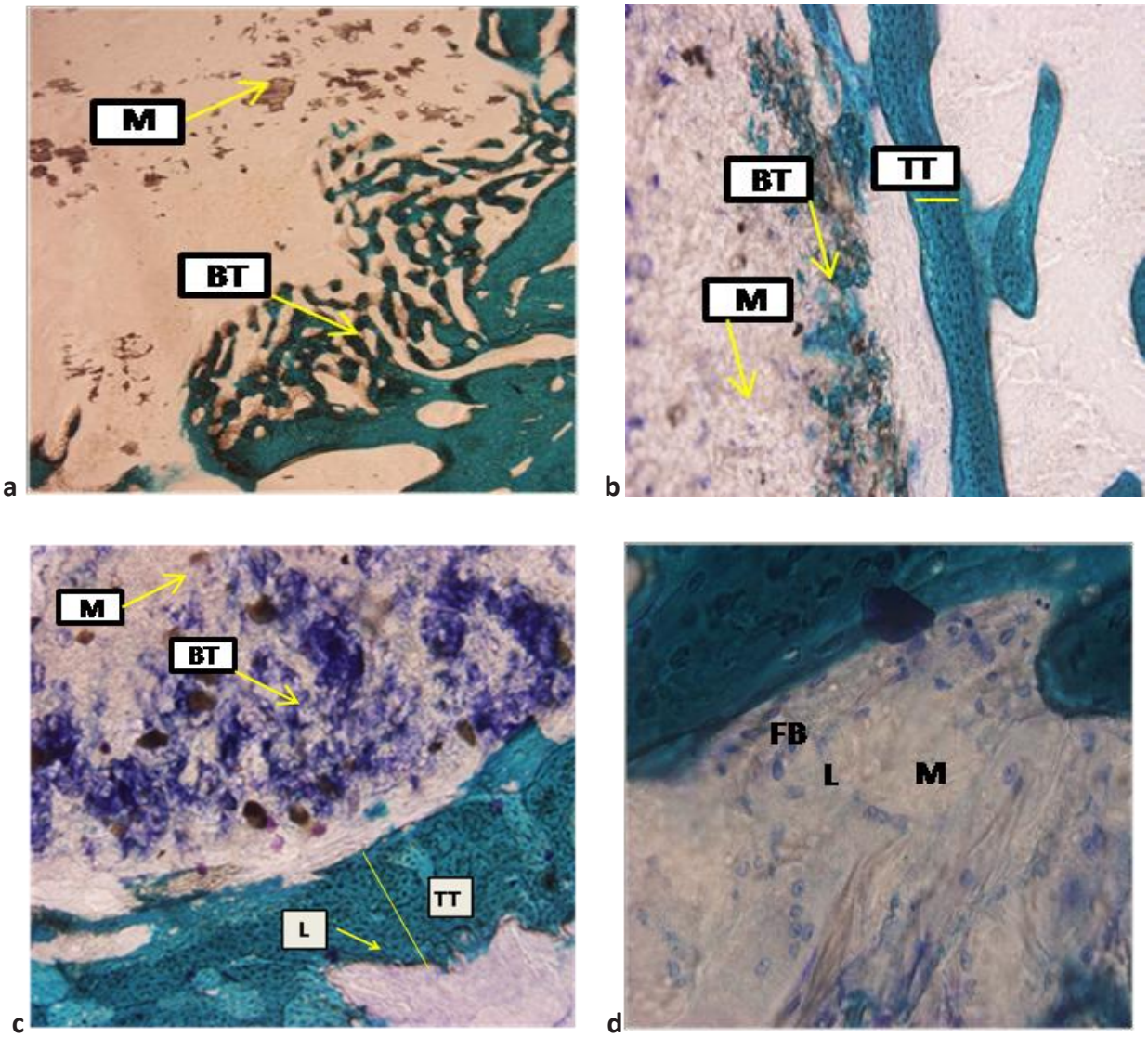

Fig.37. a) PCL and b) PCL/HA initial trabeculae invasion, observed in the peripheral zones of the implanted materials, at 4 weeks. c) PCL/HA at 12 weeks with increasing trabeculae inside the scaffold and lacunae with osteocytes within the outer new trabeculae, that have an higher thickness in comparison to those at 4 weeks. d) Fibroblasts (FB), few macrophages (M) and few leukocytes (L) are observed in the peripheral part of the implanted material. The scaffolds are still present after 4 and 12 weeks. a), b) and c) Magnification 20x; d) Magnification 50x. M= materials; L= lacunae; TT= trabeculae thickness of outer bone; BT= new bone trabeculae inside the scaffolds. Toluidine blue, Acid fuchsin and Fast Green staining.

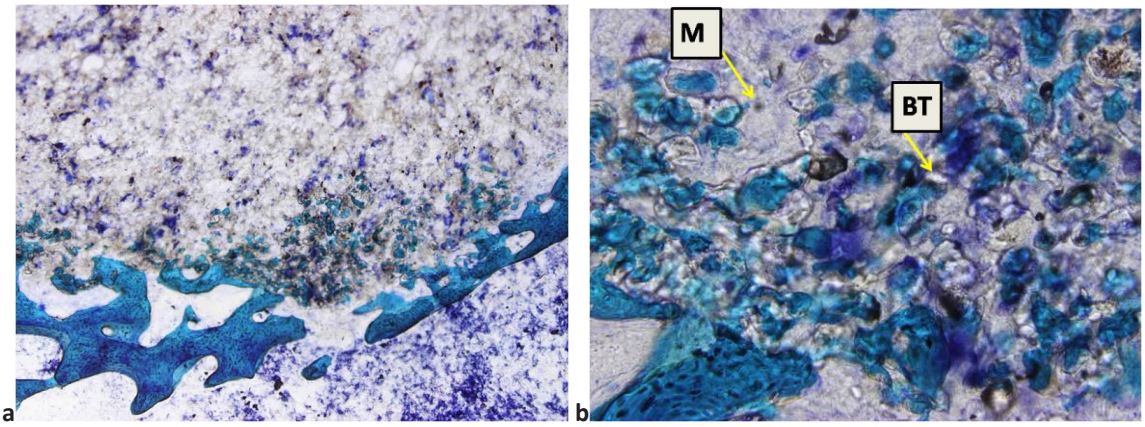

Fig.38. PCL/HA at 12 weeks. a) Magnification 4x, b) magnification 20x. M= grey material; BT= blue new bone trabeculae. Toluidine blue, Acid fuchsin and Fast Green staining.

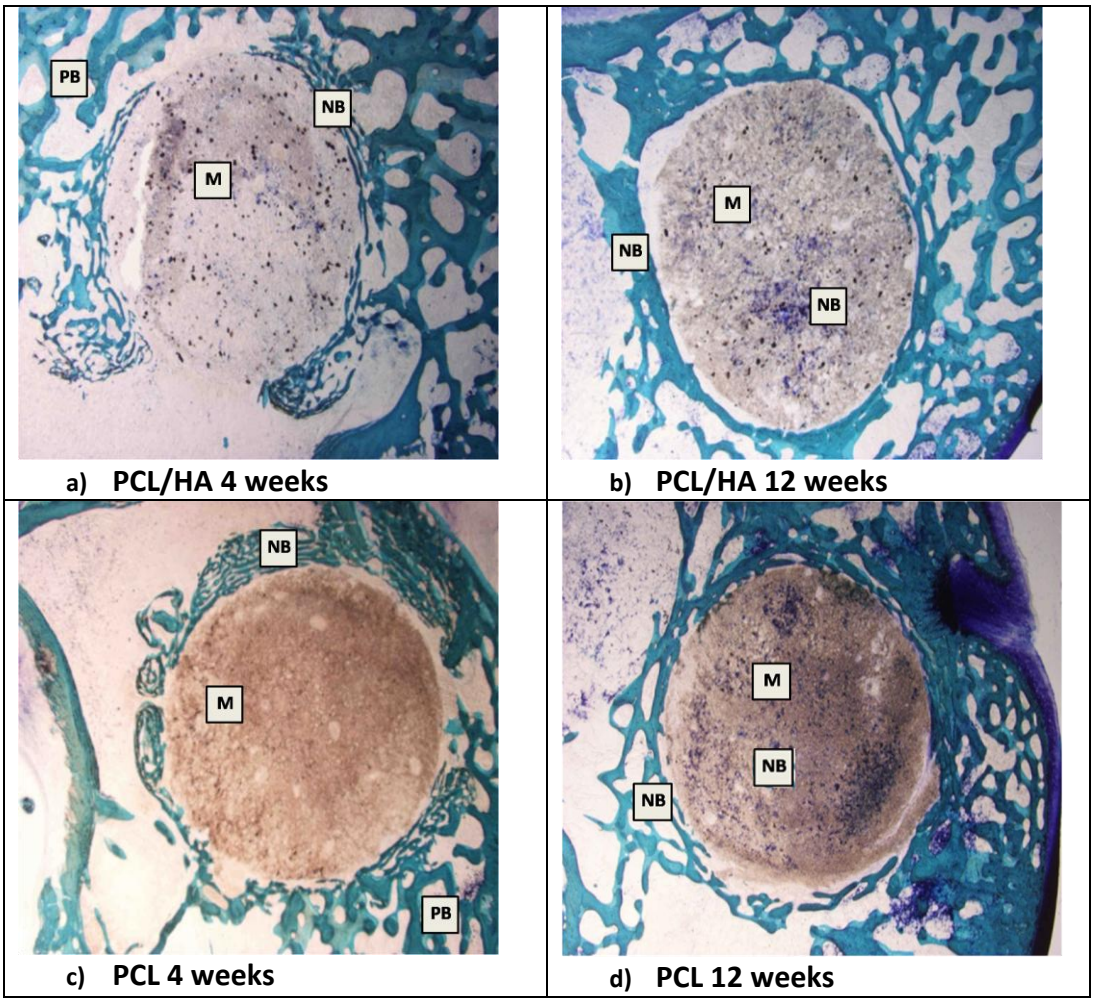

Fig.39. PCL and PCL/HA at 4 and 12 weeks. a), b) PCL/HA; c), d) PCL. a), c) 4 weeks; b), d) 12 weeks. Magnification 1,25x. M= material; NB= new bone trabeculae; PB= preexistent bone. The new bone is recognized because thinner than the preexistent old bone. Toluidine blue, Acid fuchsin and Fast Green staining.

The values of BHR, BAr/TAr and BAr/TAr_{int}, expressed as percentage, are summarized in Table 11.

As BHR values are concerned, significant differences, between the two scaffolds and the two experimental times, were not observed. It was noted that the defect is reduced nearly of 40-50% within 4 weeks and it was maintained till 12 weeks (Figure 40 a).

BAr/TAr showed significantly higher value with of PCL/HA than with PCL at 12 weeks. At 12 weeks, for each scaffolds, significantly higher values were observed than at 4 weeks (Figure 40 b). BAr/TAr_{int} was significantly higher with PCL/HA than PCL at both experimental times, moreover an improvement of this parameter was observed, for each scaffolds, at 12 weeks in comparison to 4 weeks (Figure 40 c).

As observed in figures 41 a) and b) and in Table 11, MAR values, at 4 and 12 weeks, were significantly higher with PCL/HA scaffolds in comparison to PCL scaffold. The values were also significantly higher at 12 weeks for both scaffolds in comparison to those at 4 weeks. The same trend, observed for MAR, was found also for BFR value. In Figure 42, an example of fluorescent sections for the evaluation of MAR and BFR is reported.

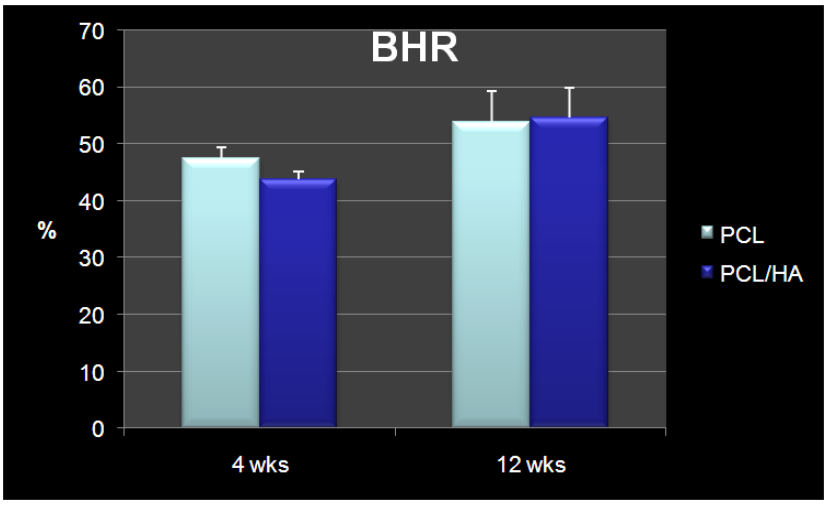

a

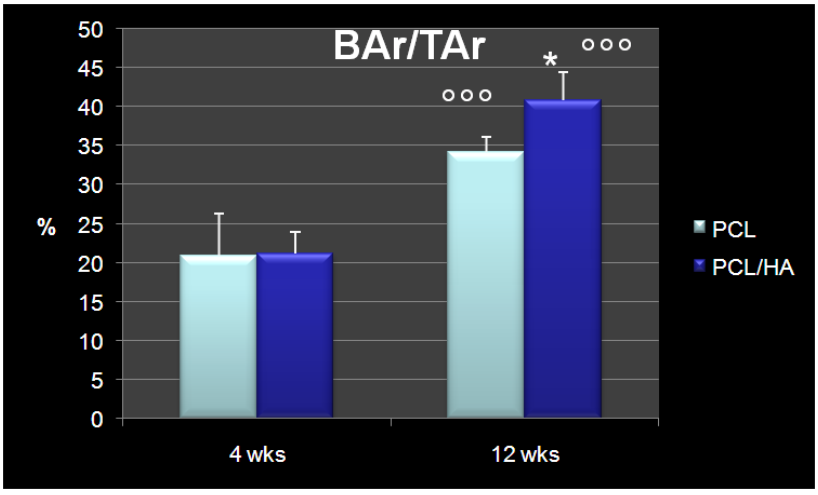

b

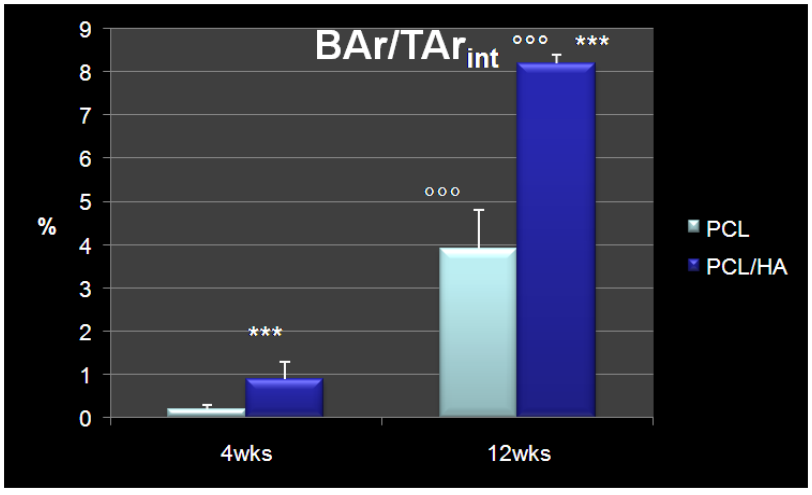

c

Fig.40. a) BHR: No differences were observed between the two materials at 4 and 12 weeks and between the two experimental times. b) BAr/TAr (%):*p < 0.05: PCL/HA *Vs* PCL at 12 wks; °°° p <0.0005: 12 wks *Vs* 4 wks for each scaffolds. At 4 weeks no differences are observed between the scaffolds. c) BAr/TAr_{int} (%):***p<0.0005: PCL/HA *Vs* PCL at 4 and 12 wks; °°° p < 0.0005: 12 wks *Vs* 4 wks for all scaffolds.

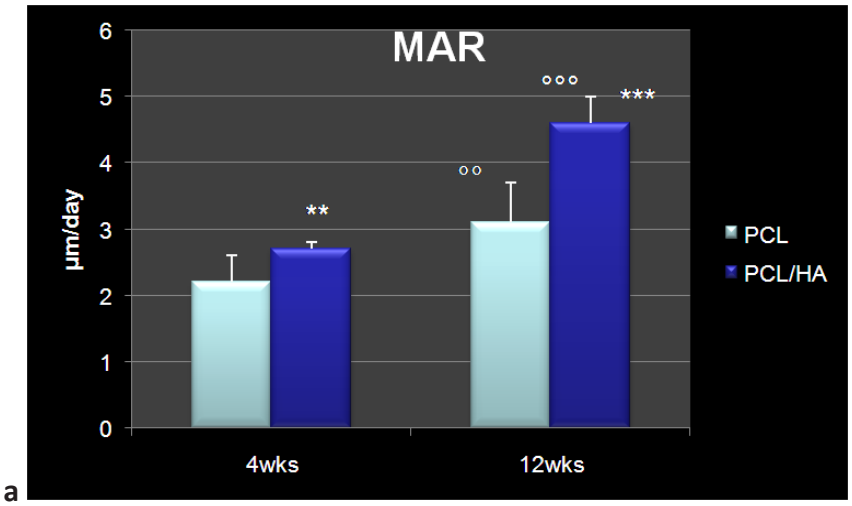

a

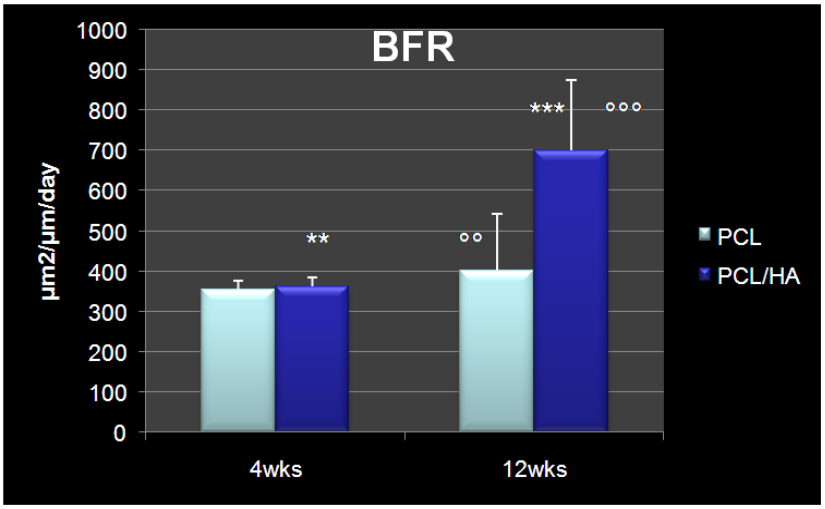

b

Fig.41. a) MAR (µm/day): ** *p*<0.005: PCL/HA *Vs* PCL at 4 wks; *** *p*<0.0005: PCL/HA *Vs* PCL at 12 wks; °° *p*<0.005: 12 wks *Vs* 4 wks for PCL; °°° *p*<0.0005: 12 wks *Vs* 4 wks for PCL/HA; b) BFR (µm^2/µm/day): ** *p*<0.005: PCL/HA *Vs* PCL at 4 wks; *** *p*<0.0005: PCL/HA *Vs* PCL at 12 wks; °° *p*<0.005: 12 wks *Vs* 4 wks for PCL; °°° *p*<0.0005: 12 wks *Vs* 4 wks for PCL/HA.

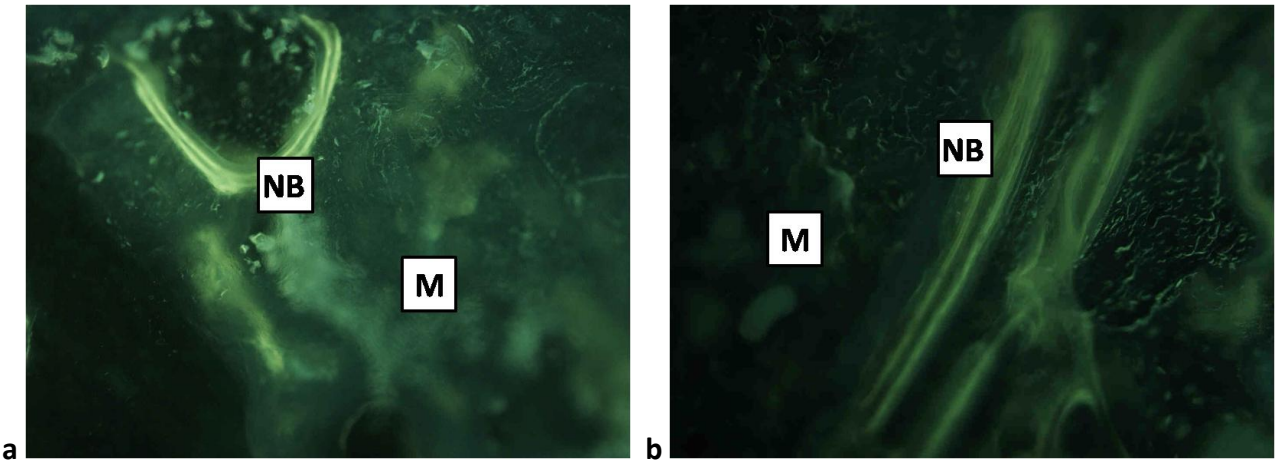

Fig.42. Examples of fluorescent sections for dynamic histomorphometry, at 4 weeks. Magnification 20x. a)PCL and b) PCL/HA. **NB**=New bone trabeculae, labelled with oxytetracycline; **M**= materials.

Tab.11. Results of static and dynamic histomorphometry and relative statistical analyses.

SCAFFOLD	EXPERIMENTAL TIME	BHR (%)	BAr/TAr (%)	BAr/TAr$_{int}$ (%)	MAR (µm/day)	BFR (µm^2/µm/day)
PCL	4 wks	47.5 ± 1.9	20.9 ± 5.3	0.2 ± 0.1	2.2 ± 0.4	352.5 ± 24.7
PCL	12 wks	53.8 ± 5.4	34.2 ± 1.9°°°	3.9 ± 0.9°°°	3.1 ± 0.6°°	401.4 ± 140.0°°
PCL/HA	4 wks	43.7 ± 1.3	21.2 ± 2.7	0.9 ± 0.4***	2.7 ± 0.1**	362.4 ± 21.1**
PCL/HA	12 wks	54.5 ± 5.4	40.8 ± 3.6*,°°°	8.2 ± 0.2***,°°°	4.6 ± 0.4***,°°°	699.2 ± 173.3 ***,°°°

- BAr/TAr (%):*p<0.05:PCL/HA *Vs* PCL at 12 wks; °°° p<0.0005:12 wks *Vs* 4 wks for each scaffolds.
- BAr/TAr$_{int}$ (%):***p<0.0005:PCL/HA *Vs* PCL at 4 and 12 wks; °°° p<0.0005:12 wks *Vs* 4 wks for all scaffolds.
- MAR (µm/day): ** p<0.005:PCL/HA *Vs* PCL at 4 wks; *** p<0.0005:PCL/HA *Vs* PCL at 12 wks; °° p<0.005:12 wks *Vs* 4 wks for PCL; °°° p<0.0005:12 wks *Vs* 4 wks for PCL/HA.
- BFR (µm^2/µm/day): ** p<0.005:PCL/HA *Vs* PCL at 4 wks; *** p<0.0005:PCL/HA *Vs* PCL at 12 wks; °° p<0.005:12 wks *Vs* 4 wks for PCL; °°° p<0.0005:12 wks *Vs* 4 wks for PCL/HA.

10. DISCUSSION AND CONCLUSIONS

In this thesis, PCL scaffold, with a well-controlled microarchitecture, was manufactured by the combination of gas foaming (GF) and selective polymer extraction (PE) from co-continuos blends technique. Gas-foaming based technique has emerged as very promising tool for the design of porous synthetic scaffolds with finely controlled biochemical and biophysical properties; this approach avoids the use of organic solvents, potentially harmful to cells and tissues. In literature, GF and PE techniques were selected and combined to regulate scaffold morphology on a single or double scale (Harris DL, et al., 1998; Sarazin P, et al., 2004; Salerno A, et al., 2007; Kanczler JM, et al., 2008). The appropriate selection of blend composition and GF process parameters allows the design of highly interconnected porous network of PCL scaffolds suitable to be used for tissue engineering. In this thesis, the microstructural parameters have been designed by selecting a 3/2 (w/w) PLC/TG and optimizing the GF processing conditions. Consequently, the final μ-bimodal PCL scaffold prepared was characterized by high interconnectivity and good mechanical responses, with porosity uniformly distributed between the macroporosity, created by the selective extraction of the TG, and the microporosity, induced by the GF process (Salerno A, et al., 2008).

Slow degrading PCL has attracted much interest since its first appearance as bone substitute and has been extensively tested as film, 3D, and nanofibrous scaffold, and for drug delivery, but these products are limited in inducing a regenerative response from bone cells, once implanted. It has been demonstrated that the incorporation of biocompatible insoluble signals, such as hydroxyapatite (HA), into polymer matrix, promotes cell activity, due to the well-known osteoconductive and osteogenic potential, as well as an improvement of mechanical properties for its reinforcement action. The idea of combining bioactive ceramics and degradable polymers to produce 3D scaffolds with high porosity is a promising strategy for the design and development of

composite system for hard tissue regeneration materials (Taddei P, et al., 2005; Koh YH, et al., 2006; Guarino V and Ambrosio L, 2008).

In this thesis, for the fabrication of composite PCL/HA scaffold, among several processing techniques to achieve a highly porous structure (i.e solvent casting, phase inversion, fiber bonding, melt based technologies, high pressure based methods, freeze drying), the phase inversion/particulate leaching technique has been chosen. This procedure of preparation involves the precipitation of a polymer solution in which salt particles are dispersed and the subsequent leaching out of the salt (Guarino V, et al., 2008). Moreover, this technique enables the incorporation of HA solid signals without relevant complications during the preparation procedure, using solvents that do not alter the osteoconductive potential of the HA filler. A highly controlled porosity, characterized by a bimodal distribution of pore size, was achieved: an open macroporous network that assures a uniform cell distribution and tissue regeneration, appeared interconnected by micropores that provide an efficient transport of soluble signaling molecules, as well as nutrients and oxygen, and metabolic waste removal.

For the bony ingrowth into a scaffold, it has been shown that the interconnected pores are important to induce mineralized bony tissue to form inside the macropores of scaffolds. Scaffolds characterized by pores with mean diameters ranging from 100 to 500 μm (macroporosity) and pores with diameters of few microns (microporosity) may provide suitable 3D substrates for both cell colonization/biosynthesis and fluid transport. Apart from pore size, other important variables in orthopaedic applications, related to the scaffold physical features, are the percentage of porosity and the interconnectivity of the pores. Klawitter and coworkers showed that the potential for bone ingrowth was found with a range of pore diameter between 40-100 μm. It has been

reported that the pore interconnection is important for angiogenesis and osteogenesis inside the scaffold by improving the fluid flow and nutrient supply (Klawitter JJ and Hulbert SF, 1971).

There are different methods to evaluate the porosity and interconnectivity of a scaffold and the most suitable techniques are represented by water immersion, mercury intrusion porosimetry, SEM and Image analysis and all of them show some drawbacks.

Water immersion is a method that only provides information on the empty space within the material. The porosity or empty space, measured by this method, includes all the micropores as well as macropores. This method is not able to provide objective and quantitative information about pore size and pore interconnection. Mercury porosimeter is based on the physical principle that a nonwetting liquid does not penetrate fine pore until sufficient pressure is applied. The required pressure is inversely proportional to the size of the pores according to the Washburn equation with the assumption that the pore is cylindrical and well connected. Therefore, the pore size distribution, obtained from mercury porosimeter, does not represent pore diameters but instead a measurement more closely related to the size of the interconnections between pores. The mercury porosimetry only provides partial information on the entire porous structure. SEM is a very useful method to demonstrate the micropore structure. However, the quantification of the pore structure is dependent on the image analysis of 2D images obtained from the scan, but the network of the pore structure is in a 3D manner, which required a 3D method to analyze it (Hiu-Yan Y, et al., 2005). It is evident, that all the previous techniques, used for the study of a material porosity, alone are not complete and can give different results because they analyze different aspects of porosity. Therefore, an alternative is required to provide more comprehensive information on the physical distribution, size, and connectivity of the pores within the porous scaffolds in a 3D space. Unlike the water immersion and SEM techniques, the Micro-CT is a

method that provides information on functional porosity and 3D interconnection apart from delivering a detailed report on parameters of the material structure objectively. The porosity of the scaffolds, measured by Micro-CT, can be calculated based on the void volume of scaffolds. With Micro-CT, the porosity is calculated from the 2D images by the percentage of void area within the porous material area, while for 3D structural evaluation, the volume of interest is reconstructed (Intranuovo F, et al., 2011). Micro-CT seems to be the most complete method to study all the porosity parameters in 2D and 3D manners (Engelke K, et al., 1993; Muller R, et al., 1998; Schmidt C, et al., 2003).

In this thesis, the overall porosity, microporosity, macroporosity percentages, at rest and after mechanical compression, were evaluated with Micro-CT technique, underling that PCL/HA scaffold showed higher overall porosity and macroporosity in comparison to PCL and that both scaffolds possessed a good interconnectivity of nearly 99%. The pore size evaluations revealed that PCL scaffold had the maximum pore size of about 500 μm and the minimum of about 7 μm or few. On the other hand, PCL/HA had pores size that reached dimensions of 900 μm, even if they are very few. For both scaffolds, pores with few microns of dimension were more than larger pores and after compression steps the number of micropores increased.

Moreover, according to the Micro-CT capability to study 2D and 3D structure of an internal object without sample preparation, Micro-CT could be considered very useful to observe cell behaviour inside a scaffold. Indeed cells, scaffolds and growth factors are combined in the *in vitro* phase, which is a crucial moment for the successful outcome of applied tissue engineering scaffold. The need to display the architecture of materials and especially the cellular distribution inside the constructs has consequently triggered different technical efforts to reach this aim. The most common method for examining cells in scaffolds is still microscopy, based on embedding the

sample, sectioning and finally histological staining. Clearly, this technique is destructive and only semi-quantitative. For this approach, fluorescence microscopy can provide a quantitative evaluation, but combined with a confocal equipment to obtain 3D images. However, the analyzed depth is very limited and the interior of opaque materials is still a drawback for a complete imaging (Dorsay SM, et al., 2009). In this thesis, to obtain analytical images, back-scattered electrons (BSE), used by SEM technique, highlighted how the interaction, between osmium and an electron beam, generated a light image of the cells. The same concept was applied to the Micro-CT technique, where the lighter the pixel in Micro-CT sections was, the higher the voxel's absorption was, to observe the cell colonization inside the scaffold analytically. The evident overlap of surface images, obtained by these alternative ways, showed that this new method is a reliable tool for cell visualization. Although currently the most widely used technique to observe the material surface colonization is electron microscopy, these results highlighted the usefulness of SEM to investigate the external coating of the construct, and also the validity of Micro-CT. Thus, SEM and Micro-CT might be two complementary approaches aimed for evaluation of an engineered construct over time from different points of view: SEM is useful to investigate the material surface, whereas Micro-CT allows the scaffold to be assessed three-dimensionally in terms of cell colonization and increasing material degradation rate (Chen Y, et al., 2011). To date, only few studies analyzed the cellular compartment in constructs or soft tissues by Micro-CT (Dorsay SM, et al., 2009; Intranuovo F, et al., 2011; Zehbe R, et al., 2010; Metsher BD, 2009; Chen Y, et al., 2011): in the future it would be very interesting to apply this "microscale" technology for tissue engineering to evaluate the scaffold and to predict a clinical outcome. In this project, a method was established to detect cells within the PCL scaffold to make correct statistical comparisons between samples. The nominal resolution used here (2.5 µm of pixel size) allowed the presence of cells to be detected, even in

Micro-CT sections far from the surface. The MG63 osteosarcoma cell line, used to assess the visualization technique, can grow in multilayers and continue to proliferate over time. Thus, this characteristic was used to ensure the presence of cell colonization even in deeper layers of the scaffold. The method, presented here, was developed after observing the X-ray attenuation histograms obtained. The method described is good for 3D quantification of cell distribution considering the intrinsic properties of Micro-CT analysis, indeed, due to its 3D analysis nature, Micro-CT allows the results obtained by qualitative surface analysis to be combined and gives a more complete understanding of cell colonization. By observing all images, both at 1 week and at 2 weeks after seeding, the PCL appeared to be completely colonized by cells seeded at all the concentration used. A difference in the volume distribution was visible by composing 3D models of the analyzed samples. Indeed, in addition to increased cell volume at 2 weeks compared to 1 week after seeding, the cells with an initial concentration of $2x10^5$ cells/cm^2 showed a more uniform colonization of the PCL scaffold over time. Surface observations (for example by SEM) or observations of the most superficial layers alone might therefore not be sufficient for a correct correlation with quantitative biological data. In fact, quantitative analysis of the surface alone both by SEM and by Micro-CT showed fewer cells at both experimental times for the $2x10^5$cells/cm^2 concentration, whereas quantitative analysis showed a more widespread internal colonization. A good cell infiltration capacity was observed within the PCL scaffold according to the topological properties of its pore structure. The results of this part of Micro-CT study suggest that not only scaffold porosity, but also the number, type and size of seeded cells, as well as the seeding technique are necessary to avoid an excessive and fast colonization of the scaffold periphery. The results could be of particular relevance also for applications of the scaffolds in *in vitro* tissue

engineering field where an engineered construct may be developed in laboratory for the subsequent implantation.

For the subsequent *in vitro* biocompatibility assessment of the scaffolds, ISO 10993 Part 5 "Tests for in vitro cytotoxicity" lists three categories of tests: extract test, direct-contact test, indirect-contact test, selected by the nature of the materials to be evaluated, the potential site of use and nature of their use. In the present study the direct-contact tests were chosen because the scaffolds were proposed as bone fillers, promoters of bone healing and as scaffolding materials for cell growth, thus they had to come in contact with bony tissue.

Biological *in vitro* evaluations were performed at 24 hours, 7 and 14 days. An established cell line (MG63), due to its reproducibility, standardization and accuracy in understanding the response, was chosen (Fini M and Giardino R, 2003).

As stated in the ISO 10993-5, after the culture period, the cytotoxic effects of tested materials on cells were evaluated by means of both qualitative and quantitative analyses. Measurements of cell adhesion, gave similar results, for both scaffolds and control, without significant differences, with a percentage of 85 and 89% for PCL and PCL/HA, respectively. Analogies were also observed in the morphology of cells seeded in empty wells and in both scaffolds: after 24 hours of culture, the cells appeared spindly with well defined cellular membranes and without lysis or reduced proliferation. Moreover, LDH activity was comparable among tested materials and control, indicating an absence of cytotoxicity of both scaffolds. Cell proliferation tests, evaluated at 24 hours, 7 and 14 days, underlined that cells grew regularly on materials and control: their proliferation significantly increased between 24 hours and 7 days and was maintained between 7 and 14 days. In particular, at 7 days PCL/HA cells showed a lower proliferation than PCL and control cells, probably due to the starting of the differentiation process. Indeed, at 7 days, PCL/HA

cells produced significantly higher level of BAP than PCL and control, and OC and CICP than PCL. At 14 days, BAP was produced significantly more by cells on PCL/HA in comparison to control. The production of OC increased between 7 and 14 days in all materials and control, in significantly manner, underlying its role as a late differentiation marker of osteoblasts, whereas the production of BAP and CICP did not show significant differences among experimental times. As about TGF-β, TNF-α and IL-6 synthesis, no differences were observed nor among scaffolds and control at both experimental times, nor between 7 and 14 days. Moreover, the production of TNF-α, was significantly lower on PCL/HA at 14 days in comparison to 7 days.

Thus, results of the *in vitro* study showed that the PCL and PCL/HA possessed a good *in vitro* biocompatibility. In fact the materials did not affect cell proliferation and did not evoke cytotoxic or inflammatory effects as explained by the TNF-α, IL-6, LDH production by the materials, that did not differ from control. Cells cultured on the scaffolds showed a good biofunctionality and bioactivity, as demonstrated by the amount of extracellular matrix components, at both experimental times. In particular, PCL/HA showed an early differentiation process, starting at 7 days and maintaining up to 14 days, demonstrated by an enhanced production of BAP, OC and CICP than PCL, especially at 7 days. In conclusion PCL/HA revealed better biocompatibility and bioactivity when compared to PCL and control.

Then, the *in vivo* evaluations were performed. ISO requires both *in vitro* and *in vivo* tests for a complete assessment of biocompatibility (ISO 10993-1. Guidance on selection of tests). As with any experimental investigation, and in animal testing, the validity of the experimental model for the researched question is of decisive importance for the evaluation of the test results. In order to be able to study the stimulating effect of various implanted materials on bone regeneration, investigations about the kinds of animal models have to be performed. Desirable attributes of an

animal model include demonstration of similarities with humans, both in terms of physiological and pathological considerations, as well as being able to observe numerous subjects over a relatively short time frame (Pearce AI, et al., 2007). When deciding on the species of animal, there are several factors that should be considered. One must define clearly the research question being addressed, prior to selecting the species of animal to be used in the study. Animal selection factors include: cost to acquire and care for animals, availability, acceptability to society, tolerance to captivity and ease of housing. In the last decades a suitable animal model was investigated to study bone repair mechanisms. Among different models, rabbit has several advantages, such as standardization of the experimental conditions, easier housing and experiment repeatability, low cost and high bone turnover rate, proponing rabbit as one of the preferred test animal for the *in vivo* step of the present thesis. Moreover, rabbits are very commonly used as model of bone healing and the efficacy of osteoinductive agents and osteoconductive scaffolds. The rabbit is also convenient in that, because it reaches skeletal maturity shortly after sexual maturity at around 6 months of age (Pearce AI, et al., 2007).

The *in vivo* tests were performed, comparing, with qualitative (histology) and quantitative (static and dynamic histomorphometry) analyses, the behaviour of the two scaffolds, in terms of bone healing defect, new bone formation inside bone defect and porous scaffold and of animal tolerability, after their implantation in a rabbit femoral condyle defect. An important aspect of the histomorphometry is represented by the dynamic parameters MAR and BFR. Histomorphometry or quantitative histology is the analysis on histological sections of bone resorption, formation and structure parameters and it is the only technique that allows a dynamic evaluation of the activity of bone modeling after labeling with tetracycline. Moreover, the new measurement procedures, through the use of the computer, allow an assessment of bone microarchitecture too. They are

employed in the evaluation of bone damage associated with particular treatments. As about dynamic histomorphometry, bone formation rate (BFR) represents the quantity of mineralized bone per trabecular perimeter per days. This parameter would reflect more frequent replacement of bone and would correspond to the higher values for both bone turnover and osteocytes density. The mineral apposition rate (MAR) is determined by dividing the mean distance between the oxytetracycline labels by the time interval between the administration of the two labels and it reflects the bone-forming capacity of osteoblasts at the bone multicellular unit (BMU) level (Schopper C, et al., 2009; Bloebaum RD, 2007; Giavaresi G, et al., 2010).

Histology and the calculated histomorphometry parameters, evaluated after 4 and 12 weeks from the scaffold implantation, showed that new bone trabeculae started to be formed in the periphery of the scaffolds at 4 weeks, and then penetrate the porosity and internal structure of the scaffolds, at 12 weeks, especially for PCL/HA scaffold. Histological analysis evidenced the absence of a thick fibrous inflammatory capsule, without inflammatory cells around the implanted materials, underling that the scaffolds were well tolerated by the animals. It was observed that both materials were present at the end of the both experimental times and they were only partially degraded.

The initial area of the defect was reduced of about 40-50%, after 4 weeks, without significant differences between the two materials and between the two experimental times, indicating that within 4 weeks the healing process started faster and then proceeded slower between 4 and 12 weeks.

The formation of new bone trabeculae outside the implanted materials (BAr/TAr) did not shown differences between the two scaffolds at 4 weeks, but at 12 weeks, PCL/HA had significantly higher values of BAr/TAr than PCL. Moreover, between 4 and 12 weeks, this value increased, with

the two scaffolds, in a significantly manner. The new bone trabeculae started to penetrate the porosity of the two scaffolds slowly, at 4 weeks, in the peripheral zones with values of BAr/TAr_{int} of about 0.2 and 0.9% for PCL and PCL/HA, respectively; at 12 weeks, this value was significantly higher than at 4 weeks, reaching a percentage of 3.9 and 8.2 for PCL and PCL/HA, respectively. Moreover, for each experimental times, PCL/HA showed significantly higher values of BAr/TAr_{int} in comparison to PCL.

As about dynamic histomorphometry, MAR and BFR showed the same trend: at 4 and 12 weeks PCL/HA values were significantly higher than those of PCL and, between 4 and 12 weeks, MAR and BFR results significantly increased in the presence of both scaffolds.

Through time, new bone formation increased outside more than inside the porous scaffold, especially for PCL/HA scaffold and the bone outside the scaffold become more dense between 4 and 12 weeks.

11. ADVANTAGES, LIMITS AND FUTURE OF THE PROJECT

This thesis has permitted the evaluation of different materials, polymeric and polymeric/ceramic scaffolds, proposed to be used as bone fillers in orthopaedic surgery, and described the most important steps, from the fabrication to the *in vivo* animal models passing through mechanical and *in vitro* tests, for the characterization of materials before their clinical use. The first steps of morphological and mechanical characterization of the scaffolds were evaluated in the laboratories in which the materials were performed. In the laboratory, where my thesis work was developed, the subsequent tests of Micro-CT evaluation of the scaffolds porosity at rest and after compression stages and *in vitro* and *in vivo* studies were done and underlined that both scaffolds are biocompatible, bioactive, biofunctional and well tolerated by cells, tissues and animals, with new bone trabeculae that started to grow inside the scaffold porous structure. Moreover, during these three years of PhD, a method for the visualization, distribution and quantification of cells inside the scaffolds was established. A limit of this research was represented by the lack of a comparison with PCL/HA scaffold in terms of cell distribution, because this new method was tested only on PCL scaffold, and once established, in the future, it will be adopted for PCL/HA too. The results of cell-scaffold interaction study demonstrated that high cell seeding efficiency and 3D colonization may be achieved by fine tuning the topological characteristics of the scaffold. In particular, the μ-bimodal scaffolds promoted selective 3D cell colonization into the macroporosity, and consequently ensured the presence of a separate porous network for fluid transport.

Due to the low degradation feature of PCL material, only a little degradation of the scaffolds was noted within 12 weeks. For this reason, in the future, further research will become necessary with longer experimental times for the *in vivo* studies.

It would be interesting to test other cell lines, used in tissue engineering, for the evaluation of scaffolds colonization, such as hMSC (human mesenchymal stromal cells) (Veronesi F, et al., 2011), and hADSC (primary human adipose derived stromal cells) (Levi B, et al., 2011), because of their ability to undergo osteogenic differentiation as well as hMSC, and the interest in these kinds of cells is greatly increasing in these last years (Salerno A, et al., 2010, Veronesi F, et al., 2011).

The implantation of one single bone substitute has been associated with different success rates ranging between 50% and 90%: for this reason the idea of ‘‘polytherapy’’ is arising in the orthopaedic field and consists in the utilization and simultaneous implantation of all the three tissue engineering fundamental components MSCs, growth factors and scaffolds, even if, further investigations are needed to optimize the harvesting, isolation, cultivation and preparation for clinical application (Arthur A, et al., 2009). Polytherapy therefore may be a logical option, especially in individuals of advanced age with associated co-morbidities and a limited capacity for tissue regeneration. In such cases, it could potentially accelerate fracture healing, facilitate early mobilization of patients, and reduce morbidity, health-care costs and complications associated with ongoing cases of impaired fracture healing. Based on experimental and clinical experiences, the application of a scaffold alone could be not enough for restoring large bone loss, particularly in complex non-unions in some patients. In order to improve decision making regarding which bone substitute has to be used to treat large defects properly, more standardized studies are necessary to better understand the use of the scaffolds.

Materials with similar chemical and physical compositions do not necessarily possess the same structural, biological and biomechanical properties or follow the same resorption pathway or even result in the same healing characteristics. Therefore, proper assessment of the biological and mechanical environment and accurate patient selection are necessary. A sound understanding of

various aspects of scaffold properties and their relation and influence towards bone healing is of importance (Janicki P and Schmidmaier G, 2011).

Further investigations on the scaffolds will be performed in terms of fabrication techniques and mechanical tests that will be refined to improve and better understand the quality of the scaffolds for orthopaedic applications.

Thanks to the adopted methodology, a future collaboration between Preclinical and Surgical Studies laboratory and other departments or Universities will be proposed for the possibility to select the best composite scaffold with more relevant promising features, and new materials with different degradability, surface chemistry and porosity for bone regeneration.

12. REFERENCES

- Amizuka N. Bone quality in the respect of bone matrix. *Clin Calcium* 2004, 14:589-93.
- Albrektsson T, Brånemark PI, Hansson HA, Lindström J. Osseointegrated titanium implants. Requirements for ensuring a long-lasting, direct bone anchorage in man. *Acta Orthop Scand* 1981;52:155-170.
- Andersson M, Hedlund J, Berglin M, Elwing H, Tang L. Molecular mobility of polymeric implants and acute inflammatory response: an experimental study in mice. *J Mater Sci Mater Med* 2007;18:283-286.
- Andersson M, Suska F, Johansson A, Berglin M, Emanuelsson L, Elwing H, Thomsen P. Effect of molecular morbility of polymeric implants on soft tissue reactions: an in vivo study in rats. *J Biomed Mater Res A* 2008;84:652-660.
- Ang KC, Leong KF, Chua CK, and Chandrasekaran M. Compressive properties and degradability of poly(ε-caprolatone)/hydroxyapatite composites under accelerated hydrolytic degradation. *J Biomed Mater Res* 2007; 80A: 655.
- Armatas GS. Determination of the effects of the pore size distribution and pore connectivity distribution on the pore tortuosity and diffusive transport in model porous networks. *Chem Eng Sci* 2006;61:4662-4675.
- Arthur A, Zannettino A, Gronthos S. The therapeutic applications of multipotential mesenchymal/stromal stem cells in skeletal tissue repair. *J Cell Physiol* 2009;218:237–45.
- Barnes GL, Kostenuik PJ, Garstenfeld LC, Einhorn TA. Growth factor regulation of fracture repair. *J Bone Min Res* 1999; 14:1805-1815.
- Beaman FD, Bancroft LW, Peterson JJ, Kransdorf MJ. Bone graft materials and synthetic substitutes. *Radiol Clin North Am* 2006; 44:451-61.

- Berridge MV, Tan AS, McCoy KD,Wang R. The biochemical and cellular basis of cell proliferation assays that use tetrazolium salts. *Biochem* 1996;4:15-19.
- Bloebaum RD, Willie BM, Mitchell BS, Hofmann AA. Relationship between bone ingrowth, mineral apposition rate, and osteoblast activity. *J Biomed Mater Res* 2007; 81A: 505-514.
- Bonfield W. Designing porous scaffolds for tissue engineering. *Phil Trans R Soc A* 2006;364, 227-232.
- Borsari V, Giavaresi G, Fini M, Torricelli P, Salito A, Chiesa R, Chiusoli L, Volpert A, Rimondini L, Giardino R. Physical characterization of different-roughness titanium surfaces, with and without hydroxyapatite coating, and their effect on human osteoblast-like cells. *J Biomed Mater Res B Appl Biomater* 2005;75:359-68.
- Branemark PI, Hansson BO, Adell R, Breine U, Lindström J, Hallén O, Ohman A. Osseointegrated implants in the treatment of the edentulous jaw. Experience from a 10-years period. *Scand J Plast Reconstr Surg* 1977;16:1-132.
- Buma P, Schreurs W, Verdonschot N. Skeletal tissue engineering- from in vitro studies to large animal models. *Biomaterials* 2004; 25: 1487-1495.
- Calori GM, Mazza E, Colombo M, Ripamonti C. The use of bone-graft sunstitutes in large bone defects: any specific needs? *Injury* 2011;42:S56-S63.
- Catauro M, Raucci MG, De Marco D, Ambrosio L. Release kinetics of ampicillin, characterization and bioactivity of TiO2/PCL hybrid materials synthesized by sol–gel processing. *J Biomed Mater Res* 2006;77A:340–50.
- Chen Y, Zhou S, Li Q. Microstructure design of biodegradable scaffold and its effect on tissue regeneration. *Biomaterials* 2011;32:5003-5014.

- Chim H, Hutmacher DW, Chou AM, Oliveira AL, Reis RL, LimTC, Schantz JT. A comparative analysis of scaffold material modifications for load-bearing applications in bone tissue engineering. *Int J Oral Maxillofac Surg* 2006; 35:928.
- Davies JE. Understanding peri-implant endosseous healing. *J Dent Edu* 2003; 67:932-949.
- Delloye C, Cnockaert N, Cornu O. Bone substitutes in 2003: an overview. *Acta Orthop Belg* 2003; 69:1
- Dimitriou R, Tsiridis E, Giannoudis PV. Current concepts of molecular aspects of bone healing. *Injury* 2005; 36:1392-1404.
- Dorsay SM, Lin-Gibson S, Simon CG Jr. X-ray microcomputed tomography for the measurement of cell adhesion and proliferation in polymer scaffolds. *Biomaterials* 2009; 30:2967-2974.
- Engelke K, Graeff W, Meiss L, Hahn M, Delling G. High spatial resolution imaging of bone mineral using computed microtomography. Comparison with microradiography and un- decalcified histologic sections. *Invest Radiol* 1993;28:341–349.
- Fini M and Giardino R. In vitro and in vivo tests for the biological evaluation of candidate orthopedic materials: benefits and limits. *J Appl Biomater Biomech* 2003;1:155-163.
- Fini M, Carpi A, Borsari V, Tschon M, Nicolini A, Sartori M, Mechanick J, Giardino R. Bone remodeling, humoral networks and smart biomaterial technology for osteoporosis. *Front Biosci* 2010;1:468-482.
- Fini M, Giavaresi G, Giardino R, Cavani F, Cadossi R. Histomorphometric and mechanical analysis of the hydroxyapatite-bone interface after electromagnetic stimulation: an experimental study in rabbits. *J Bone Joint Surg Br* 2006; 88:123-128.

- Fini M, Motta A, Torricelli P, Giavaresi G, Nicoli Aldini N, Tschon M, Giardino R, Migliaresi C. The healing of a confined critical size cancellous defects in the presence of silk fibroin hydrogel. *Biomaterials* 2005;26:3527-3536.
- Fox CF and Skalak R, eds. *Tissue Engineering.* New York: Alan R. Liss, Inc., 1988.
- Frantzl P. Biomimetic materials research: what can we really learn from nature's structural materials? *J R Soc Interface* 2007;4:637-642.
- Frost HM. Cybernetic aspects of bone modeling and remodeling, with special reference to osteoporosis and whole-bone strength. *Am J Hum Biol* 2001;13:235-48.
- Gallagher CJ. Advances in bone biology and new treatments for bone loss. *Maturitas* 2008; 60:65-69.
- Gatti AM and Knowles JC, 2002. Biocompatibility and biological tests in R Barbucci (ed) Integrated biomaterial science, Kluwer Academic/Plenum Publishers, New York, 2002.
- Gelinsky M, Welzel PB, Simon P, Bernhardt A, Konig U. Porous three-dimensional scaffolds made of mineralized collagen: preparation and properties of a biomimetic nanocomposite material for tissue engineering of bone. *Chem Eng J* 2007;137:84-96.
- Gentile P, Chiono V, Tonda-Turo C, Ferreira AM, Ciardelli G. Polymeric membranes for guided bone regeneration. *Biotechnol J* 2011;6:1187-1197.
- Gerstenfeld LC, Cullinane DM, Barnes GL, Graves DT, Einhorn TA. Fracture healing as a post-natal developmental process: molecular, spatial, and temporal aspects of its regulation. *J Cell Biochem* 2003; 88:873-884.
- Giavaresi G, Fini M, Salvege J, Nicoli Aldini N, Giardino R, Ambrosio L, Nicolais L, Santin M. Bone regeneration potential of a soybean-based filler: experimental stucy in a rabbit cancellous bone defects. *J Mater Sci Mater Med* 2010; 21:615-626.

- Gloria A, De Santis R, Ambrosio L. Polymer-based composite scaffolds for tissue engineering. *J Appl Biomater Biomech* 2010;8:57-67.
- Guarino V and Ambrosio L. The synergic effect of poly-lactide fiber and calcium phosphate particles reinforcement in poly ε-caprolactone based composite scaffolds. *Acta Biomater* 2008;4:1778.
- Guarino V, Causa F, Ambrosio L. Bioactive scaffolds for bone and ligament tissue. *Expert rev Med Devices* 2007;4:405-418.
- Guarino V, Causa F, Netti PA, Ciapetti G, Pagani S, Martini D, Baldini N, Ambrosio L. The role of hydroxyapatite as solid signal on performance of PCL porous scaffolds for bone tissue re generation. *J Biomed Mater Res Part B* 2008;86B:584-557.
- Guarino V, Taddei P, Di Foggia M, Fagnano C, Ciapetti G, Ambrosio L. The influence of hydroxyapatite particles on in vitro degradation behavior of Poly ε-Caprolactone-based composite scaffolds. *Tissue eng A* 2009; 11:3655-3668.
- Gunatillake PA and Adhikari R. Biodegradable synthetic polymers for tissue engineering. *Eur Cell Mater* 2003;5:1-16.
- Habibovic P and de Groot K. Osteoinductive biomaterials-properties and relevance in bone repair. *J Tissue Eng Regen Med* 2007;1:25-32.
- Harris DL, Kim B, Mooney DJ. Open pore biodegradable matrices formed with gas foaming. *J Biomed Mater Res* 1998;42:396-402.
- Heffner J, Brown L, Barbieri C. Diagnostic value of tests that discriminate between exudative and transudative pleural effusions. Primary Study Investigators. *Chest* 1997;111:970–980.

- Henriksen K, Neutzsky-Wulff AV, Bonewald LF, Karsdal MA. Local communication on and within bone controls bone remodeling. *Bone* 2009;44:1026-1033.
- Hing KA. Bone repair in the twenty-first century: biology, chemistry or engineering?. *Phil Trans R Soc Lond A* 2004;362:2821-2850.
- Hiu-Yan Y, Ling Q, Kwong-Man L, Ming Z, Kwok-Sui L, Chun-yiu CJ. Novel approach for quantification of porosity for biomaterial implants using Microcomputed tomography (μ-CT). *J Biomed Mater Res Part B* 2005;75B:234-242.
- Horch HH, Sader R, Pautke C, Neff A, Deppe H, Kolk A. Synthetic, pure-phase beta-tricalcium phosphate ceramic granules (Cerasorb) for bone regeneration in the reconstructive surgery of the jaw. *Int J Oral Maxillofac Surg* 2006;35:708-713.
- Huang CP, Chen XM, Chen ZQ. Osteocyte: the impresario in the electrical stimulation for bone fracture healing. *Med hypotheses* 2008;70:287-290.
- Hutmacher DW, Schantz JT, Lam CXF, Tan KC, Lim TC. State of the art and future directions of scaffold-based bone engineering from a biomaterials perspective. *J Tissue Eng Regen Med* 2007;1:245-260.
- Hutmacher DW. Scaffolds in tissue engineering bone and cartilage. *Biomaterials* 2000;21: 2529.
- Ingber DE, Mow VC, Butler D, Niklason L, Huard J, Mao J, Yannas I, Kaplan D, Vunjak-Novakovic G. Tissue engineering and developmental biology: going biomimetic. *Tissue Eng* 2006;12:3265-3283.
- Intranuovo F, Howard D, White LJ, Johal RK, Ghaemmaghami AM, Favia P, Howdle SM, Shakesheff KM, Alexander MR. Uniform cell colonization of porous 3-D scaffolds achieved using radial control of surface chemistry. *Acta Biomater* 2011;7:3336-3344.

- Janicki P and Schmidmaier G What should be the characteristics of the ideal bone graft substitute? Combining scaffolds with growth factors and/or stem cells. *Injury* 2011;42:S77–S81.
- Kanczler JM, Ginty PJ, Barry JJA, Clarke NMP, Howdle SM, Shakesheff KM, Oreffo RO. The effect of mesenchymal populations and vascular endothelial growth factor delivered from biodegradable polymer scaffolds on bone formation. *Biomaterials* 2008;29:1892-1900.
- Kao ST and Scott DD. A review of bone substitutes. *Oral Maxillofac Surg Clin North Am* 2007;19:513-521.
- Kawamura K, Kawate K, Yajima H, Kobata Y, Takakura Y. Vascularized scapular grafting for treatment of osteonecrosis of the humeral head. *J Reconstr Microsurg* 2008;24:559-64.
- Khan YM, Katti DS, Laurencin CT. Novel polymer synthesized ceramic composite-based system for bone repair: an in vitro evaluation. *J Biomed Mater Res* 2004;69A:728.
- Kilpadi KL, Sawyer AA, Prince CW, Chang PL, Bellis SL. Primary human marrow stromal cells and Saos-2 osteosarcoma cells use different mechanisms to adhere to hydroxylapatite. *J Biomed Mater Res A* 2004;68:273-85.
- Kim BS, P IK, Hoshiba T, Jiang HL, Choi YJ, Ai T. Design of artificial extracellular matrices for tissue engineering. *Prog Polym Sci* 2011;36:238-268
- Kishimoto T, Akira S, Narazaki M, Taga T. Interleukin-6 family of cytokines and gp130. *Blood* 1995;86:1243–54.
- Klawitter JJ and Hulbert SF. Application of porous ceramics for the attachment of load-bearing internal orthopedic applications. *Cell Transplant* 1971;3:339.
- Kneser U, Schaefer DJ, Polykandriotis E, Horch RE. Tissue engineering of bone: the reconstructive surgeon's point of view. *J Cell Mol Med* 2006;10:7-19.

- Koh YH, Bae CJ, Sun JJ, Jun IK, Kim HE. Macrochanneled poly (ε-caprolactone)/hydroxyapatite scaffold by combination of bi-axial machining and lamination. *J Mater Sci Mater Med* 2006;17:773.
- Kolk A, Handschel J, Drescher W, Rothamel D, Kloss F, Blessmann M, Heiland M, Wolff KD, Smeets R. Current trends and fracture perspectives of bone substitute materials-from space holders to innovative biomaterials. J Craniomaxillofac Surg 2012;1-13.
- Laz PJ, Stowe JQ, Baldwin MA, Petrella AJ, Rullkoetter PJ. Incorporating uncertainty in mechanical properties for finite element-based evaluation of bone mechanics. *J Biomech* 2007;40:2831.
- LeGeros RZ. Properties of osteoconductive biomaterials: calcium phosphates. *Clin Orthop relat Res* 2002;395:81-98.
- Levi B, Nelson ER, Brown K, James AW, Xu D, Dunlevie R, Wu JC, Lee M, Wu B, Commons GW, Vistnes D, Longaker MT. Differences in osteogenic differentiation of adipose-derived stromal cell from murine, canine, and human sources in vitro and in vivo. Plast Reconstr Surg 2011;128:373-386.
- MacEwan DJ. TNF receptor subtype signalling: differences and cellular consequences. *Cell Signal* 2002;14:477-492.
- Marsh DR and Li G. The biology of fracture healing: optimizing outcome. Br Med Bull 1999; 55:856-869.
- McIntire LV. WTEC panel on tissue engineering research: final report, Academic Press, San Diego, 2003.
- Metsher BD. Micro-CT for development biology: a versatile tool for high-contrast 3D imaging and histological resolutions. *Dev Dyn* 2009;238:632-640.

- Moroni L, De Wijn JR, Van Blitterswijk C. Integrating novel technologies to fabricate smart scaffolds. *J Biomater Sci Polymer Edn* 2008;19:543-572.
- Muller R, Van Campenhout H, Van Damme B, Van Der PG, Dequeker J, Hildebrand T, Ruegsegger P. Morphometric analysis of human bone biopsies: a quantitative structural comparison of histological sections and micro-computed tomography. *Bone* 1998;23:59–66.
- Nandi SK, Roy S, Mukherjee P, Kundi B, De DK, Basu D. Orthopaedic applications of bone graft & graft substitutes: a review. *Indian J Med Res* 2010;132:15-30.
- Nathan AS, Baker BM, Nerurkar NL, Mauck RL. Mechano-topographic modulation of stem cell nuclear shape on nanofibrous scaffolds. *Acta Biomater* 2011;7:57-66.
- Naujoks C, Langenbach F, Berr K, Depprich R, Kübler N, Meyer U, Handschel J, Kögler G. Biocompatibility of osteogenic predifferentiated human cord blood stem cells with biomaterials and the influence of the biomaterial on the process of differentiation. *J Biomater Appl* 2011;25:497-512.
- Negrou G, Piticescu RM, Chitanu GC, Mihailescu IN, Zdrentu L, Miroiu M. Biocompatibility evaluation of a novel hydroxyapatite-polymer coating for medical implants (*in vitro* tests). *J Mater Sci Mater Med* 2008;9:1537-1544.
- Ohgaki T, Toda H, Kobayashi M, Uesugi K, Niinom M, Akahori T, Kobayashi T, Makii K, Aruga Y. In situ observations of compressive behavior of aluminum foams by local tomography using high-resolution tomography. *Phil Mag* 2006;86:4417-4438.
- Ohtsuki C, Kamitakahara M, Miyazaki T. Bioactive ceramic-based materials with designed reactivity for bone tissue regeneration. *J R Soc Interface* 2009;6:S349-60.

- Otsuki B, Takemoto M, Fujibayashi S, Neo M, Kokubo T, Nakamura T. Pore throat size and connectivity determine bone and tissue ingrowth into porous implants: three-dimensional Micro-CT based structural analyses of porous bioactive titanium implants. *Biomaterials* 2006;27:5829-5900.
- Parfitt AM, Drezner MK, Glorieux FH, Kanis JA, Malluche H, Meunier PJ, Ott SM, Recker RR. Bone histomorphometry: standardization of nomenclature, symbols, and units. Report of the ASBMR Histomorphometry Nomenclature Committee. *J Bone Miner Res* 1987;2:595-610. A)
- Parfitt AM, Simon LS, Villanueva AR, Krane SM. Procollagen type I carboxy-terminal extension peptide in serum as a marker of collagen biosynthesis in bone: correlation with iliac bone formation rates and comparison with total alkaline phosphatase. *J Bone Miner Res* 1987;2:427-436. B)
- Pearce AI, Richards RG, Milz S, Schneider E, Pearce SG. Animal models for implant biomaterial research in bone: a review. *Eur Cell Mater* 2007;13:1-10.
- Peterson GL. A simplification of the protein assay method of Lowry et al. which is more generally applicable. *Anal Biochem* 1977;83:346-56.
- Price CP. Multiple forms of human serum alkaline phosphatase: detection and quantization. *Ann Clin Biochem* 1993;30:355-372.
- Puchacz E, Lian JB, Stein GS, Wozney J, Huebner K, Croce C. Chromosomal localization of the human osteocalcin gene. J *Endocrinol* 1989;124:2648–2650.
- Rezwan K, Chen QZ, Blaker JJ, Boccaccini AR. Biodegradable and bioactive porous polymer/inorganic composite scaffolds for bone tissue engineering. *Biometarials* 2006;27:3413-3431.

- Salerno A, Guarnieri D, Iannone M, Zeppetelli S, Di Maio E, Iannace S, Netti PA. Engineered μ-bimodal poly(ε-caprolactone) porous scaffold for enhanced hMSC colonization and proliferation. *Acta Biomater* 2009;5:1082-93.
- Salerno A, Guarnieri D, Iannone M, Zeppetelli S, Netti PA. Effect of micro- and macroporosity of bone tissue three-dimensional-poly (ε-Caprolactone) scaffold on human mesenchymal stem cells invasion, proliferation, and differentiation in vitro. *Tissue eng: part A* 2010;16:2661-2673.
- Salerno A, Oliviero M, Di Maio E, Iannace S, Netti PA. Design and preparation of μ-bimodal porous scaffold for tissue engineering. *J Appl Polym Sci* 2007;106:3335-3342.
- Sanz-Herrera JA, Doblaré M, García-Aznar JM. Scaffold microarchitecture determines internal bone directional growth structure: a numerical study. *J Biomech* 2010;43:2480-6.
- Sarazin P, Roy X, Favis BD. Controlled preparation and properties of porous poly(L-lactide) obtained from a co-continuous blend of two biodegradable polymers. *Biomaterials* 2004;25:5965-5978.
- Schmidt C, Priemel M, Kohler T, Weusten A, Muller R, Amling M, Eckstein F. Precision and accuracy of peripheral quantitative computed tomography (pQCT) in the mouse skeleton compared with histology and microcomputed tomography (microCT). *J Bone Miner Res* 2003;18:1486–1496.
- Schopper C, Moser D, Spassova-Tzekova E, Russmuller G, Goriwoda W, Lagogiannis G, Ewers R, Redl H. Mineral apposition rate provide significant information on long-term effects in BMP-induced bone regeneration. *J Biomed Mater Res* 2009;89A: 679-686.
- Sen MK and Miclau T. Autologous iliac crest bone graft: Should it still be the gold standard for treating nonunions? *Injury* 2007;38:S75-S80.

- Simchi A, Tamjid E, Pishbin F, Boccaccini AR. Recent progress in inorganic and composite coatings with bactericidal capability for orthopaedic applications. *Nanomedicine* 2011;7:22-39.
- Soheim E. Growth factors in bone. *Int Orthop* 1998;22:410-416.
- Standring S. Functional anatomy of the musculoskeletal system. In: Grays anatomy. The Anatomical Basis of Clinical Practice. (Ed) Standring S. Churchill Livingstone. 40th Ed. 2008.
- Stock SR. Recent advances in x-ray microtomography applied to materials. *Int mater Rev* 2008; 58:129-181.
- Summer-Smith G. Non-union of fractures. In: Sumner-Smith G Bone in clinical orthopaedics, Thieme eds, New York 2002, pp 349-378.
- Sundelacruz S and Kaplan DL. Stem cell-and scaffold-based tissue engineering approaches to osteochondral regenerative medicine. *Semin Cell Dev Biol* 2009;20:646-655.
- Taddei P, Tinti A, Reggiani M, Fagnano C. In vitro mineralization of bioresorbable poly(ε-caprolactone)/apatite composites for bone tissue engineering: a vibrational and thermal investigation. *J Mol Struct* 2005;744:135.
- Takai E, Mauck RL, Hung CT, Guo XE. Osteocyte viability and regulation of osteoblast function in a 3D trabecular bone explant under dynamic hydrostatic pressure. *J Bone Miner Res* 2004;19:1403-1410.
- Takemoto M, Fujibayashi S, Otsuki B, Matsushita T, Kokubo T, Nakamura T. 3-D analysis of pore structure of porous biomaterials using micro focus X-ray computed tomography. *Bioceramics* 2006;18:1095-1098.

- Thompson MS, Epari DR, Bieler F, Duda GN. In vitro models for bone mechanobiology: applications in bone regeneration and tissue engineering. *Proc Inst Mech Eng H* 2010;224:1533-41.
- Tschon M, Fini M, Giavaresi G, Torricelli P, Rimondini L, Ambrosio L, Giardino G. In vitro and in vivo behaviour of biodegradable and injectable PLA/PGA copolymers related to different matrices. *Int J Artif Organs* 2007;30:352-362.
- Urist MR and Dawson E. Intertransverse process fusion with the aid of chemosterilized autolyzed antigen-extracted allogenic (AAA) bone. *Clin Orthop Relat Res* 1981;97-113.
- Veronesi F, Torricelli P, Borsari V, Tschon M, Rimondini L, Fini M. Mesenchymal Stem Cells in the Aging and Osteoporotic Population. *Crit Rev Eukaryot Gene Expr* 2011; 21:363-377.
- Wan AC, Ying JY. Nanomaterials for in situ cell delivery and tissue regeneration. *Adv Drug Deliv Rev* 2010;62:731-40.
- Wang M. Developing bioactive composite materials for tissue replacement. *Biomaterials* 2003;24:2133–51.
- Wang W, Ouyang Y, Poh CK. Orthopaedic implant technology: biomaterials from past to future. *Ann Acad Med Singapore* 2011;40:237-8.
- Warden SJ. Breaking the rules for bone adaptation to mechanical loading. *J Appl Physiol* 2006;100:1441-1442.
- Weigel T, Schinkel G, Lendlein A. Design and preparation of polymeric scaffolds for tissue engineering. *Exp Rev Med Devices* 2006;3:835-851.
- Whyte MP. Hypophosphatasia and the role of alkaline phosphatase in skeletal mineralization. *Endocr Rev* 1994;15:439-461.

- Williams DF. Definition in biomaterials. In: Progress in biomedical engineering. Amsterdam Elsevier.1987, p. 67
- Williams DF. Review: on the mechanisms of biocompatibility. *Biomaterials* 2008;29:2941-2953.
- Wintermantel E and Mayer J. Anisotropic biomaterials strategies and developments for bone implants. In: Encyclopedic handbook of biomaterials and bioengineering. Part B-1. Eds Wise DL, Trantolo DJ, Altobelli DE, Yaszemiski JD, Gressner JD, Schwarts ER. New York. Marcel Dekker. 1995. P-3-42.
- Wolff J. Das Gesetz der transformation des knochens. Hirscwald, Berlin, 1892
- Yamada Y, Boo JS, Nagasaka ROT, Okazaki Y, Hata KI, Ueda M. Bone regeneration following injection of mesenchymal stem cells and fibrin glue with biodegradable scaffold. *J Cranio Maxillofac Surg* 2003;31:27-33.
- Yan Y, Li S, Zhang R, Lin F, Wu R, Lu Q, Xiong Z and Wang X. Rapid prototyping and manufacturing technology: principle, representative techniques, applications, and development trends. *Tsinghua Sci Technol* 2009;14:1-12.
- Yu H, Matthew HW, Wooley PH, Yang SY. Effect of porosity and pore size on microstructures and mechanical properties of poly-ε-Caprolactone-hydroxyapatite composites. *J Biomed Mater Res Part B* 2008;86B:541-547.
- Zarb G and Albrektsson T. Osseointegration- a requirement for the periodontal ligament?- an editorial. *Int J Periodont rest Dent* 1991;11:88-91.
- Zehbe R, Goebbels J, Ibold Y, Gross U, Shubert H. Three-dimensional visualization of in vivo cultivated chondrocytes inside porous gelatin scaffolds: a tomographic approach. *Acta Biomater* 2010;6:2097-2107.

- Zhang C, Hu YY, Cui FZ, Zhang SM, Ruan DK. A study on a tissue-engineered bone using rhBMP-2 induced periosteal cells with a porous nano-hydroxyapatite/collagen/poly(L-lactic acid) scaffold. *Biomed Mater* 2006;1:56-62.
- Zhou H and Lee J. Nanoscale hydroxyapatite particles for bone tissue engineering. *Acta Biomater* 2011; 7:2769-81.

13. ACKNOWLEDGEMENTS

I would like to thank Prof. Roberto Giardino who accepted and gave to me the possibility and the opportunity to study and perform my PhD project at the Preclinical and Surgical Studies Laboratory of Rizzoli Orthopaedic Institute of Bologna.

I am also grateful to thank my patient tutor and responsible of the laboratory, Dr. Milena Fini, for her assistant and experience during these 3 years of my PhD.

I thank the two groups of University of Naples for providing materials, particularly Prof. Ambrosio and Prof. Netti PA.

I would like to thank all of my friends and colleagues also for their moral support: Dr Francesca Salamanna, Maria Sartori and Annapaola Parrilli, and Dr Paola Torricelli and Gianluca Giavaresi for their valuable advices.